

National Bureau of Standards
Library, N.W. Bldg
MAY 17 1965



Technical Note

No. 306

STUDIES OF SOLAR FLARE EFFECTS AND OTHER IONOSPHERIC DISTURBANCES WITH A HIGH FREQUENCY DOPPLER TECHNIQUE

V. Agy, D. M. Baker, and R. M. Jones



U. S. DEPARTMENT OF COMMERCE
NATIONAL BUREAU OF STANDARDS

THE NATIONAL BUREAU OF STANDARDS

The National Bureau of Standards is a principal focal point in the Federal Government for assuring maximum application of the physical and engineering sciences to the advancement of technology in industry and commerce. Its responsibilities include development and maintenance of the national standards of measurement, and the provisions of means for making measurements consistent with those standards; determination of physical constants and properties of materials; development of methods for testing materials, mechanisms, and structures, and making such tests as may be necessary, particularly for government agencies; cooperation in the establishment of standard practices for incorporation in codes and specifications; advisory service to government agencies on scientific and technical problems; invention and development of devices to serve special needs of the Government; assistance to industry, business, and consumers in the development and acceptance of commercial standards and simplified trade practice recommendations; administration of programs in cooperation with United States business groups and standards organizations for the development of international standards of practice; and maintenance of a clearinghouse for the collection and dissemination of scientific, technical, and engineering information. The scope of the Bureau's activities is suggested in the following listing of its four Institutes and their organizational units.

Institute for Basic Standards. Electricity. Metrology. Heat. Radiation Physics. Mechanics. Applied Mathematics. Atomic Physics. Physical Chemistry. Laboratory Astrophysics.* Radio Standards Laboratory: Radio Standards Physics; Radio Standards Engineering.** Office of Standard Reference Data.

Institute for Materials Research. Analytical Chemistry. Polymers. Metallurgy. Inorganic Materials. Reactor Radiations. Cryogenics.** Office of Standard Reference Materials.

Central Radio Propagation Laboratory.** Ionosphere Research and Propagation. Troposphere and Space Telecommunications. Radio Systems. Upper Atmosphere and Space Physics.

Institute for Applied Technology. Textiles and Apparel Technology Center. Building Research. Industrial Equipment. Information Technology. Performance Test Development. Instrumentation. Transport Systems. Office of Technical Services. Office of Weights and Measures. Office of Engineering Standards. Office of Industrial Services.

* NBS Group, Joint Institute for Laboratory Astrophysics at the University of Colorado.

** Located at Boulder, Colorado.

NATIONAL BUREAU OF STANDARDS

Technical Note 306

Issued April 28, 1965

STUDIES OF SOLAR FLARE EFFECTS AND OTHER IONOSPHERIC DISTURBANCES WITH A HIGH FREQUENCY DOPPLER TECHNIQUE

V. Agy, D. M. Baker, and R. M. Jones

Central Radio Propagation Laboratory

National Bureau of Standards

Boulder, Colorado

NBS Technical Notes are designed to supplement the Bureau's regular publications program. They provide a means for making available scientific data that are of transient or limited interest. Technical Notes may be listed or referred to in the open literature.



Table of Contents

	<u>Page</u>
List of Tables	v
List of Figures	vii
Nomenclature	ix
Abstract	xi
1. Introduction	1
2. Theoretical Considerations	7
2.1 An Equivalence Theorem for Doppler Shifts	9
2.2 Changing Ionospheric Parameters	11
2.3 Frequency Deviations due to Rate of Change of Electron Density as Function of Height	21
3. Solar Flare Observations with the Doppler Technique	31
3.1 Percentage of Solar Flares Detected	32
3.2 Duration, Rise Time, and Delay Time of Frequency Deviation	37
3.3 Path Length Dependence of Frequency Deviations	40
3.4 Frequency Dependence of Frequency Deviations	44
4. Selected Events Detected by Doppler Technique	47
4.1 Solar Flares	47
4.2 Geomagnetic Variations	55
5. Discussion	60
6. Acknowledgements	64
7. References	65
8. Appendix I: The Doppler Shift Written as an Integral	67
9. Appendix II: Equivalence Theorem for Doppler Shifts	72
10. Appendix III: Relationship Between Doppler Shift and Virtual Height	74

Table of Contents

	<u>Page</u>
11. Appendix IV: Catalog of Sudden Frequency Deviations Observed from October 1960 through December 1962	78

List of Tables

	<u>Page</u>
1.1 Circuits over which Doppler measurements have been made by CRPL	4
2.1 Tabulation of data for flare effects of November 22, 1961 and April 17, 19, and 20, 1962	28
3.1 Percentage of flares reported from October 1, 1960 to December 31, 1962 which were accompanied by SFD's	32
11.1 Catalog of sudden frequency deviations observed from October 1960 through December 1962	85



List of Figures

	<u>Page</u>
2.1 Doppler shift, Δf , for vertical propagation with reflection in a changing parabolic F layer	14
2.2 Doppler shift, Δf , for oblique propagation with reflection in a changing parabolic F layer	15
2.3 Doppler shift, Δf , for vertical propagation with fixed mirror-like reflection above a changing parabolic E layer	17
2.4 Doppler shift, Δf , for vertical propagation through a valley of changing depth between parabolic E and F layers.	19
2.5 Doppler shift, Δf , for oblique propagation through a valley of changing depth between parabolic E and F layers.	20
2.6 Comparison of $f_v \Delta f$ vs f_v with ionogram for SFD at 2014 UT on November 22, 1961.	24
2.7 Comparison of $f_v \Delta f$ vs f_v with ionogram for SFD at 2252 UT on April 17, 1962	25
2.8 Comparison of $f_v \Delta f$ vs f_v with ionogram for SFD at 1935 UT on April 19, 1962	26
2.9 Comparison of $f_v \Delta f$ vs f_v with ionogram for SFD at 1959 UT on April 20, 1962	27
2.10 Relationship between maximum frequency deviations observed on 4 and 5 Mc/s at vertical incidence, Boulder, Colorado	30
3.1 Variations of the percentage of reported solar flares detected, mean solar flux at 2800 Mc/s, and mean Zürich sunspot number during the period October 1, 1960 through December 31, 1962.	34
3.2 Percentage of reported solar flares detected by the Doppler technique as a function of month, October 1960 through December 1962.	35
3.3 Percentage of reported solar flares detected by the Doppler technique as a function of time of day, October 1960 through December 1962.	36
3.4 Percentage of reported solar flares detected by the Doppler technique as a function of solar zenith angle at the midpoint of the WWV to Boulder path, October 1960 through December 1962 .	38
3.5 Durations of sudden frequency deviations observed from October 1960 through December 1962	39
3.6 Rise times of sudden frequency deviations observed from October 1960 through December 1962	41
3.7 Time difference between maximum positive frequency deviation and maximum phase of optical flare, October 1960 through December 1962	42

3.8	Frequency deviation of WWV-10 Mc/s observed at Shickley, Nebraska (1780 km) versus that observed at Boulder, Colorado (2400 km) . . .	43
3.9	Frequency deviation of WWV-10 Mc/s versus that of WWV-20 Mc/s, both observed at Boulder, Colorado	45
3.10	Frequency deviation of WWV-10 Mc/s versus that of WWV-15 Mc/s, both observed at Boulder, Colorado	46
4.1	Sudden frequency deviation observed during importance 1 flare on September 4, 1961, WWV-10 Mc/s received at Boulder	48
4.2	Sudden frequency deviation observed during importance 3+ flare on November 12, 1960, WWV-20 Mc/s received at Boulder.	50
4.3	Sudden frequency deviation observed during importance 3 flare on September 28, 1961, WWV-10 and WWV-20 Mc/s received at Boulder.	51
4.4	Sudden frequency deviation observed during importance 2 flare on April 19, 1962, WWV-10 and WWV-15 Mc/s received at Boulder. .	53
4.5	Sudden frequency deviation observed during importance 2 flare on April 19, 1962. 4 and 5 Mc/s vertical incidence at Boulder .	54
4.6	Sudden commencement observed by the Doppler technique at 2108 UT on September 30, 1961. WWV-10 and WWV-20 Mc/s received at Boulder.	56
4.7	Sudden commencement observed by the Doppler technique at 0219 UT on February 22, 1962. WWV-10 Mc/s received at Shickley, Nebraska, and WWV-10 and WWV-15 Mc/s received at Boulder, Colorado	57
4.8	Correlation between frequency variations observed at both oblique and vertical incidence and changes in the magnetic field observed at Boulder	59
10.1	Comparison of theoretical $f\Delta f$ versus f with ionogram	77
11.1	Sample Doppler record illustrating the range in magnitude of the sudden frequency deviations detected	80

Nomenclature

ΔA	change in non-deviative absorption, nepers
b	thickness of slab of ionization in non-deviative region, km
c	speed of light in vacuum, km/s
D	great circle distance between transmitter and receiver, km
f	frequency
f_c	critical frequency of parabolic layer, Mc/s
f_E	critical frequency of parabolic E layer, Mc/s
f_F	critical frequency of parabolic F layer, Mc/s
f_H	gyrofrequency, Mc/s
f_N	electron plasma frequency, Mc/s
f_v	$f \cos\phi_0$, equivalent vertical-incidence frequency, Mc/s
f_{vv}	plasma frequency of valley between two parabolic layers, Mc/s
Δf	Doppler shift, c/s
h	reflection height, km
h'	virtual height, km
h_m	height of maximum electron density of parabolic layer, km
h_{mE}	height of maximum electron density of parabolic E layer, km
h_{mF}	height of maximum electron density of parabolic F layer, km
h_o	height of bottom of parabolic layer, km, or a height in non-deviative region below which dN/dt can be considered to be zero.
h_{oE}	height of bottom of parabolic E layer, km
h_{oF}	height of bottom of parabolic F layer, km
k	$\frac{f_N^2}{N}$, $8.05 \times 10^{-11} (\text{Mc/s})^2 \text{ m}^3$
N	electron density, m^{-3}

P	phase path, km
s	path length
t	time
X	$\frac{f_N^2}{f^2}$
y_m	$h_m - h_o$, semithickness of parabolic layer
Y	f_H/f
Y_L	$Y \cos\theta$
Y_T	$Y \sin\theta$
z	height as variable of integration
μ	phase refractive index
μ'	group refractive index
μ_o	phase refractive index at transmitter
ν	electron collision frequency
ρ	f_V/f_E
ϕ	angle between wave normal and vertical
ϕ_o	angle between wave normal and vertical at transmitter
θ	angle between wave normal and magnetic field

Abstract

This report presents some results of work done with a Doppler technique for studying ionospheric disturbances. The theoretical results include a calculation of the frequency shifts to be expected from changes in the parameters of a parabolic model ionosphere and a method of determining the height variation of the time rate of change of electron density during ionospheric disturbances. It is shown that the frequency shift, with oblique propagation, is the same as that with vertical propagation on the equivalent vertical-incidence frequency. The experimental results include a comprehensive catalog of all flare effects observed from 1 October 1960 through 31 December 1962, a statistical study of these flare effects, and the Doppler records of some solar flare effects detected during this period. A model in which the time rate of change of electron density is zero below the bottom of the E layer, and constant above that height, explains the frequency dependence of the maximum Doppler shifts observed during some solar flares.



STUDIES OF SOLAR FLARE EFFECTS AND OTHER IONOSPHERIC
DISTURBANCES WITH A HIGH FREQUENCY DOPPLER TECHNIQUE

V. Agy, D. M. Baker, and R. M. Jones
Central Radio Propagation Laboratory

1. Introduction

The "Doppler technique" developed and described by Watts and Davies [1960] appears to be a powerful tool for probing the ionosphere, especially during times of rapid change. It has been shown to be effective, for example, in the study of solar-flare effects and of variations occurring at the time of a magnetic sudden commencement [Davies, 1962b]. The term "sudden frequency deviation", abbreviated to SFD (initially suggested by Chan and Villard [1963]), has been adopted to refer to solar-flare induced variations in the received frequency of a high frequency, ionospherically propagated radio signal.

In effect, the frequency f of the received signal from a highly stable CW transmitter is monitored continuously. If the phase path P changes with time, a shift in the received frequency is produced which may be written [Davies, 1962a]:

$$\Delta f = - \frac{f}{c} \frac{dP}{dt} \quad (1.1)$$

where c is the speed of light in vacuum. (This may be written

$$\Delta f = - \frac{f}{c} \frac{d}{dt} \int \mu \ ds \quad (1.2)$$

if the anisotropy of the ionosphere is neglected.)

The present monitoring technique involves recording, at a speed of .02 ips on magnetic tape, the beat between the received signal and that of a stable local oscillator. The beat frequency is set initially at a few cycles per second. If the tape is played back at 30 ips, this beat frequency is readily analyzed on a standard audio frequency analyzer and changes in the original frequency of one tenth of a cycle per second or more can easily be observed and measured. The transmitted and reference frequencies must be stable to within a few parts in 10^9 per day.

A simple theory, consisting of two special cases, for determining the layers affected during an ionospheric disturbance has been described by Davies [1962a] and by Davies, Watts, and Zacharisen [1962]. One case shows that for several probing frequencies propagating in the same mode (i.e., same ground path length, same number of hops, reflected from same layer) the Doppler shift varies inversely with carrier frequency ($\Delta f \propto 1/f$) when the change in phase path is due solely to changes in ionization in the non-deviative portion of the ionosphere. In the other case the frequency deviation varies directly with frequency ($\Delta f \propto f$) if the phase path change is due entirely to a vertical movement of the height of reflection.

Davies [1963] has suggested that in the non-deviative region the height determination can be improved by comparing the phase path change (ΔP) to the absorption suffered by the radio wave. An atmospheric model specifying electron collision frequency (ν) as a function of height can then be used to locate the "slab" of ionization assumed responsible for both effects. Similar work has been carried out by Kanellakos, Chan, and Villard [1962]. These studies have helped to establish the fact that

solar-flare effects are relatively frequent at heights above the D region of the ionosphere.

Davies [1962c] has also shown that the Doppler technique can be used for study of ionospheric drifts.

Those circuits over which Doppler measurements have been made by CRPL are given in table 1.1. Related techniques involving the direct measurement of phase change are also in use. The increasing use of these techniques and the high precision of the actual measurements (both of Doppler shift and of phase change) suggest that attention be given to further development of the theory so that the approach may be exploited to the fullest extent.

This paper presents work done with the Doppler technique by the Ionosphere Research Section of the Ionosphere Research and Propagation Division of CRPL. The theoretical treatment develops two methods of determining the heights at which ionospheric disturbances occur. Both approaches neglect the earth's magnetic field and the curvature of the ionosphere.

The first method approximates the ionosphere by one or two parabolic profiles and then determines the frequency dependence of the Doppler shift produced by the rate of change of the parameters (i.e., critical frequency, minimum height, height of maximum electron density, thickness of layer, and valley depth) defining the ionospheric model. If, then, the Doppler shifts are known for a number of frequencies at vertical and/or oblique incidence during a disturbance, it is possible to determine the time rate of change of the parameters which could have produced the observed Doppler shifts. This method is not difficult to apply since the

Table 1.1
Circuits over which Doppler measurements have been made by CRPL

Transmitter	Receiver	Path Length (km)	Freq. Mc/s	Period of Operation
Beltsville, Md. (WWV)	Boulder, Colorado	2430	5	02/09/63-07/15/63
"	"		10	12/15/60-12/20/60, 01/11/61-- (1)
"	"		15	12/21/60-01/10/61, 01/17/62-- (1)
"	"		20	10/02/60-06/02/61 09/08/61-01/17/62
"	Shickley, Nebraska	1780	10	08/12/61-04/18/62
Maui, Hawaii (WWVH)	Anchorage, Alaska	4480	15	06/08/62-12/03/62
"	Midway Island (3)	2200	5	05/31/62-07/10/62 10/25/62-11/06/62 (night)
"	"		10	05/31/62-07/10/62 10/25/62-11/06/62
"	"		15	05/31/62-07/10/62 10/25/62-11/06/62 (2) (day)
"	Wake Island (3)	3900	10	05/26/62-07/29/62
"	"		15	05/28/62-07/29/62

Maui, Hawaii (WVH) Makapuu Pt., Oahu,
Hawaii (4) 140 5 11/10/62-08/29/63

Pt. Barrow, Alaska Anchorage, Alaska 1160 9.9475 02/23/62-12/03/62

Tripoli, Libya Accra, Ghana 3300 19.904 09/11/61-10/14/61

Monrovia, Liberia " 1180 10.1018 10/19/62-- (1)

" " 20.2036 10/22/62-- (1)

" Natal, Brazil 2990 10.1018 11/30/62-- (1)

" " 20.2036 11/14/62-- (1)

Sunset (Boulder),
Colorado Boulder, Colo. 25 2.100 06/02/61-09/08/61

" " 4.000 08/04/61-- (1)

" " 5.054 07/30/61-- (1)

" Ft. Collins, Colo. 75 4.000 02/01/62-03/01/62

Erie, Colorado Boulder, Colorado 15 2.100 02/25/63-06/21/63

(1) Circuit in operation as of July 1964

(2) Either 5 and 10 or 10 and 15 Mc/s in operation during this period

(3) Subject to interference from JY, Tokyo

(4) Hawaiian records obtained by Dr. Walter Steiger of the University of Hawaii

layer parameters are easily determined from the ionogram and the solution for the time rate of change involves solving only a few simultaneous linear equations.

The second approach gives a solution for the time rate of change of electron density as a function of height when the Doppler shift as a function of the equivalent vertical-incidence frequency can be given. It can be applied to any monotonic ionospheric profile, but the accuracy of the solution depends on the amount of data available.

Most solar flare effects in the ionosphere produce characteristic effects on the Doppler records. The early recognition of this fact led to the suggestion that the Doppler technique be used for flare patrol work. Much of the record analysis and the experimental effort has dealt with flare effects--specifically with the percentage of flares detected, the time characteristics of the frequency deviations, and the magnitude of the effects relative to probing frequency, path length, and solar zenith angle. The section of the report dealing with the observations gives the empirical results derived to date and a catalog of solar flare effects as observed on the CRPL Doppler records from 1 October 1960 through 31 December 1962. A few sets of observations are treated according to the methods described in the theoretical section.

2. Theoretical Considerations

In order for the Doppler technique to be of value as a tool for ionospheric research, a theory is needed which adequately relates the observed frequency variations to the ionospheric changes producing them. A simple theory for vertical incidence (neglecting the earth's magnetic field) has been developed by Davies [1962a, 1962b]. According to this theory, if changes take place in a non-deviative slab of thickness b in which the rate of change of ionization can be considered constant with height, then

$$\Delta f = \frac{kb}{cf} \frac{dN}{dt} . \quad (2.1)$$

In this case the observed frequency deviation is inversely proportional to the operating frequency. However, if the only change is a vertical movement of the height at reflection, then

$$\Delta f = - 2 \frac{f}{c} \frac{dh}{dt} \quad (2.2)$$

and the frequency deviation is directly proportional to the operating frequency. These equations can be applied to oblique incidence if b is replaced by $b/\cos \phi_0$ and dh/dt is replaced by $dh/dt \cos \phi_0$, where ϕ_0 is the angle of incidence on the ionosphere.

If both types of change occur at the same time (i.e., if the change in height of reflection and a change in the non-deviative region occur simultaneously but independently) then

$$\Delta f = \frac{kb}{cf} \frac{dN}{dt} - 2 \frac{f}{c} \frac{dh}{dt} . \quad (2.3)$$

If such independent changes did occur and measurements of Δf were made on two different frequencies, then $b dN/dt$ and dh/dt could be determined from

(2.3) [Davies, 1962d].

Davies [1963] has further shown that for a thin, non-deviative slab in which the collision frequency is $\nu(\ll \omega)$

$$\frac{\Delta A}{\Delta P} = - \frac{\nu}{c}, \quad (2.4)$$

where ΔA is the change in non-deviative absorption in nepers and ΔP is the change in phase path given by

$$\Delta P(t) = - \frac{c}{f} \int_{t_0}^t \Delta f \, dt. \quad (2.5)$$

Hence, if both $\Delta A(t)$ and $\Delta f(t)$ are measured, it is possible to determine $\nu(t)$ from (2.4) and (2.5). If the collision frequency profile $\nu(h)$ is known, then the average height $h(t)$ at which the additional electron density is produced can be found. However, even where this method is applicable it is rather insensitive due to the lack of knowledge of the variation of collision frequency with height.

The simple theory has not explained all the frequency deviations observed. The theoretical work covered in this report is a beginning in the development of a theory which will explain the Doppler observations at both vertical and oblique incidence. The major aim has been to develop a method of determining the height variation of dN/dt from the Doppler observations. A knowledge of dN/dt as a function of height during a solar flare would be helpful in determining which wave length bands are enhanced during the flare. A knowledge of the enhancement of radiation during a flare should help in gaining an understanding of the processes taking place in the sun.

2.1. An Equivalence Theorem for Doppler Shifts

For oblique propagation relations similar to (2.1) and (2.2) can be derived if the earth's magnetic field and the curvature of the ionosphere are neglected. The resulting relations are:

$$\Delta f = \frac{kb}{cf \cos \phi_o} \frac{dN}{dt} \quad (2.6)$$

for a change of ionization in a non-deviative slab, and

$$\Delta f = -2 \frac{f \cos \phi_o}{c} \frac{dh}{dt} \quad (2.7)$$

for a vertical movement of the height of reflection. In these equations ϕ_o is the angle of incidence on the ionosphere. These two equations can be written as

$$\Delta f = \frac{kb}{f_v c} \frac{dN}{dt} \quad (2.8)$$

and

$$\Delta f = -2 \frac{f_v}{c} \frac{dh}{dt} \quad (2.9)$$

where $f_v = f \cos \phi_o$. A comparison of (2.8) and (2.9) with (2.1) and (2.2) reveals that, in these simple cases, the Doppler shift observed on a wave frequency f , incident on the ionosphere at an angle ϕ_o , would be the same as that observed on a frequency f_v incident vertically on the ionosphere. This "equivalence" between the Doppler shifts observed for vertical and oblique propagation is easily seen for these simple cases. In Appendix II it is shown that such an equivalence holds in the general case, if the earth's magnetic field and the curvature of the ionosphere are neglected. Hence, an equivalence theorem for Doppler shifts can be stated as follows:

$$\Delta f(f, \phi_o) = \Delta f(f \cos \phi_o, 0) \quad (2.10)$$

where $\Delta f(f, \phi_0)$ is the Doppler shift, on a frequency f , incident on the ionosphere at an angle ϕ_0 . The frequency f_V is called the equivalent vertical-incidence frequency.

As derived, this equivalence relation applies only for no magnetic field. However, it is probably a good approximation even with the magnetic field for frequencies which are large compared to the gyrofrequency. Therefore, rather than attempting to treat vertical-incidence and oblique-incidence data separately, it seems more advantageous to use the equivalence theorem to reduce the oblique-incidence data to equivalent vertical-incidence data, and to apply a single theory to the combined data. In this connection it may be noted that with oblique-incidence observations the amount of useful data may exceed the number of probing frequencies used. At oblique incidence more than one propagation mode is often possible (e.g., E and F layer propagation, one- and two-hop propagation, etc.), and the Doppler shifts observed on the different modes may be quite different. In such a case, if the propagation modes can be identified, the Doppler shift observed on each gives an independent piece of data.

This equivalence theorem should be very useful in analyses of Doppler data obtained on different paths and from different parts of the world, and it will provide a convenient means whereby various observers can exchange their data. Of course, before data from different paths or different regions can be meaningfully compared certain corrections, such as corrections for the number of hops or the differences in solar zenith angle, may have to be applied to the observed frequency deviations.

2.2. Frequency Deviations Due to Changing Ionospheric Parameters

Although in many cases the ionosphere can be described adequately only by specifying the height distribution of electron density, it is often convenient to represent the ionosphere by a suitable model (e.g., parabolic). If the distribution does not change in character (if, for example, a parabolic distribution remains parabolic) it is possible to find Δf as a function of the time derivatives of the parameters defining the distribution. Primarily for illustrative purposes and for comparison with the first order theory [Davies, 1962a], the algebra and the computations have been carried out for several model ionospheres. Both vertical and oblique propagation are considered. The earth's magnetic field and the curvature of the earth and ionosphere are neglected.

For vertical propagation of a wave, the phase path P is given by

$$P = 2 \int_0^h \mu \, dz , \quad (2.11)$$

where h is the reflection height. For oblique propagation, the phase path is given by

$$P = \int_s \mu \, ds , \quad (2.12)$$

where s is the path length.

If the ionospheric profile consists of parabolic layers, then the plasma frequency f_N in each layer is given by

$$f_N^2 = f_c^2 \left[2 \left(\frac{z - h_o}{h_m - h_o} \right) - \left(\frac{z - h_o}{h_m - h_o} \right)^2 \right] , \quad (2.13)$$

for $h_O \leq z \leq 2 h_m - h_O$. In each layer, the phase refractive index μ for a wave of frequency f is given by

$$\mu = \sqrt{1 - \frac{f_N^2}{f^2}} = \sqrt{1 - \frac{f_c^2}{f^2}} \left(2 \left[\frac{z - h_O}{h_m - h_O} \right] - \left[\frac{z - h_O}{h_m - h_O} \right]^2 \right). \quad (2.14)$$

For vertical propagation this expression for the refractive index may be used in (2.11) to find the phase path in terms of the parameters defining the model ionosphere. The time derivative of P may then be found in terms of the time derivatives of the layer parameters, and the Doppler shift, Δf , is then given by (1.1). Similarly the Doppler shift for oblique propagation could be found from (2.14), (2.12), and (1.1) using the fact that the transmission distance is constant (i.e., the transmitter and receiver are fixed). However, because of the equivalence theorem presented in section 2.1, the calculations need be performed only for vertical propagation. The Doppler shift for oblique propagation can then be found by substituting $f \cos \phi_O$ for f in the equations for vertical propagation. Indeed, the equivalence theorem was discovered while working with changing parabolic layers.

Three models considered will now be discussed separately.

Model 1: reflection in a changing parabolic layer (figure 2.1a).

For this case

$$\Delta f = - \frac{f}{c} \frac{\partial P}{\partial h_O} \frac{dh_O}{dt} - \frac{f}{c} \frac{\partial P}{\partial h_m} \frac{dh_m}{dt} - \frac{f}{c} \frac{\partial P}{\partial f_c} \frac{df_c}{dt} \quad (2.15)$$

where

$$\begin{aligned}
 -\frac{f}{c} \frac{\partial P}{\partial h_o} &= \frac{f_c}{c} \left[-x - \frac{1-x^2}{2} \ln \frac{1+x}{1-x} \right] \\
 -\frac{f}{c} \frac{\partial P}{\partial h_m} &= \frac{f_c}{c} \left[-x + \frac{1-x^2}{2} \ln \frac{1+x}{1-x} \right] \\
 -\frac{f}{c} \frac{\partial P}{\partial f_c} &= \frac{y_m}{c} \left[-x + \frac{1+x^2}{2} \ln \frac{1+x}{1-x} \right]
 \end{aligned} \tag{2.16}$$

and

$$x = \frac{f}{f_c} \tag{2.17}$$

for vertical propagation, or

$$x = \frac{f \cos \phi_o}{f_c} \tag{2.18}$$

$$\tan \phi_o = \frac{D}{(2h_o + x y_m \ln \frac{1+x}{1-x})} \tag{2.19}$$

for oblique propagation. Plots of the coefficients in (2.15)

$[-f/c \partial P/\partial h_o, -f/c \partial P/\partial h_m, -f/c \partial P/\partial f_c]$ versus f , for specific values of the parameters h_o , h_m , and f_c , are given in figure 2.1 for vertical propagation. Similar curves are shown in figure 2.2 for oblique propagation over paths of 200, 1000, and 2400 km. For a layer defined by values of h_o , h_m , and f_c different from those chosen, figures 2.1 and 2.2 can still be applied by using equation (2.16) to scale the curves.

For the special case $dh_o/dt = dh_m/dt = dh/dt$ and $df_c/dt = 0$, (2.15) reduces to (2.2), the expression for the Doppler shift caused by vertical movement of the ionosphere (or of the height of reflection).

Doppler shift, Δf , for vertical propagation with reflection in a changing parabolic F layer

$$f_c = 10 \text{ Mc/s}, h_0 = 200 \text{ km}, h_m = 300 \text{ km}$$

$$\Delta f = -\frac{f}{c} \frac{\partial P}{\partial h_0} \frac{dh_0}{dt} - \frac{f}{c} \frac{\partial P}{\partial h_m} \frac{dh_m}{dt} - \frac{f}{c} \frac{\partial P}{\partial f_c} \frac{df_c}{dt}$$

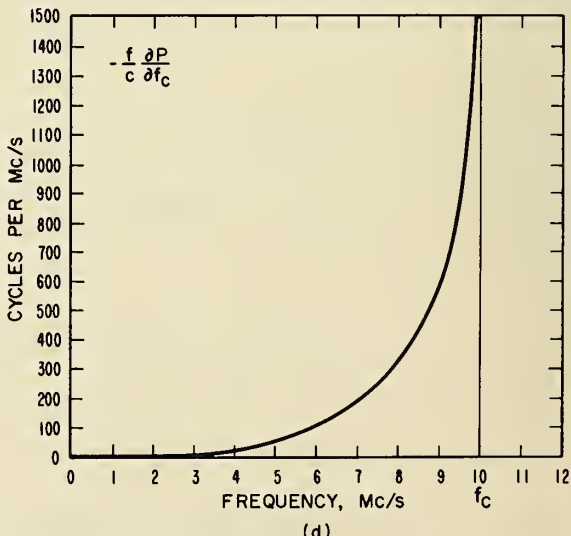
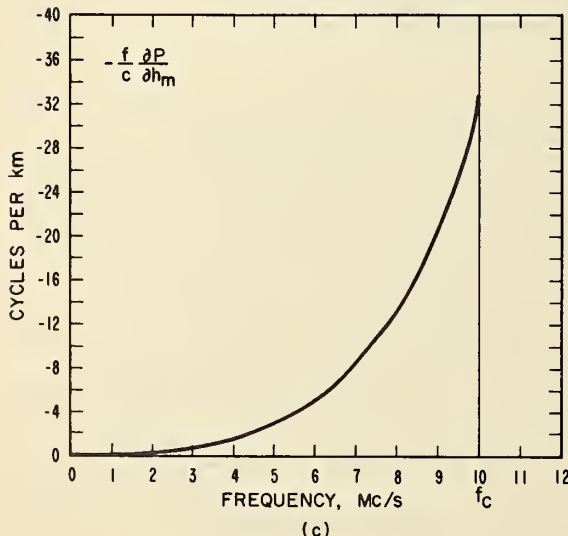
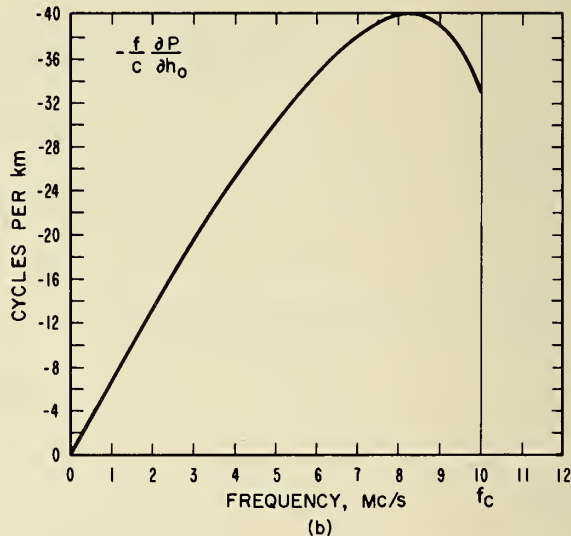
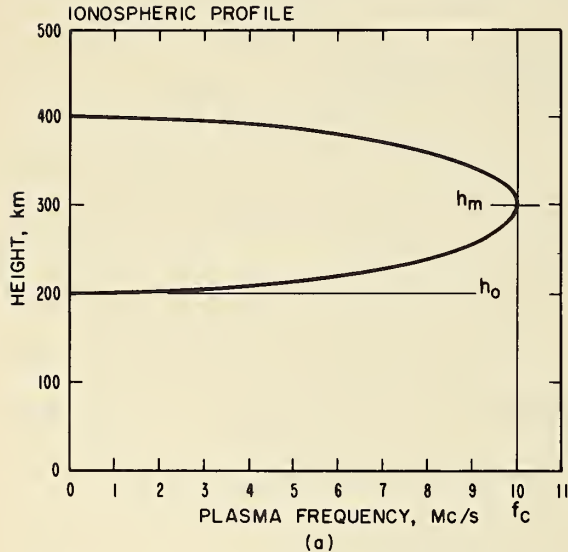


Figure 2.1

Doppler shift, Δf , for oblique propagation with reflection in a changing parabolic F layer

$$f_c = 10 \text{ Mc/s}, h_0 = 200 \text{ km}, h_m = 300 \text{ km}$$

$$\Delta f = -\frac{f}{c} \frac{\partial P}{\partial h_0} \frac{dh_0}{dt} - \frac{f}{c} \frac{\partial P}{\partial h_m} \frac{dh_m}{dt} - \frac{f}{c} \frac{\partial P}{\partial f_c} \frac{df_c}{dt}$$

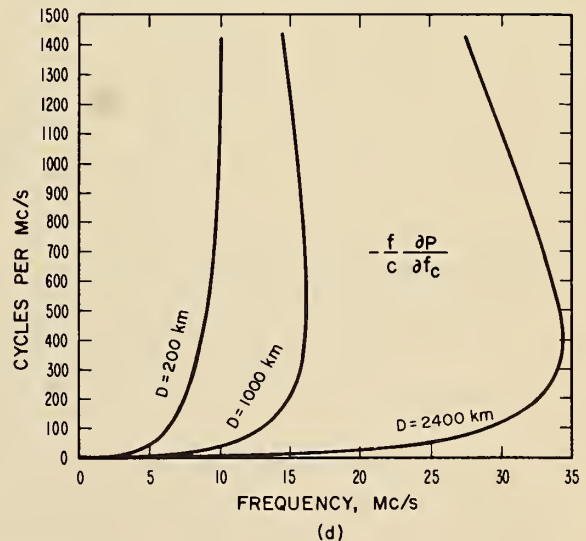
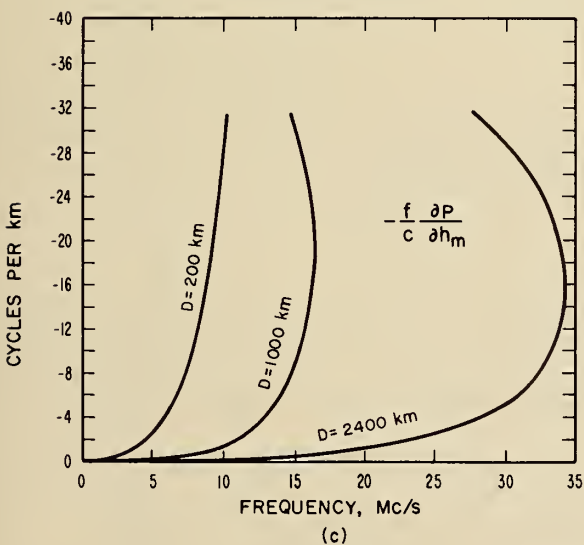
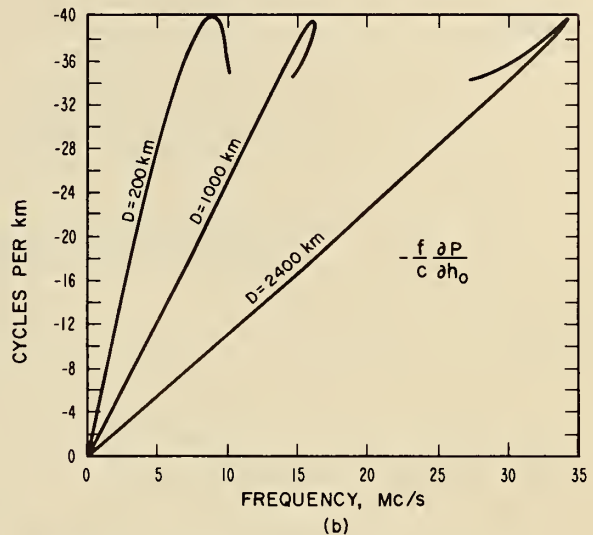
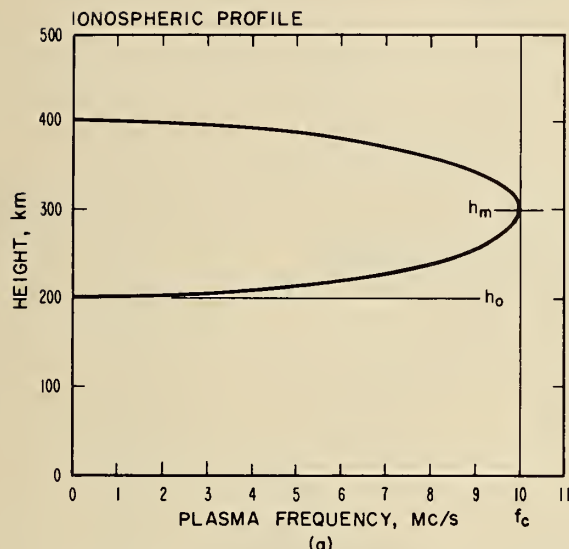


Figure 2.2

Model 2: propagation through a changing parabolic layer with reflection from a mirror reflector (figure 2.3a). In this case

$$\Delta f = - \frac{f}{c} \frac{\partial P}{\partial f_c} \frac{df_c}{dt} - \frac{f}{c} \frac{\partial P}{\partial y_m} \frac{dy_m}{dt} \quad (2.20)$$

where

$$- \frac{f}{c} \frac{\partial P}{\partial f_c} = \frac{y_m}{c} \left[-2x + (1 + x^2) \ln \frac{x+1}{x-1} \right] \quad (2.21)$$

$$- \frac{f}{c} \frac{\partial P}{\partial y_m} = \frac{f_c}{c} \left[2x + (1 - x^2) \ln \frac{x+1}{x-1} \right]$$

and

$$x = \frac{f}{f_c} \quad (\text{eq. 2.17})$$

for vertical propagation, or

$$x = \frac{f \cos \phi_o}{f_c} \quad (\text{eq. 2.18})$$

$$\tan \phi_o = \frac{D}{(2h_o + 2x y_m \ln \frac{x+1}{x-1})} \quad (2.22)$$

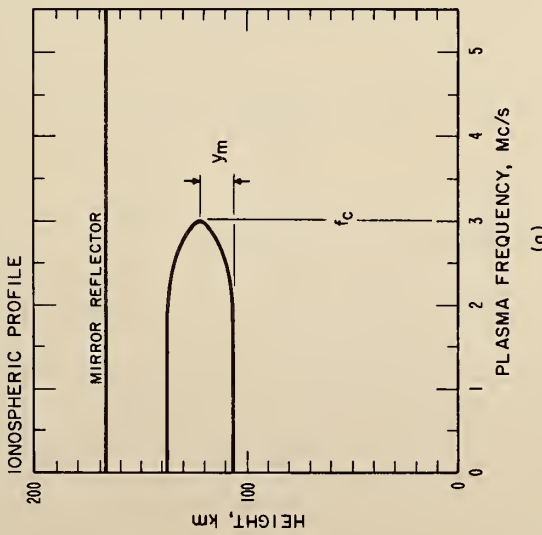
for oblique propagation.

For vertical propagation with specific values of f_c and y_m the coefficients $-f/c \partial P/\partial f_c$ and $-f/c \partial P/\partial y_m$ are shown as functions of frequency in figure 2.3. The dashed curves in this figure show what the behavior would be if Δf were inversely proportional to frequency. For frequencies much greater than the critical frequency of the parabolic layer (i.e., when the parabolic layer can be considered non-deviative) the Doppler shift clearly exhibits an inverse frequency dependence as is predicted by (2.1).

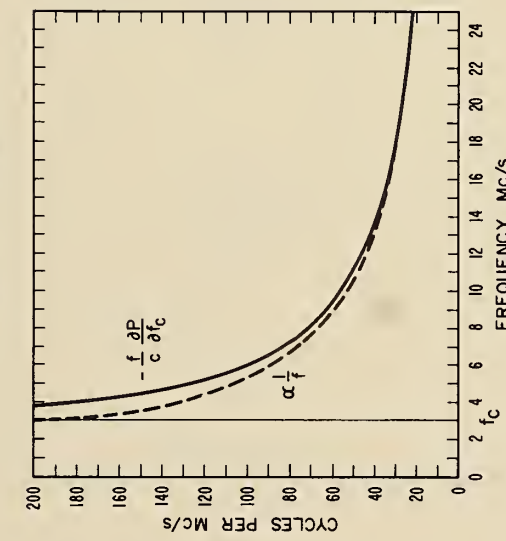
Doppler shift, Δf , for vertical propagation with fixed mirror-like reflection above a changing parabolic E layer

$$f_c = 3 \text{ Mc/s}, y_m = 20 \text{ km}$$

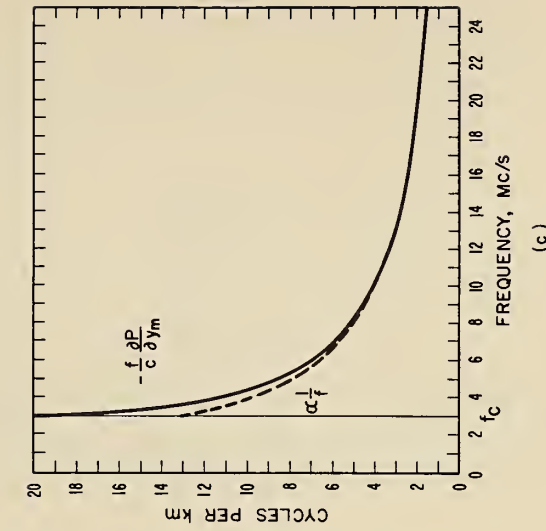
$$\Delta f = -\frac{f}{c} \frac{\partial P}{\partial f_c} \frac{df_c}{dt} - \frac{f}{c} \frac{\partial P}{\partial y_m} \frac{dy_m}{dt}$$



(a)



(b)



(c)

Figure 2.3

Model 3: propagation through one parabolic layer and a valley of changing depth with reflection in a second parabolic layer (figure 2.4a).

For this model

$$\Delta f = - \frac{f}{c} \frac{\partial P}{\partial \rho} \frac{d\rho}{dt} \quad (2.23)$$

where

$$-\frac{f}{c} \frac{\partial P}{\partial \rho} = \frac{2f_E}{c} \frac{h_{MF} - h_{ME} - y_F \sqrt{1 - \left(\frac{f_V}{f_E}\right)^2} - y_E \sqrt{1 - \left(\frac{f_V}{f_E}\right)^2}}{\sqrt{x^2 - 1}} \quad (2.24)$$

$$\rho = \frac{f_V}{f_E} \quad (2.25)$$

$$\frac{d\rho}{dt} = \frac{1}{f_E} \frac{df_V}{dt} \quad (2.26)$$

and

$$x = \frac{f}{f_V} \quad (2.27)$$

for vertical propagation, or

$$x = \frac{f \cos \phi_0}{f_V} \quad (2.28)$$

for oblique propagation. The formula for $\tan \phi_0$ is not given because of its complexity.

The frequency dependence of $-f/c \partial P/\partial \rho$ for $\rho = 0.05$ and 0.95 is shown in figure 2.4b and 2.4c for vertical propagation and figure 2.5b and 2.5c for oblique propagation. The dashed curves vary as $1/f$. For vertical propagation through a changing non-deviative valley ($\rho = 0.05$ or

Doppler shift, Δf , for vertical propagation through a valley of changing depth between parabolic E and F layers

$$f_E = 3 \text{ Mc/s}, f_V = \rho \cdot f_E, f_F = 10 \text{ Mc/s}$$

$$h_{0E} = 100 \text{ km}, h_{mE} = 120 \text{ km}, h_{0F} = 200 \text{ km}, h_{mF} = 300 \text{ km}$$

$$\Delta f = -\frac{f}{c} \frac{\partial P}{\partial \rho} \frac{d\rho}{df}$$

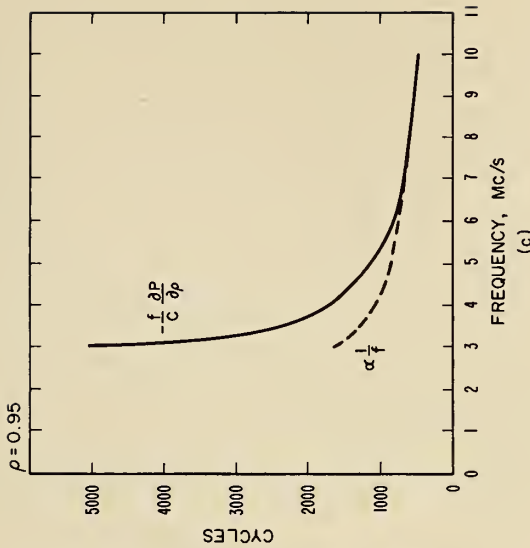
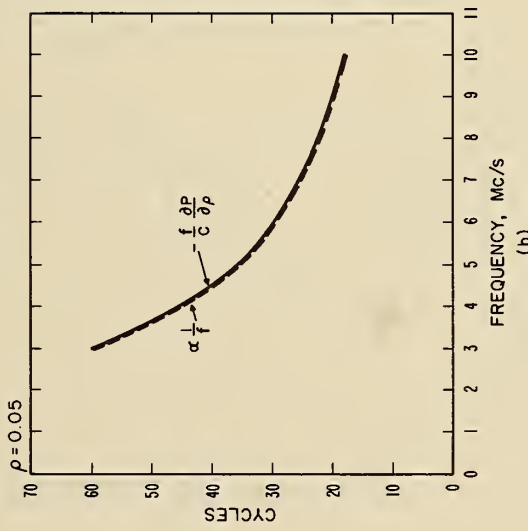
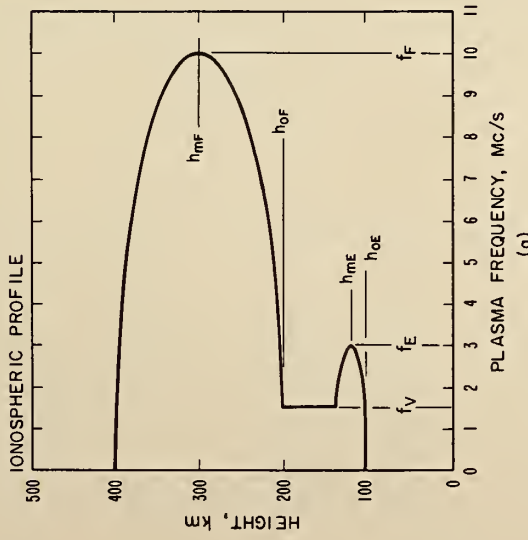


Figure 2.4

Doppler shift, Δf , for oblique propagation through a valley of changing depth between parabolic E and F layers

$$f_E = 3 \text{ Mc/s}, \quad f_V = \rho \cdot f_E, \quad f_F = 10 \text{ Mc/s}$$

$$h_{mE} = 100 \text{ km}, \quad h_{mF} = 120 \text{ km}, \quad h_{oF} = 200 \text{ km}, \quad h_{mF} = 300 \text{ km}, \quad D = 1500 \text{ km}$$

$$\Delta f = -\frac{f}{c} \frac{\partial P}{\partial \rho} \frac{d\rho}{dt}$$

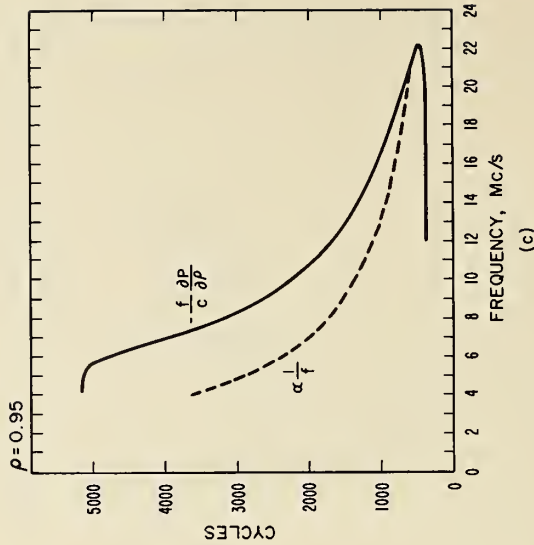
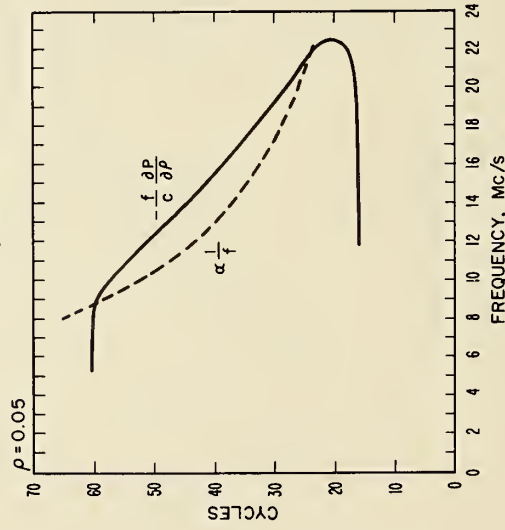
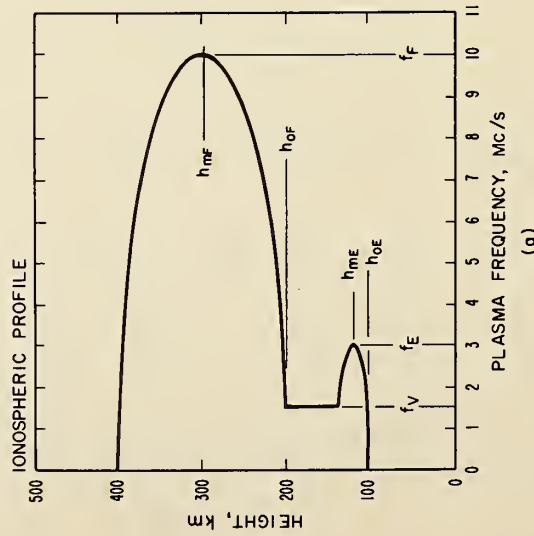


Figure 2.5

for higher frequencies when $\rho = 0.95$) the Doppler shift is inversely proportional to frequency as shown in figure 2.4b and 2.4c. However, at oblique incidence when the valley is non-deviative the Doppler shift does not show a $1/f$ dependence, as shown in figure 2.5b and 2.5c. This is due to the frequency dependence of the angle of incidence ϕ_0 .

As shown in figures 2.2 and 2.5 for high frequencies at oblique incidence ($f > f_c$) two values of the Doppler shift become possible. In each case one possible Doppler shift would be observed on the low-angle ray and the other on the high-angle ray.

2.3. Rate of Change of Electron Density as a Function of Height

Although the methods developed in the preceding section may be useful in some cases, their usefulness is limited by the necessity of approximating the ionospheric profile by parabolic layers. This section presents a method for determining the rate of change of electron density as a function of height using the true height profile directly.

It is shown in Appendix I that the Doppler shift can be written as an integral over the ray path. For vertical propagation

$$\Delta f = -2 \frac{f}{c} \int_0^h \frac{\partial \mu}{\partial t} dz \quad (2.29)$$

Neglecting the earth's magnetic field this becomes

$$\Delta f = \frac{k}{f_c} \int_0^h \frac{\partial N / \partial t dz}{\sqrt{1 - kN/f^2}} \quad (2.30)$$

If the true height profile, $N(h)$ is known and if Δf is known as a function of frequency, then (2.30) can be inverted to give $\partial N/\partial t$ as a function of height. If $N(h)$ is monotonic (2.30) reduces to Abel's equation, the solution of which is

$$\frac{\partial N}{\partial t}(f_N) = \frac{c}{k} \frac{2}{\pi} \frac{df_N}{dh} \frac{d}{df_N} \int_0^{f_N} \frac{f \Delta f df}{\sqrt{f_N^2 - f^2}} \quad (2.31)$$

[Whitaker and Watson, 1952]. If $f_N(h)$ is known, then $\partial N/\partial t(h)$ can be found from $\partial N/\partial t(f_N)$. If a valley exists so that $N(h)$ is not monotonic, then $\partial N/\partial t$ cannot be determined uniquely in or above the valley.

If the magnetic field is not neglected and if it is assumed that the Doppler shift due to changes in the magnetic field itself are negligible, then (2.29) can be solved by numerical methods to give a unique solution for $\partial N/\partial t(h)$ for a monotonic true height profile. A computer program has been written which will perform this calculation if $N(h)$ and $\Delta f(f)$ are known. The method is analogous to that used in true height reduction from ionograms [Budden, 1955]. Unfortunately, the data available for any particular event have not determined the frequency dependence of Δf sufficiently well to warrant application of this technique.

An interesting special case arises when $\partial N/\partial t$ is zero below a height h_o (below the deviative regions) and constant above h_o . The Doppler shift for this case has been calculated in Appendix III. The result, which is exact if the effect of the earth's magnetic field is neglected, but only approximate otherwise, is

$$\Delta f = \frac{k}{f_c} \frac{\partial N}{\partial t} (h' - h_o), \quad (2.32)$$

where h' is the virtual height of reflection for the frequency f .

According to the equivalence theorem for Doppler shifts, (2.32) should also be approximately true for oblique propagation if f is replaced by f_v .

Several of the measurements made at Boulder of the maximum Δf observed during solar flares agree with (2.32). This indicates that these measurements can be explained by $\partial N/\partial t$ that is zero below the E layer and constant with height in the E and F regions. The agreement of the data with (2.32) is illustrated in two ways.

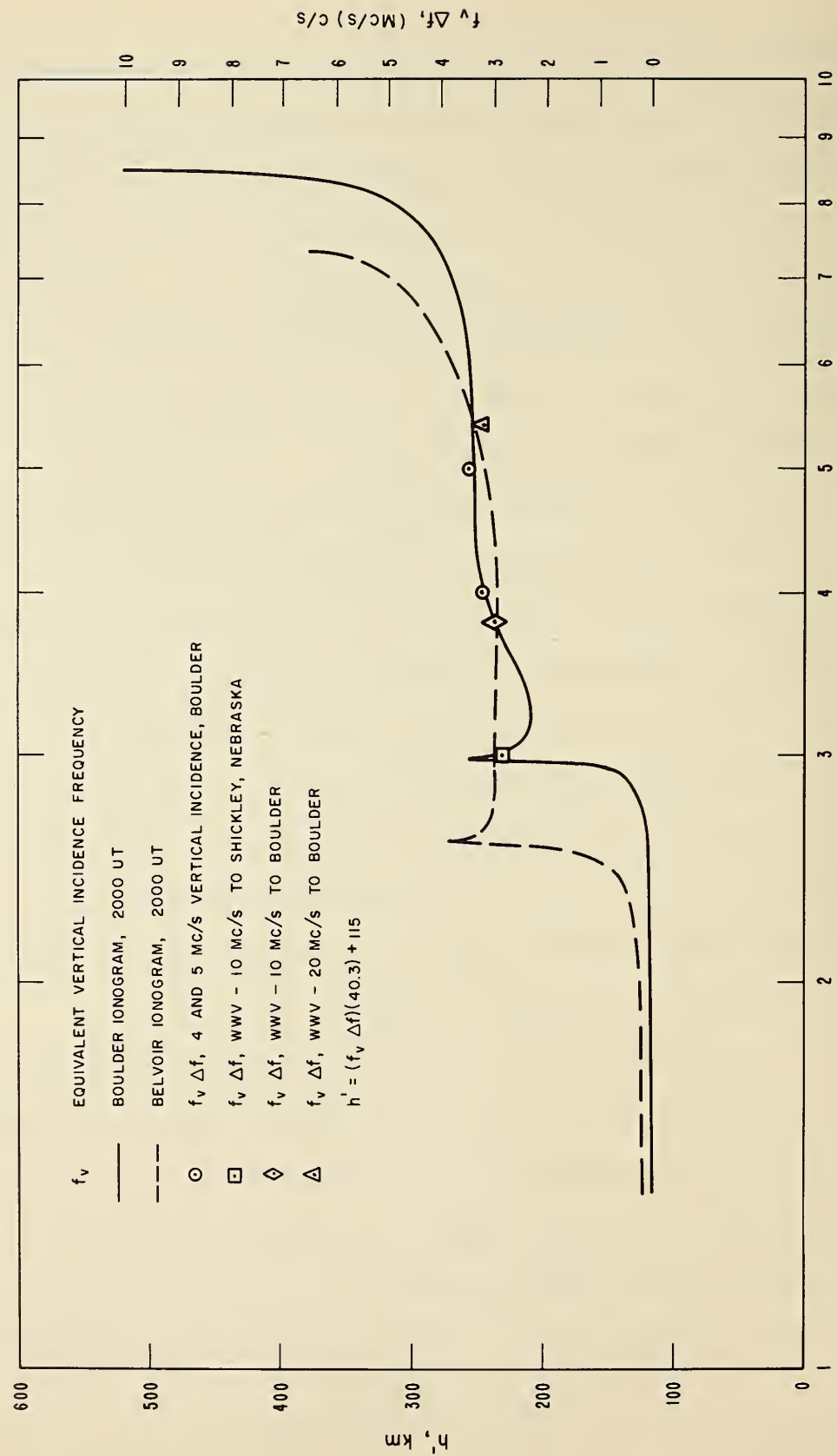
First, (2.32) indicates that a plot of $f\Delta f$ versus f should look approximately like the appropriate ionogram. The agreement is shown for four specific events in figures 2.6, 2.7, 2.8, and 2.9, where plots of $f_v\Delta f$ versus f_v have been superimposed on tracings of the ionograms obtained at the end points of the path shortly before the flares.

The scale used to plot $f_v\Delta f$ was adjusted so that the 4 Mc/s value and one E-layer value (except for 22 November 1961, where, due to lack of E-layer data, h_o was chosen to be at the bottom of the E-layer) would coincide with the Boulder ionogram. The adjustment of the scale in this manner determines h_o and $\partial N/\partial t$ in (2.32).

The data for these four events are given in table 2.1, along with the value of $\partial N/\partial t$ determined. For the oblique paths, the equivalent vertical-incidence frequencies were determined by using transmission curves [Smith, 1939; Davies, 1965] on the ionograms, and the observed frequency deviations have been divided by the number of hops.

Second, if measurements are made on two frequencies (4 and 5 Mc/s in

Comparison of $f_v \Delta f$ vs f_v with ionogram for SFD
at 2014 UT on November 22, 1961



Comparison of $f_v \Delta f$ vs f_v with ionogram for SFD
at 2252 UT on April 17, 1962

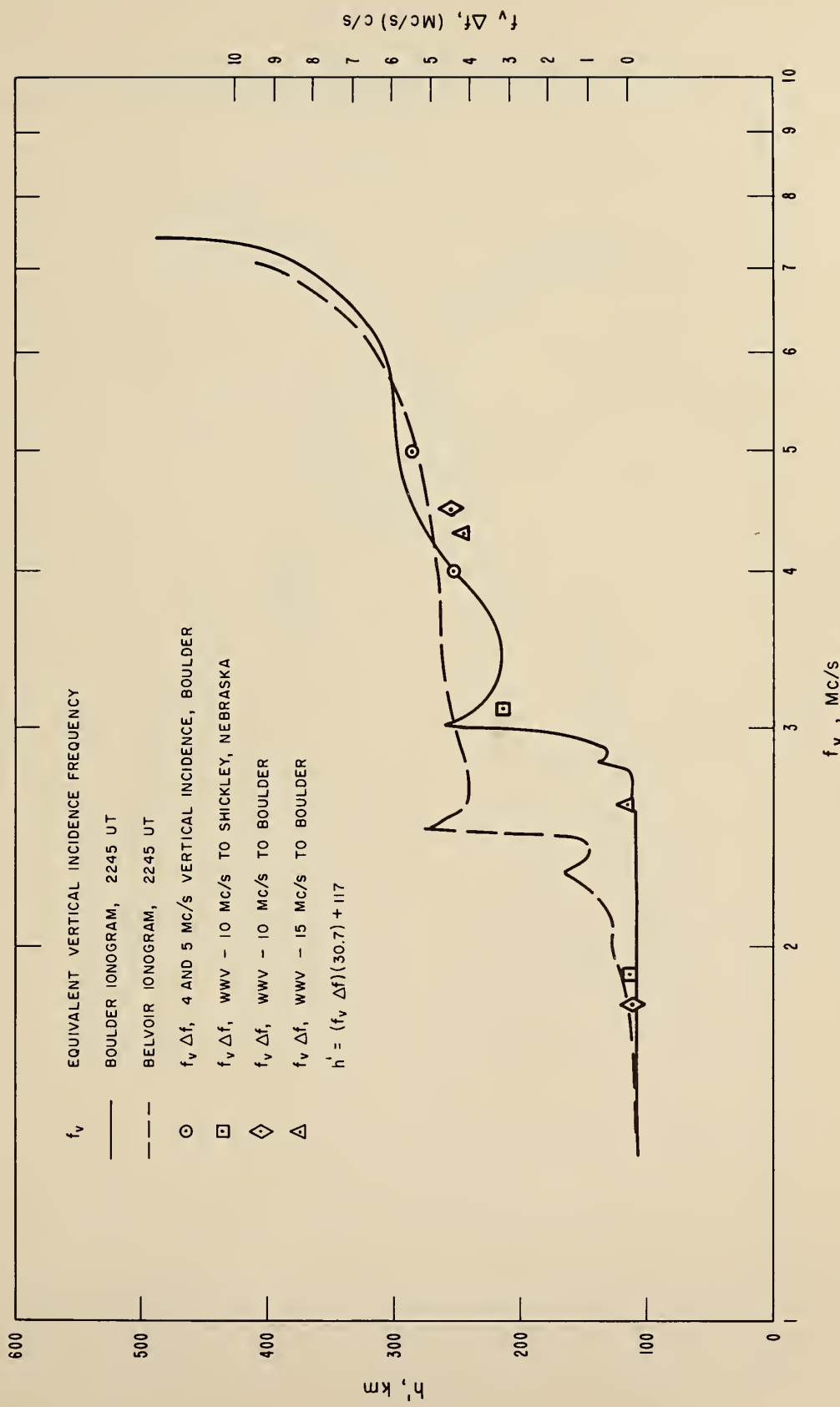


Figure 2.7

Comparison of $f_v \Delta f$ vs f_v with ionogram for SFD at 1935 UT on April 19, 1962

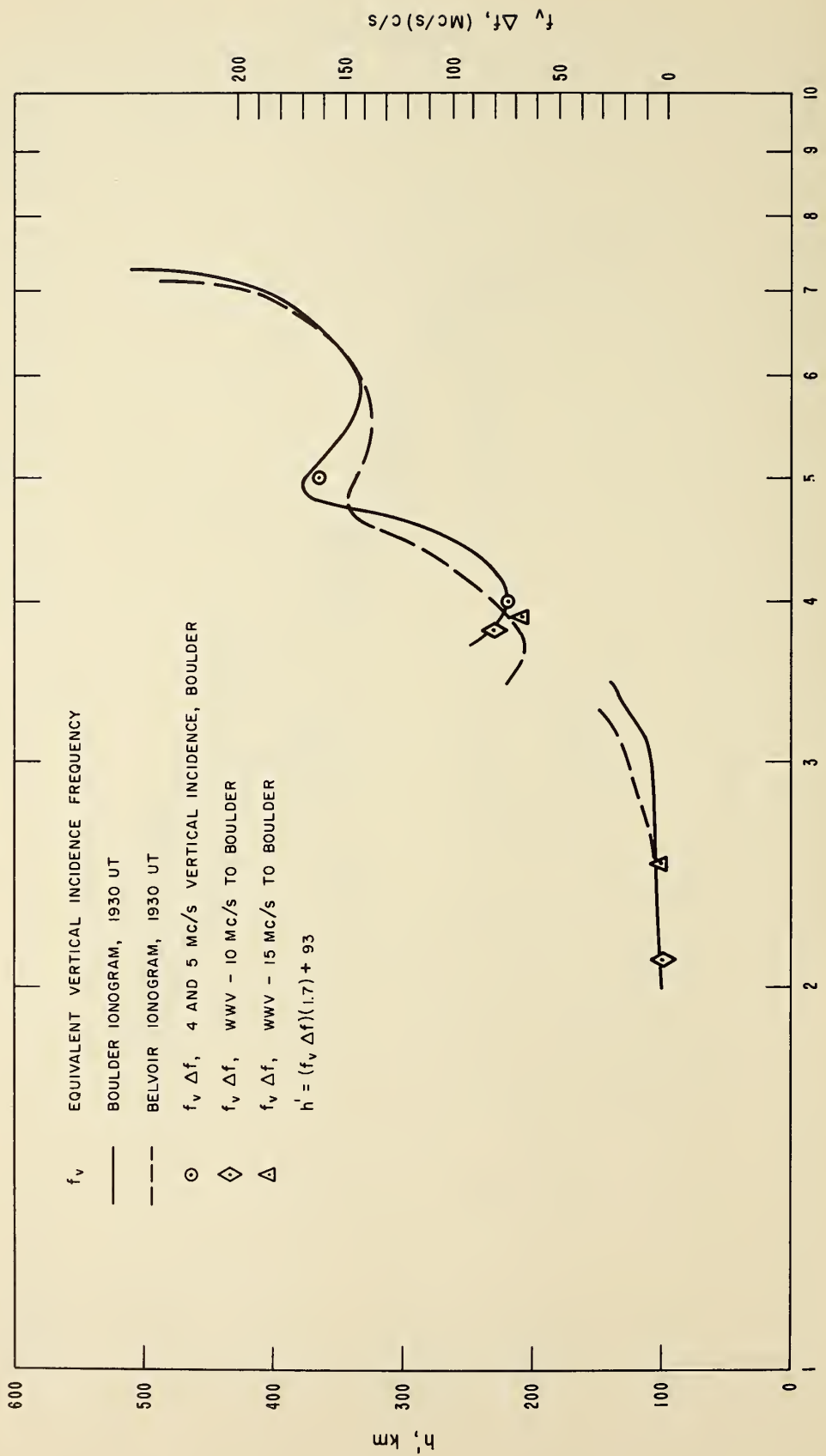


Figure 2.8

Comparison of $f_v \Delta f$ vs f_v with ionogram for SFD
at 1959 UT on April 20, 1962

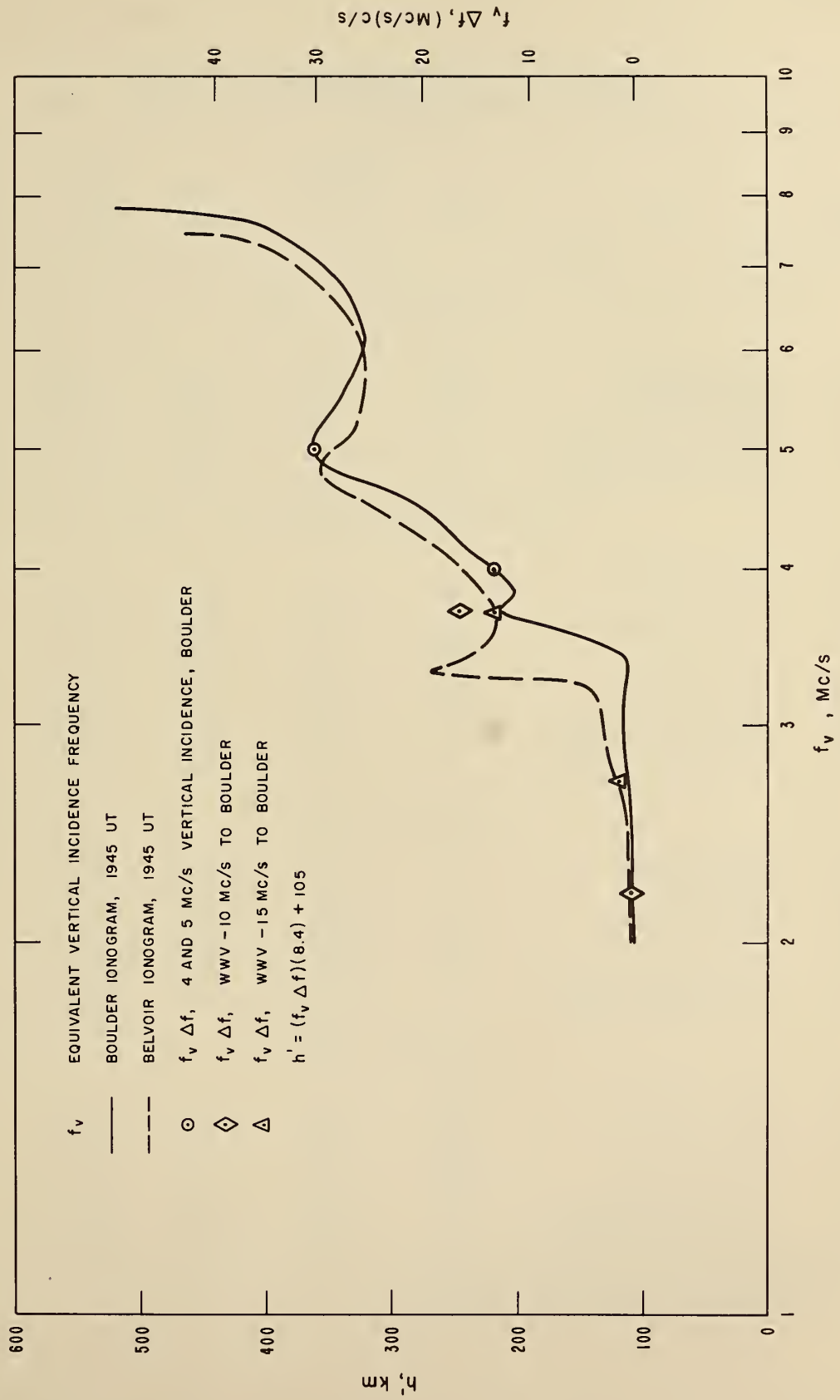


Figure 2.9

Table 2.1

Tabulation of data for flare effects of
November 22, 1961, and April 17, 19, and 20, 1962

f Mc/s	Path	Mode	Maximum Observed Δf c/s	f_v Mc/s	$f_v \Delta f^*$ Mc/s · c/s	$\partial N / \partial t$ cm ⁻³ sec ⁻¹
November 22, 1961						
20	WWV-Boulder	F	0.6	5.4	3.2	92
10	WWV-Boulder	F-F	1.6	3.8	3.0	
10	WWV-Shickley	F	0.95	3.0	2.8	
5	Vert inc Boulder	F	0.7	5.0	3.5	
4	Vert inc Boulder	F	0.8	4.0	3.2	
April 17, 1962						
15	WWV-Boulder	E	0.0	2.6	0.0	120
		F	1.0	4.3	4.3	
10	WWV-Boulder	E	0.0	1.8	0.0	
		F-F	1.9	4.7	4.5	
10	WWV-Shickley	E	0.0	1.9	0.0	
		F	1.0	3.1	3.1	
5	Vert inc Boulder	F	1.1	5.0	5.5	
4	Vert inc Boulder	F	1.1	4.0	4.4	
April 19, 1962						
15	WWV-Boulder	E	2.0	2.5	5.0	2200
		F	18.0	3.9	70.2	
10	WWV-Boulder	E	2.0	2.1	4.2	
		F-F	43.0	3.8	81.7	
5	Vert inc Boulder	F	32.0	5.0	160.0	
4	Vert inc Boulder	F	19.0	4.0	76.0	
April 20, 1962						
15	WWV-Boulder	E-E	1.2	2.7	1.6	450
		F	3.8	3.7	14.0	
10	WWV-Boulder	E-E	0.7	2.2	0.8	
		F-F	9.0	3.7	16.7	
5	Vert inc Boulder	F	6.0	5.0	30.0	
4	Vert inc Boulder	F	3.4	4.0	13.6	

* Δf corrected for number of hops

this case) at vertical incidence, then (2.32) predicts that

$$\Delta f_5 = \frac{4}{5} \frac{h'_5 - h_0}{h'_4 - h_0} \Delta f_4 \quad (2.33)$$

where Δf_4 , Δf_5 , h'_4 , and h'_5 are the frequency deviations and virtual heights of reflection for 4 and 5 Mc/s. The agreement of the data with (2.33) is shown in figure 2.10b. In each case h_0 was taken to be the bottom of the E layer. Figure 2.10a shows Δf_4 versus Δf_5 .

The preceding analyses show that a $\partial N/\partial t$ which is zero below the E layer and constant in the E and F regions will explain the maximum Doppler shifts measured during several solar flares.

Relationship between maximum frequency deviations observed on
4 and 5 Mc/s at vertical incidence, Boulder, Colorado

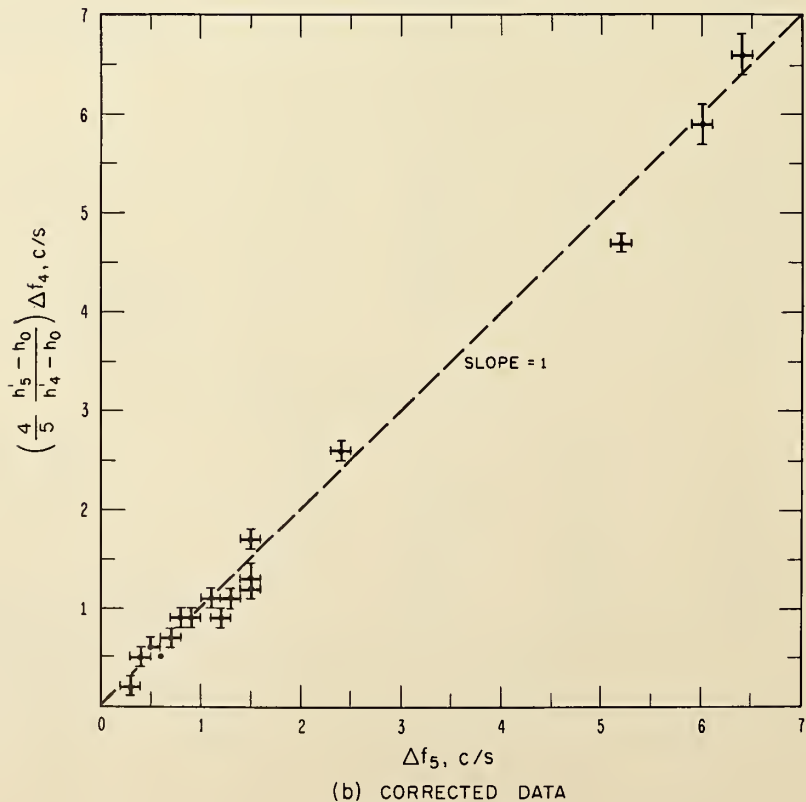
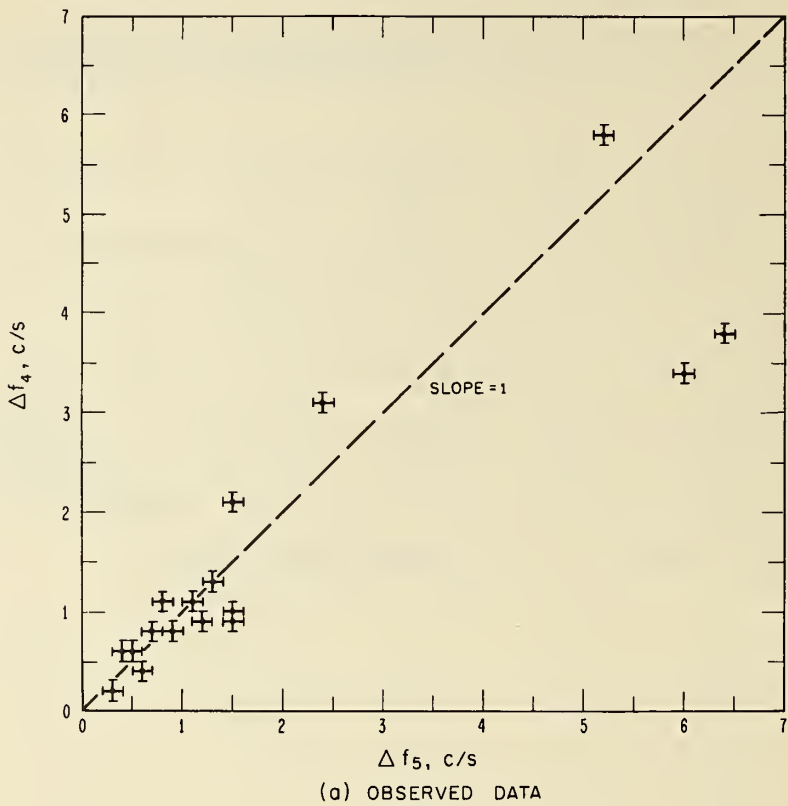


Figure 2.10

3. Solar Flare Observations with the Doppler Technique

The following discussion of flare effects deals with the sudden frequency deviations observed between October 1, 1960 and December 31, 1962 on the following frequencies and propagation paths: (1) WWV-10, -15 and -20 Mc/s, Beltsville, Maryland to Boulder, Colorado; (2) WWV-10 Mc/s, Beltsville, Maryland to Shickley, Nebraska; (3) 4.000 and 5.054 Mc/s, Sunset, Colorado to Boulder, Colorado. Table 1.1 gives the periods during which these paths and frequencies were in use.

The analysis in this section has been restricted to those sudden frequency deviations which could be correlated with solar flares reported in the CRPL-F Series, Part B, Solar-Geophysical Data. A list of all sudden frequency deviations observed between October 1, 1960 and December 31, 1962, whether they could be correlated with a known solar flare or not, is given in Appendix IV.

The shape, duration, and magnitude of sudden frequency deviations vary considerably from flare to flare. However, the general characteristics of an SFD, as illustrated in figure 4.1, are a rapid positive frequency deviation followed by a smaller negative frequency shift and a gradual recovery to the pre-flare conditions. The negative frequency deviation is sometimes absent. The maximum frequency deviation varies from a few tenths of a cycle per second to tens of cycles per second, and the duration may vary from less than a minute to ten minutes or more. The specific events, to be discussed in Section 4, illustrate the variability of the sudden frequency deviations observed.

3.1. Percentage of Solar Flares Detected by Doppler Technique

The percentages of the reported flares which can be correlated with sudden frequency deviations are given in table 3.1 as a function of flare importance. In computing these percentages, and all the percentages to follow in this section, care was taken to exclude any reported flares which occurred during periods of unusable records for the WWV to Boulder path. Also, only flares reported during conditions of ground sunlight at the midpoint of the WWV to Boulder path were included.

Table 3.1

Percentage of flares reported from October 1, 1960, to December 31, 1962, which were accompanied by SFD's

Flare H _α Importance	Number of Flares Reported	Percentage with SFD
1-	2994	10
1	648	21
2	55	49
3	10	80
1,2,3	713	24
All	3707	13

Although no simple relationship exists between the optical (H_α) importance of a flare and its associated effect on the ionosphere, it can be stated that the greater the optical importance of a flare the greater the probability that it will cause a sudden frequency deviation.

These percentages which have been calculated as a function of flare

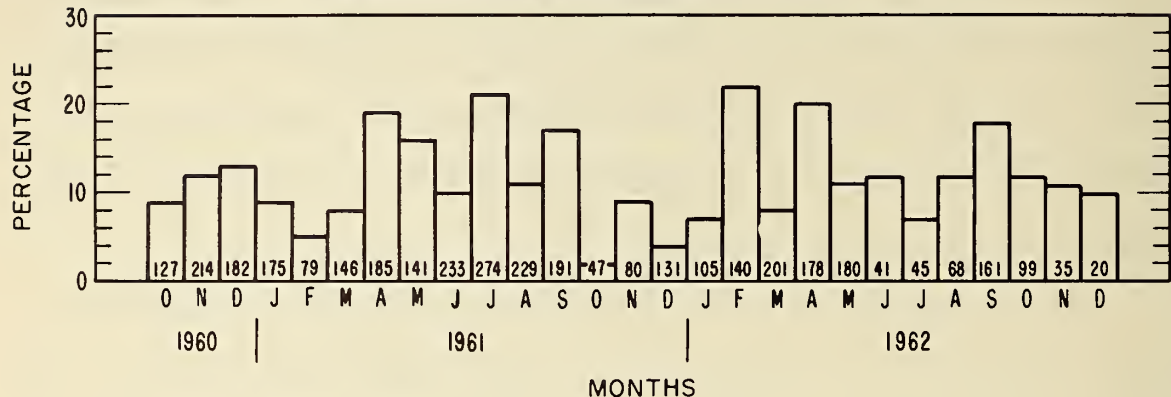
importance are naturally dependent upon the importance assigned to each flare. Unfortunately there is often disagreement among various observatories as to the importance of a given flare. Consequently, in many cases the flare importance used is somewhat arbitrary. In the present analysis, whenever the importance of a flare could not be assigned by a consideration of the most frequently reported importance and/or the reported observing conditions at each observatory, preference has usually been given to the smaller reported importance.

The percentages of the flares which were accompanied by sudden frequency deviations, for each month from October 1960 through December 1962, are shown in figure 3.1a. The number at the bottom of each column gives the number of flares upon which the percentage is based. The variations in the mean solar flux at 2800 Mc/s and the mean Zurich sunspot number for the same period are shown in figures 3.1b and 3.1c respectively. The percentage of flares detected shows neither a systematic seasonal dependence nor any well-defined variation with the mean level of solar activity. The lack of a systematic seasonal variation in the percentage of the flares detected is shown more clearly by figure 3.2 in which all data for a given month are combined.

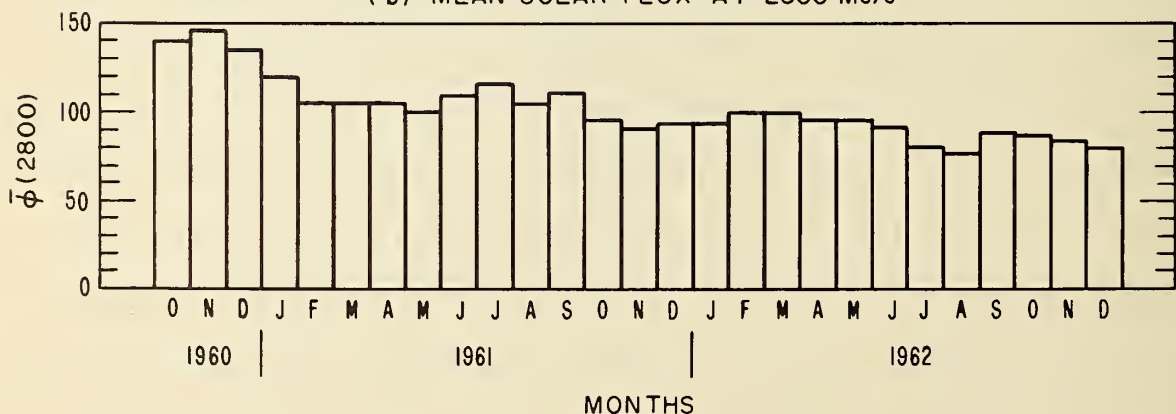
Figure 3.3 shows the percentage of the flares accompanied by sudden frequency deviations as a function of the time of day at the midpoint of the WWV to Boulder path. A diurnal variation is evident in 3.3a, 3.3c, and 3.3d. The lack of diurnal variation in the data for flares of optical importances 2 and 3 can be attributed to the small number of such flares during the period. Again the number at the bottom of each column

VARIATIONS OF THE PERCENTAGE OF REPORTED SOLAR FLARES
 DETECTED, MEAN SOLAR FLUX AT 2800 Mc/s,
 AND MEAN ZURICH SUNSPOT NUMBER DURING THE PERIOD
 OCTOBER 1, 1960 THROUGH DECEMBER 31, 1962

(a) PERCENTAGE OF REPORTED FLARES DETECTED



(b) MEAN SOLAR FLUX AT 2800 Mc/s



(c) MEAN ZURICH SUNSPOT NUMBER

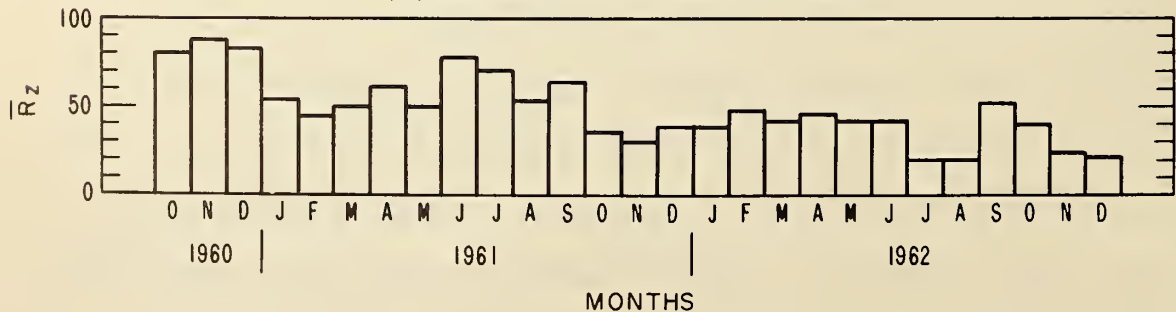


Figure 3.1

PERCENTAGE OF REPORTED SOLAR FLARES
DETECTED BY THE DOPPLER TECHNIQUE AS A
FUNCTION OF MONTH
OCTOBER 1, 1960 THROUGH DECEMBER 31, 1962

(a) ALL FLARES

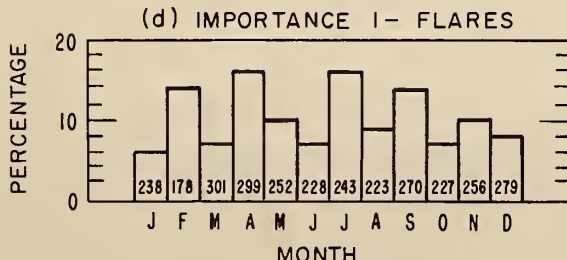
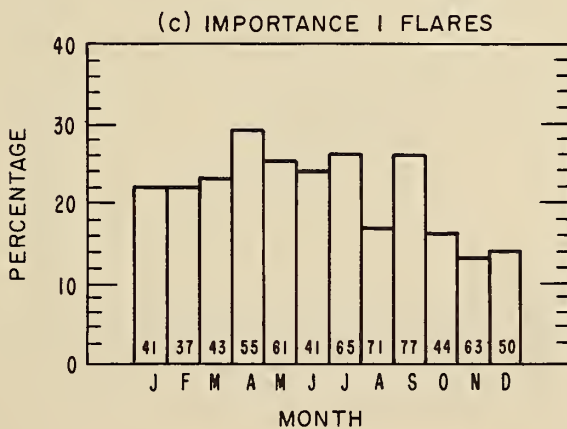
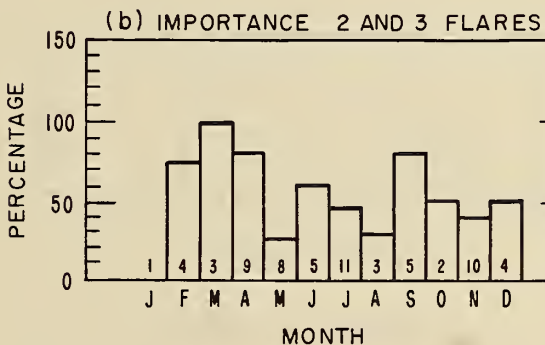
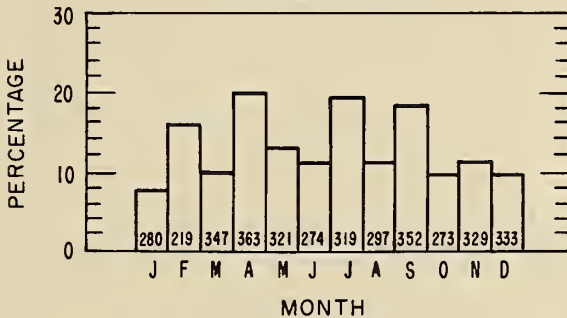


Figure 3.2

PERCENTAGE OF REPORTED SOLAR FLARES
DETECTED BY THE DOPPLER TECHNIQUE AS A
FUNCTION OF TIME OF DAY
OCTOBER 1, 1960 THROUGH DECEMBER 31, 1962

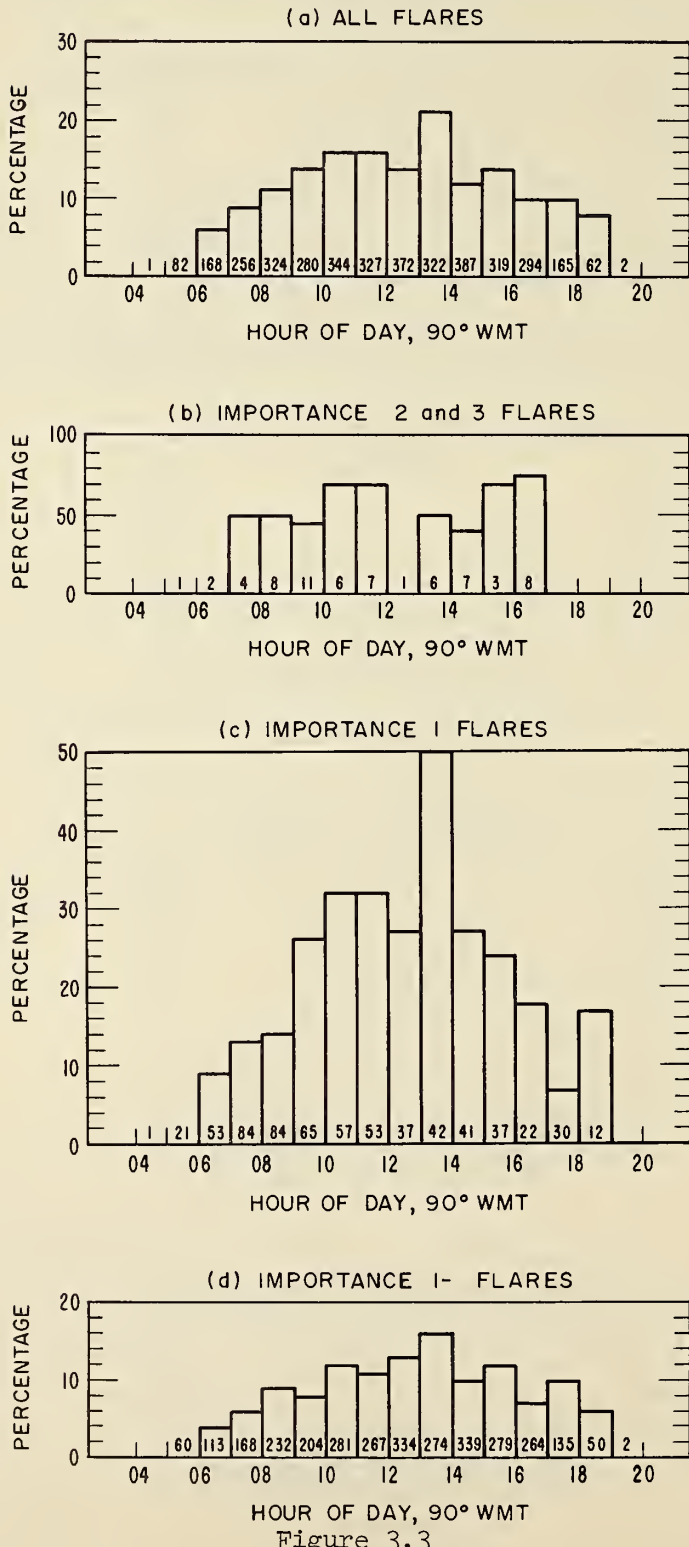


Figure 3.3

gives the number of flares on which the percentage is based.

The solar-zenith-angle dependence of the percentage of flares detected is shown explicitly in figure 3.4. In this figure the percentage of flares detected is shown as a function of the solar zenith angle at the midpoint of the WWV to Boulder path. In figures 3.4a and 3.4d there is a peak for zenith angles of 30 to 40 degrees. The decrease in the percentage detected as the zenith angle increases is to be expected; however, the decrease for zenith angles less than 30 degrees is surprising and may be due to sampling errors.

In summary, the data presented in this section indicate that the percentage of solar flares which are accompanied by sudden frequency deviations tends to increase with increasing optical importance, shows no pronounced seasonal variation, but does exhibit a marked diurnal and solar zenith angle variation with a maximum near local noon. A final conclusion regarding the apparent lack of correlation between the percentage of flares detected and the general level of solar activity will require observation over a greater portion of the solar activity cycle.

3.2. Duration, Rise Time, and Delay Time of Sudden Frequency Deviations

The general time characteristics of sudden frequency deviations are presented in this section. The number of sudden frequency deviations with a given duration is shown in figure 3.5. The duration has been taken to be the time elapsed between the beginning of the positive frequency deviation and the return to the preflare conditions. Often the duration defined in this way cannot be measured precisely due to the

PERCENTAGE OF REPORTED SOLAR FLARES DETECTED
BY THE DOPPLER TECHNIQUE AS A FUNCTION
OF SOLAR ZENITH ANGLE AT MIDPOINT OF
WWV TO BOULDER PATH,
OCTOBER 1, 1960 THROUGH DECEMBER 31, 1962

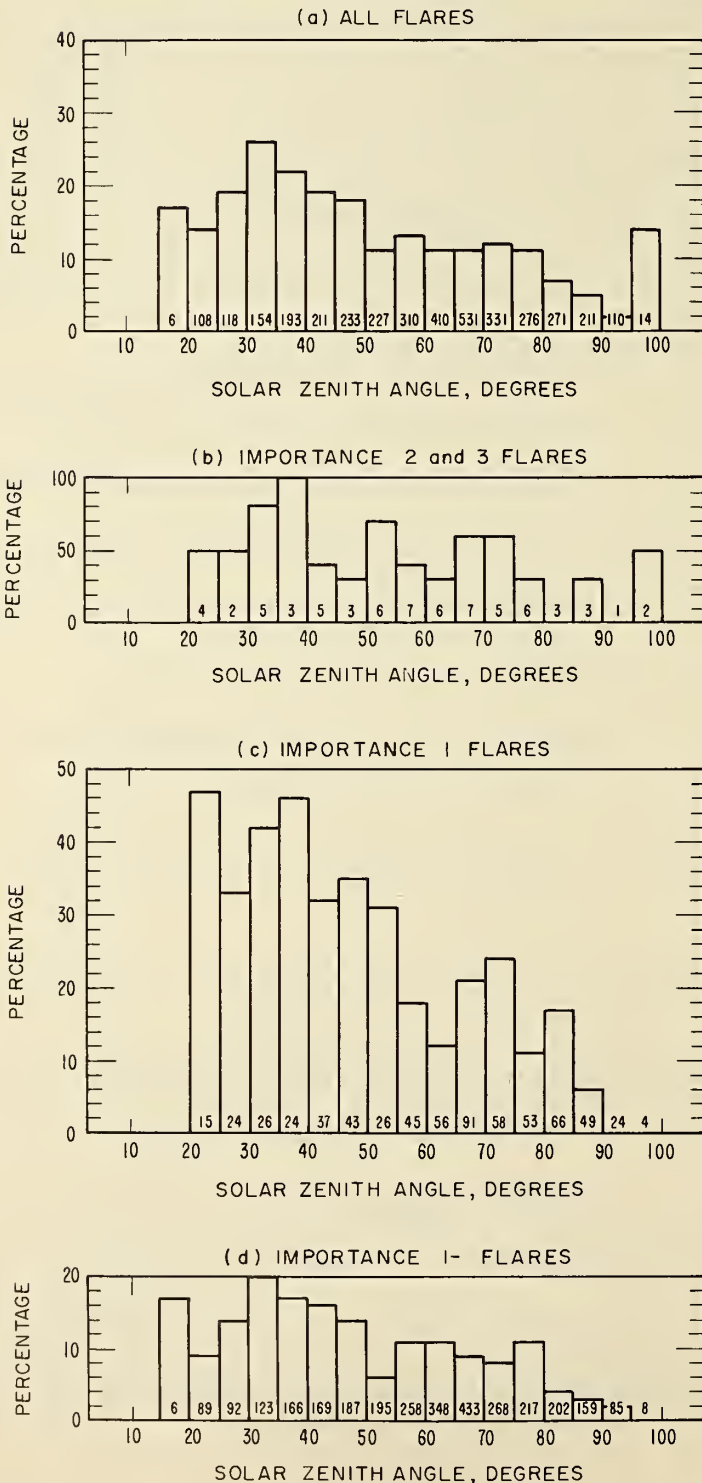


Figure 3.4

DURATIONS OF SUDDEN FREQUENCY DEVIATIONS
 OBSERVED FROM
 OCTOBER 1, 1960 TO DECEMBER 31, 1962
 $\text{DURATION} = t_{\text{end}} - t_{\text{beg}}$

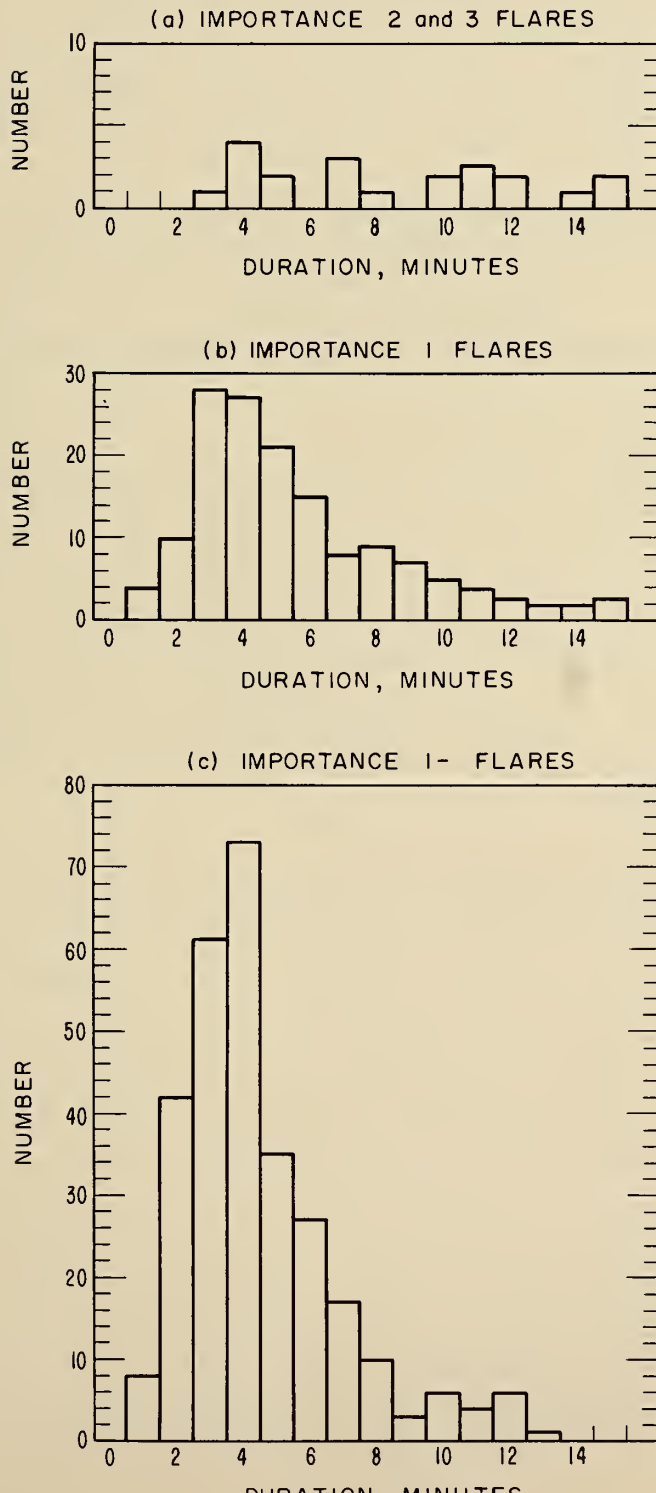


Figure 3.5

difficulty in determining the exact time at which the flare-related frequency deviation ends; however, figure 3.5 does serve to give a general idea of the durations of the flare effects observed by the Doppler technique. The observed durations range from one minute to more than fifteen minutes with the most common durations being from two to five minutes.

Figure 3.6 shows that the most common "rise time", the time from the beginning of the sudden frequency deviation to the maximum positive deviation, is one or two minutes. Very few sudden frequency deviations have rise times greater than three minutes.

The time relationship between the maximum positive frequency deviations of sudden frequency deviations and the maximum phase of the corresponding solar flares is shown in figure 3.7. The maxima of most sudden frequency deviations occur one to four minutes before the flare maxima. In very few cases does the maximum frequency deviation occur after the maximum of the solar flare.

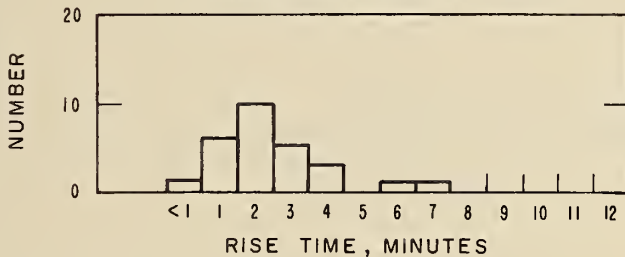
3.3. Path Length Dependence of Frequency Deviations

Figure 3.8 shows the solar flare induced frequency deviations of WWV-10 Mc/s received at Shickley, Nebraska (1780 km), plotted against those of WWV-10 Mc/s received at Boulder, Colorado (2400 km). The slope of the broken line is given by the ratio of the ground path lengths. This figure indicates that the frequency deviations for a fixed frequency vary directly with the path length for paths in the neighborhood of 2000 km. Kanellakos, Chan, and Villard [1962] have found that the flare induced frequency deviations on 15 and 18 Mc/s vary approximately directly

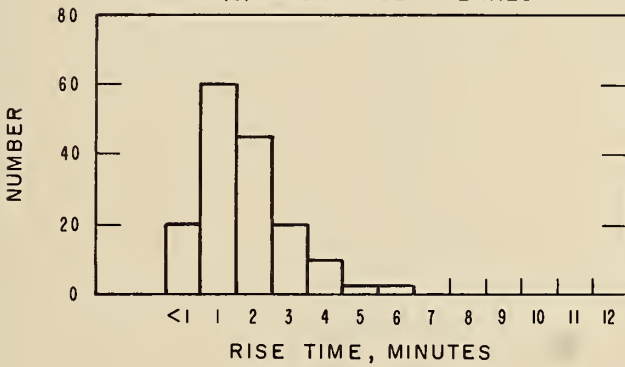
RISE TIMES OF SUDDEN FREQUENCY DEVIATIONS
 OBSERVED FROM OCTOBER 1, 1960
 TO DECEMBER 31, 1962

$$\text{RISE TIME} = t_{\max} - t_{\text{beg}}$$

(a) IMPORTANCE 2 AND 3 FLARES



(b) IMPORTANCE 1 FLARES



(c) IMPORTANCE I- FLARES

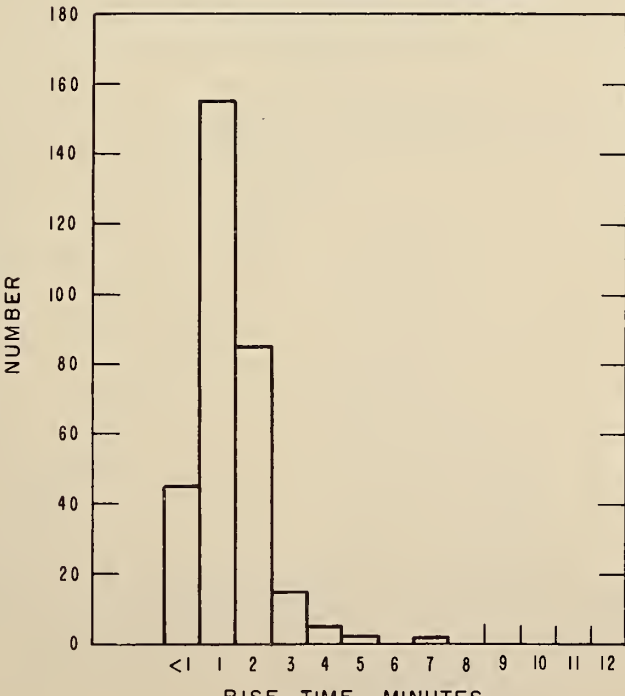


Figure 3.6

TIME DIFFERENCE, ΔT_{\max} , BETWEEN MAXIMUM POSITIVE FREQUENCY DEVIATION AND MAXIMUM PHASE OF SOLAR FLARE
 OCTOBER 1, 1960 THROUGH DECEMBER 31, 1962
 $\Delta T_{\max} = t_{\max} (\text{SFD}) - t_{\max} (\text{FLARE})$

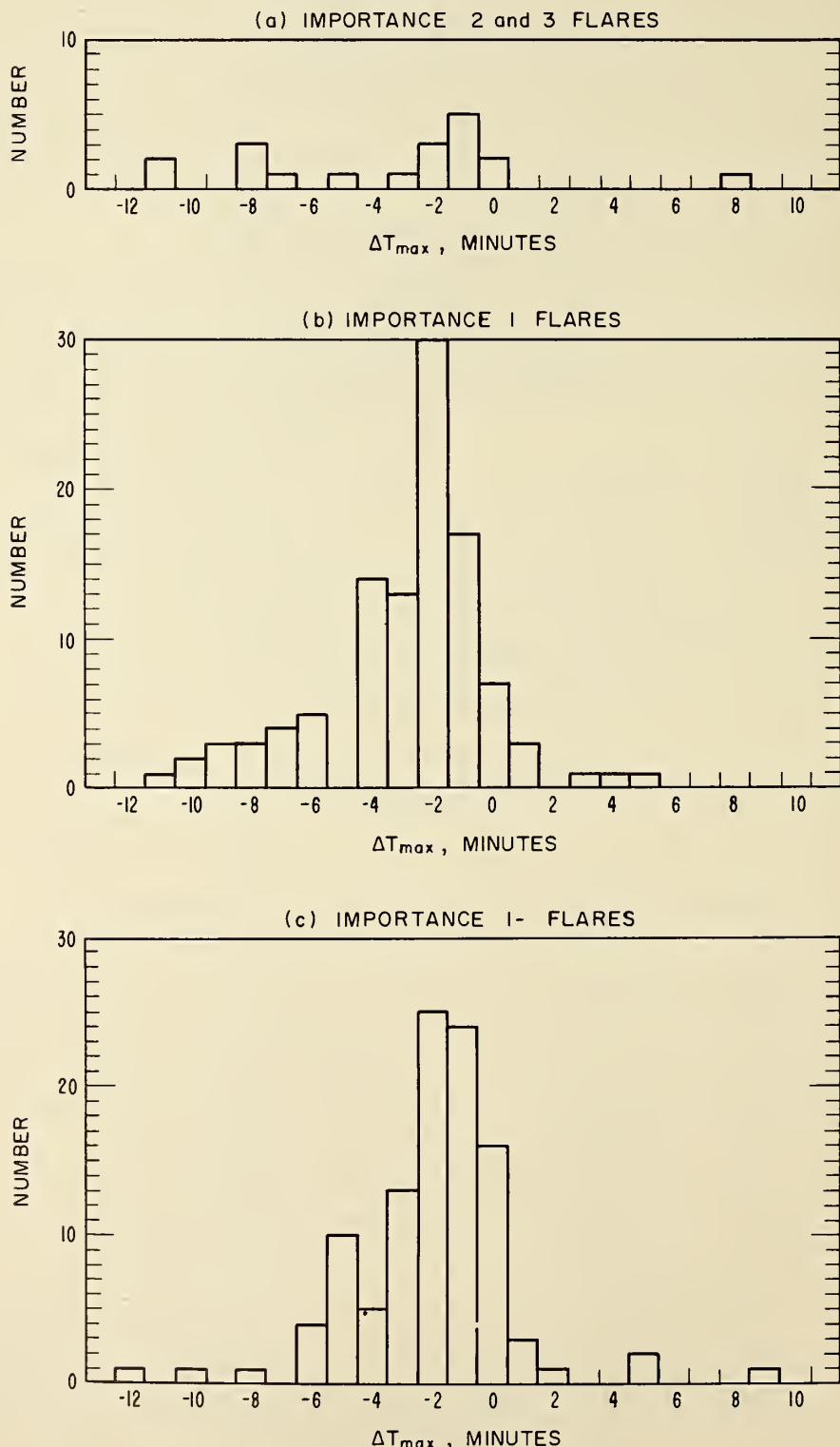


Figure 3.7

FREQUENCY DEVIATION OF WWV-10 Mc/s OBSERVED AT
SHICKLEY, NEBRASKA (1780 km) VERSUS THAT OBSERVED AT
BOULDER, COLORADO (2400 km)

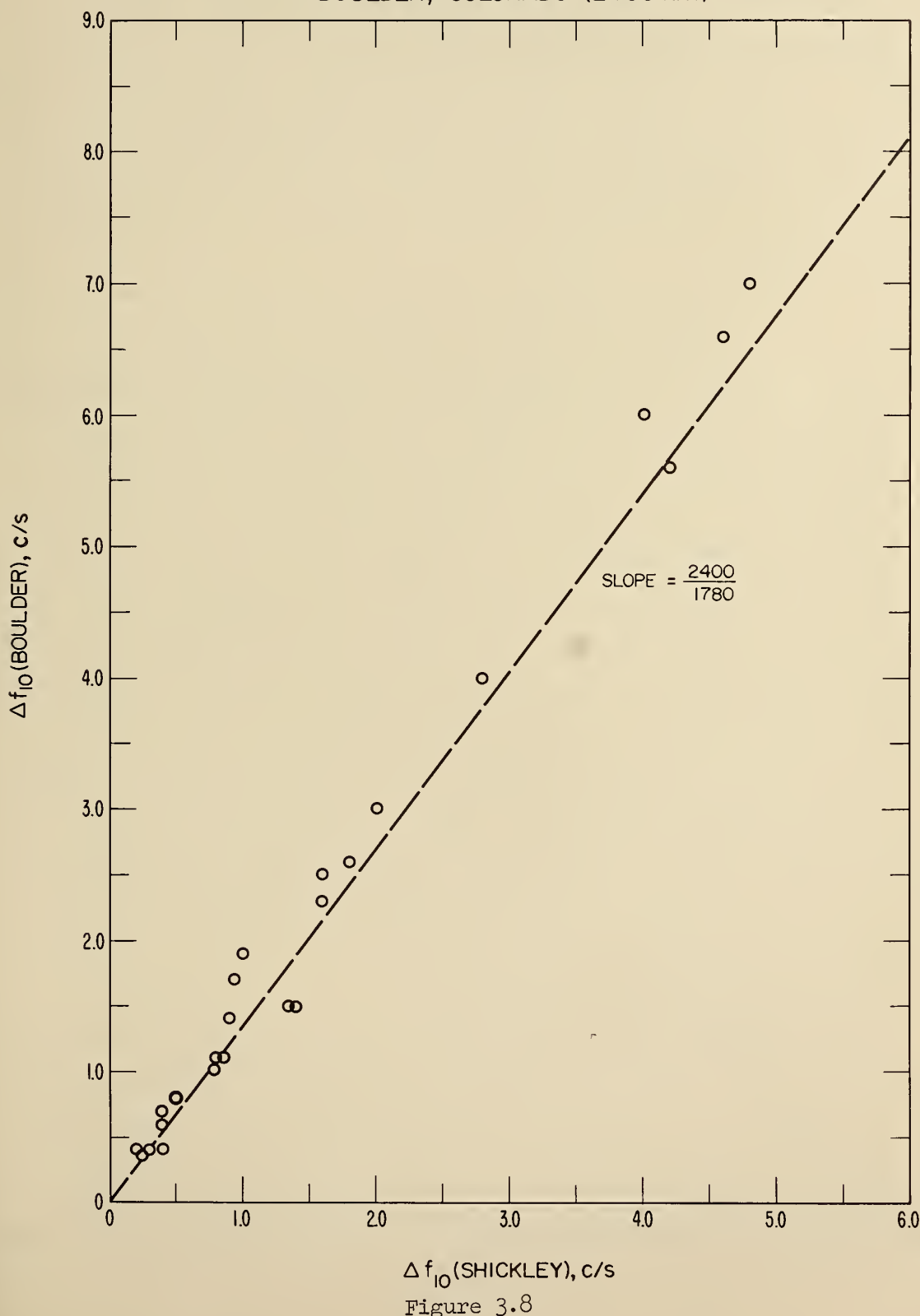


Figure 3.8

with path length for paths of 2450 and 5650 km. Therefore, it appears that for oblique paths, the effect of solar flares on the frequency of ionospherically propagated signals varies directly with the ground path length. It is to be expected that this direct path length dependence will hold only for paths which are of such length that the ratio of the ground path lengths is approximately the same as the ratio of the path lengths in the ionosphere.

3.4. Frequency Dependence of Frequency Deviations

Figure 3.9 shows the maximum positive frequency deviation observed on WWV-20 Mc/s versus that observed on WWV-10 Mc/s, both frequencies being received at Boulder (2400 km); similarly, figure 3.10 shows the relationship between the deviations observed on WWV-15 and WWV-10 Mc/s. In each case the dashed line indicates the behavior expected if the frequency deviation were inversely proportional to the operating frequency. The deviations observed on these oblique paths tend to vary inversely with the operating frequency, although there are some significant departures from an inverse dependence. These two figures show only the observed data. Due to the difficulty in determining the propagation modes for this long path, the data have not been analyzed in terms of equivalent vertical-incidence frequency.

The relationship between the maximum positive frequency deviations observed on 4 and 5 Mc/s at near vertical incidence at Boulder has been shown in figure 2.10. A plot of the observed data, figure 2.10a, shows no systematic frequency dependence. However, as shown by figure 2.10b, the frequency deviations agree well with the behavior predicted by (2.33).

FREQUENCY DEVIATION OF WWV - 10 MC/S
 VERSUS THAT OF WWV - 20 MC/S,
 BOTH OBSERVED AT BOULDER, COLORADO (2400 km)

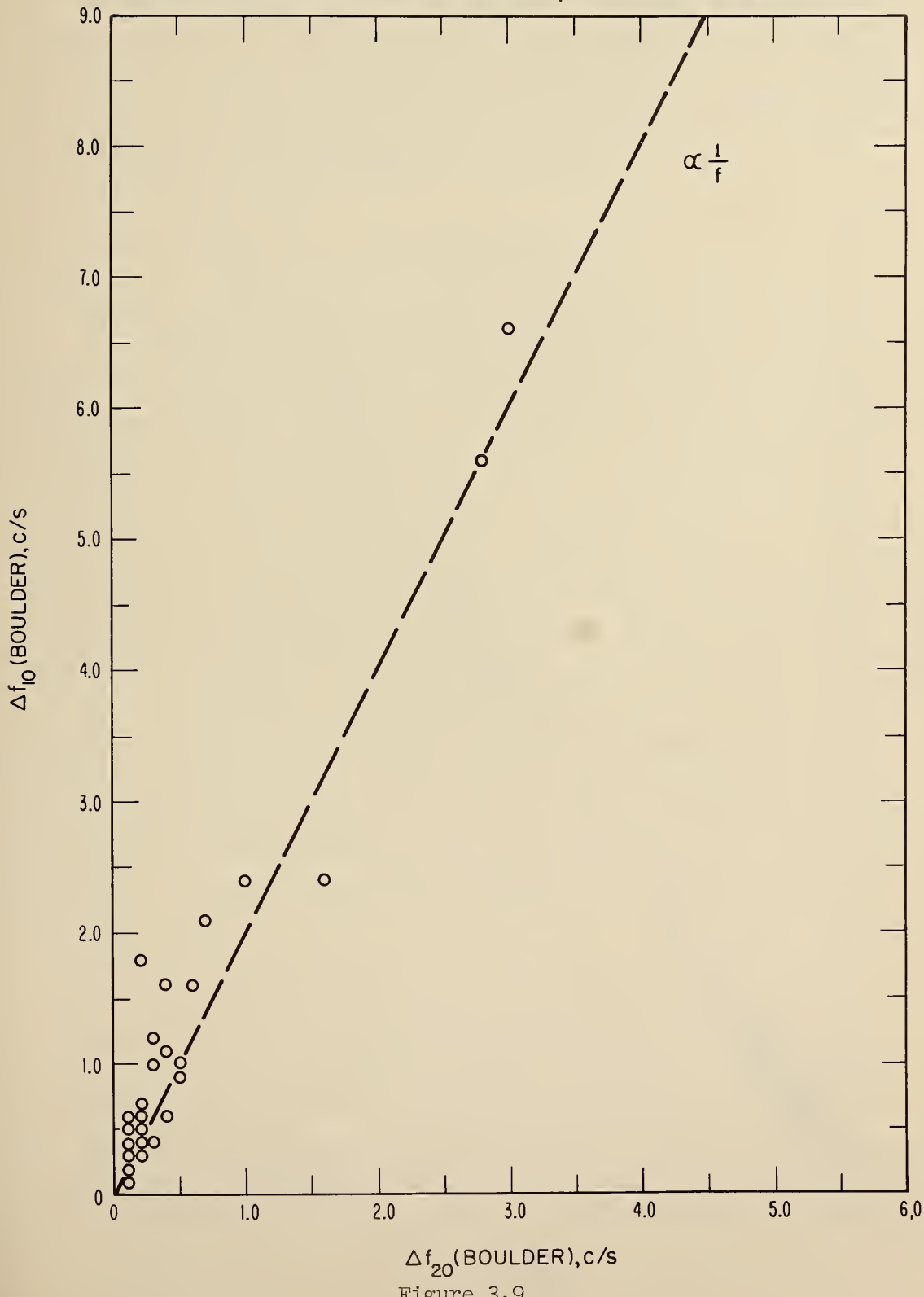


Figure 3.9

FREQUENCY DEVIATION OF WWV - 10 MC/S
VERSUS THAT OF WWV - 15 MC/S,
BOTH OBSERVED AT BOULDER, COLORADO (2400 km)

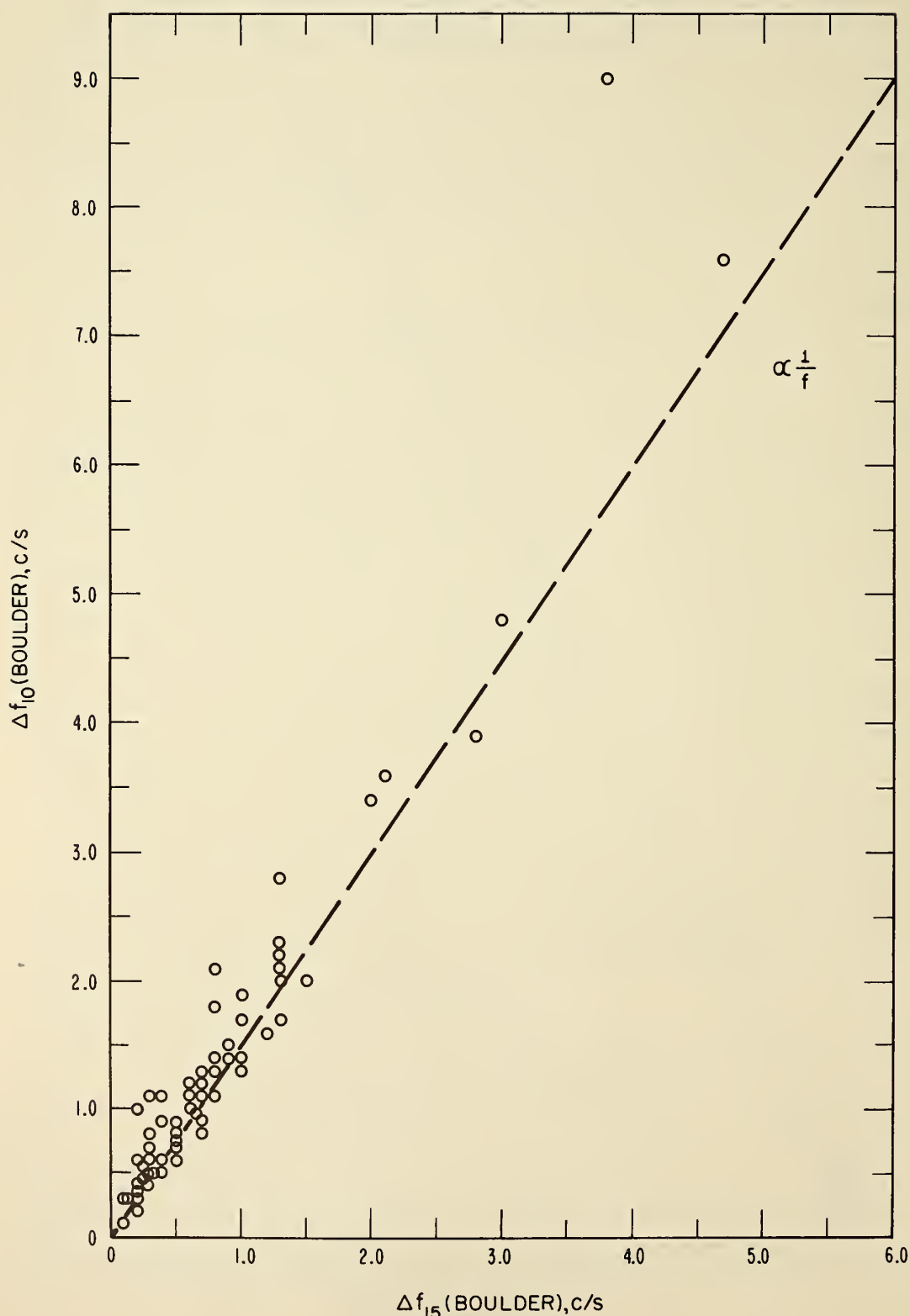


Figure 3.10

4. Selected Events Detected by the Doppler Technique

In this section are included examples of the events detected by the Doppler technique. The types of frequency deviation illustrated include those associated with solar flares, with geomagnetic sudden commencements, and with certain other geomagnetic variations.

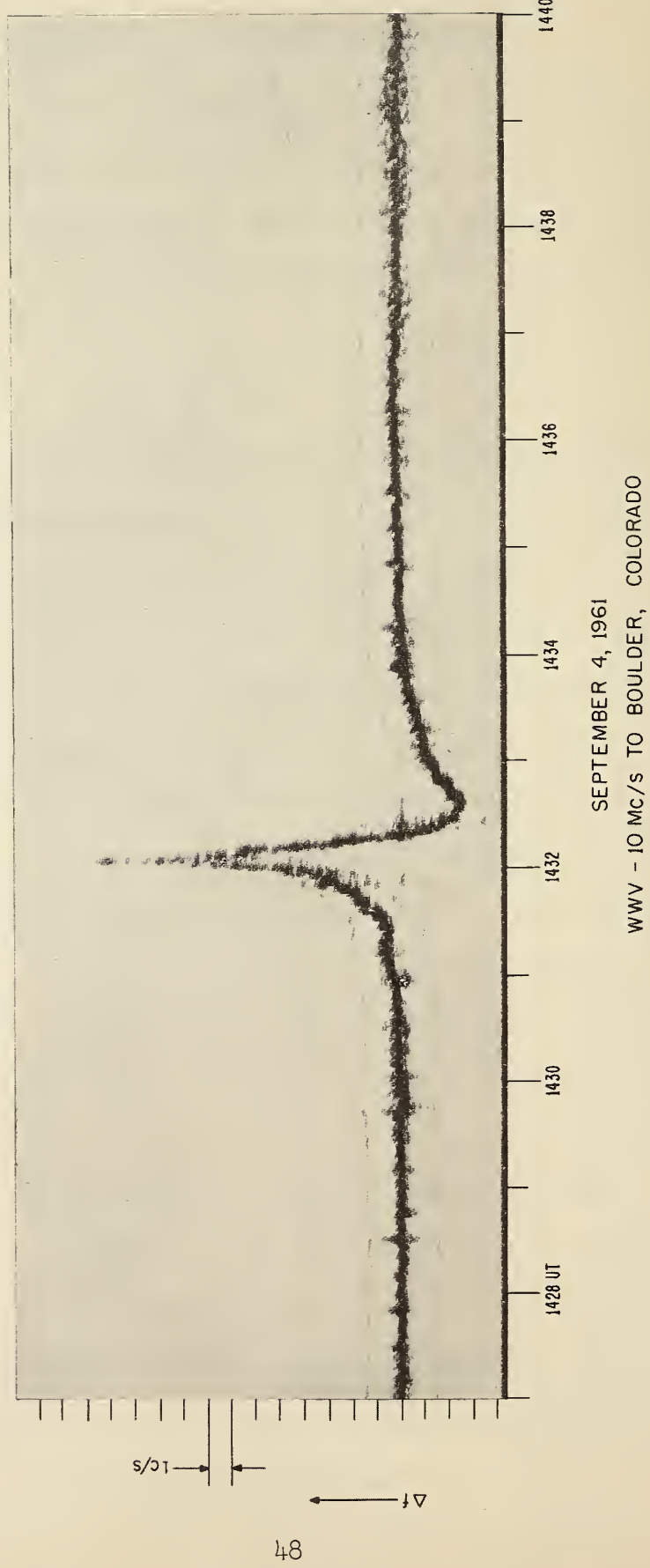
4.1. Solar Flares

Frequency deviations accompanying solar flares (SFD's) can be observed only in the sunlit hemisphere. They show great variation in magnitude, shape, and duration, but always begin with an increase in the received frequency. The initial positive phase may or may not be followed by a negative deviation. A typical sudden frequency deviation is of much shorter duration than the optical flare and tends to occur between the beginning and maximum phase of the H α flare. Those flares which produce significant increases in the electron density in the lower regions of the ionosphere cause increased absorption of the HF signals used in the Doppler technique; however, no change in absorption has been detected during most of the sudden frequency deviations observed. A detailed study must be made on the relationships between SFD's and other flare associated effects.

A "classical" sudden frequency deviation is shown in figure 4.1. This effect was observed during a flare, of optical importance 1, on 4 September 1961. The times of the optical flare were reported as 1424-1435-1512 UT (beginning-maximum-end). The sudden frequency deviation is very simple in this case: a rapid rise to a sharp peak, a negative

Sudden frequency deviation observed during importance 1 flare on
September 4, 1961, WWV-10 Mc/s received at Boulder

SOLAR FLARE, IMPORTANCE 1, 1425 - 1435 - 1512 UT



deviation, and a recovery to the pre-flare conditions. The entire effect takes place between the beginning and maximum phase of the optical flare. The maximum positive deviation is considerably larger than the negative deviation. Such "classical" sudden frequency deviations are rarely observed.

An unusually complex sudden frequency deviation is shown in figure 4.2. This effect was observed during a flare on 12 November 1960 (1315-1330-1425D, importance 3+) which was accompanied by a sea-level cosmic ray increase. The time variations of this frequency deviation indicate that the x-ray flux causing the ionospheric changes must have undergone rapid and complex variations with time. The duration of this event is greater than is usually observed; nevertheless, the major frequency variations are over before the optical flare reaches its maximum phase. This event has been discussed by Knecht and Davies [1961a, 1961b]; Munro [1961]; Davies, Watts, and Zacharisen [1962]; and Davies [1963].

Figure 4.3 shows a sudden frequency deviation observed on WWV-10 Mc/s and WWV-20 Mc/s received at Boulder on 28 September 1961 (optical flare 2202-2224-2530 UT, importance 3). This event illustrates a feature often observed on oblique-incidence Doppler records; namely, a splitting of the traces due to E- and F-layer propagation. These traces are labeled in figure 4.3a; the F-layer trace shows a large deviation while the E-layer trace shows only a small shift. Moreover, the E-layer trace lacks the oscillations of the F-layer trace. The small frequency shift suffered by the E-layer propagation mode during this event indicates that the major portion of the changes detected by this technique occurred above the height of reflection in the E layer. This event has been discussed

Sudden frequency deviation observed during importance 3+ flare on
November 12, 1960, WWV-20 Mc/s received at Boulder

SOLAR FLARE, IMPORTANCE 3+, 1315 - 1330 - 1425D

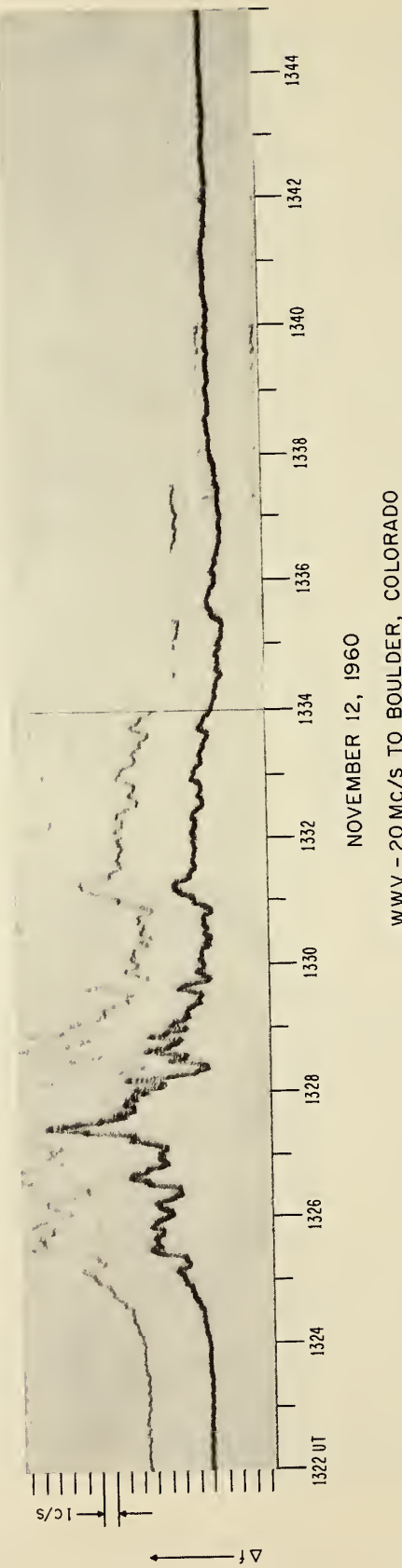
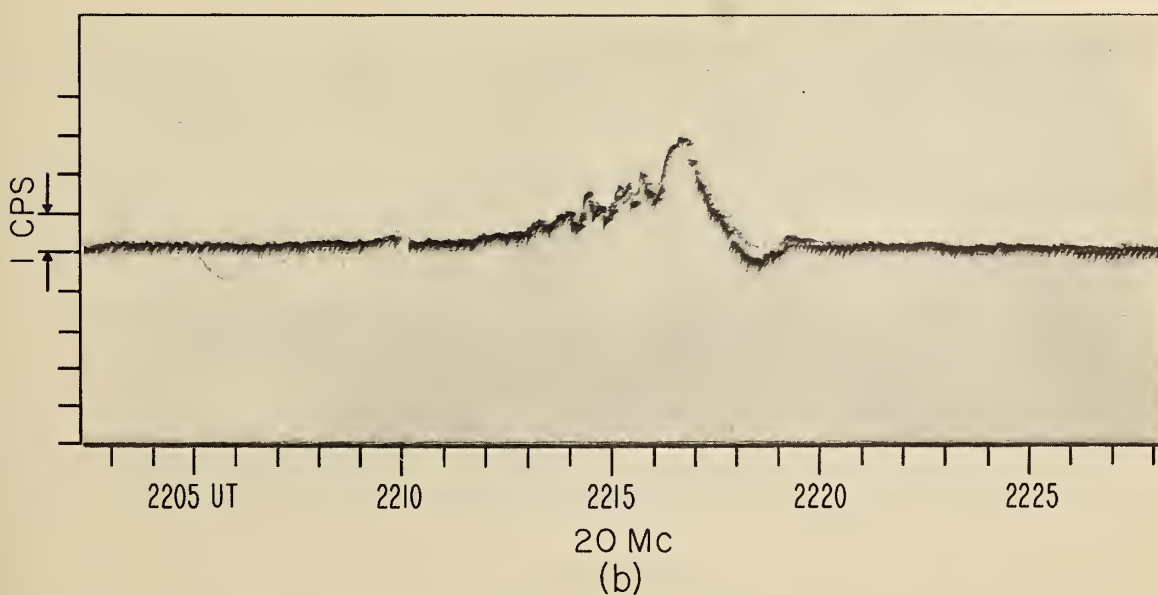
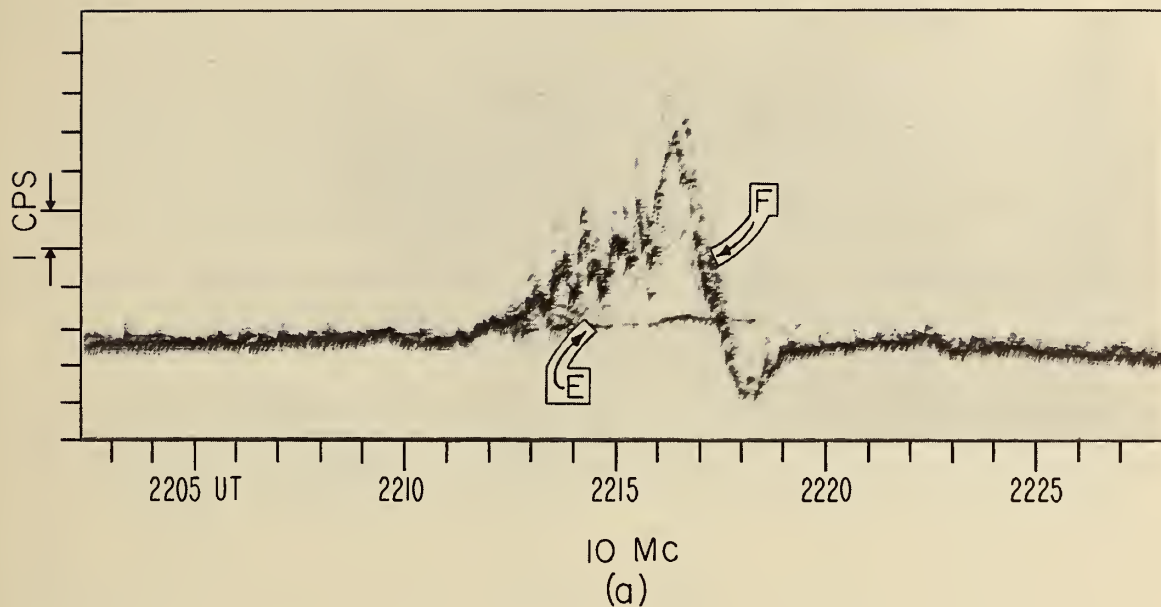


Figure 4.2

Sudden frequency deviation observed during importance 3 flare on September 28, 1961, WWV-10 and WWV-20 Mc/s received at Boulder



SEPTEMBER 28, 1961
WWV

Figure 4.3

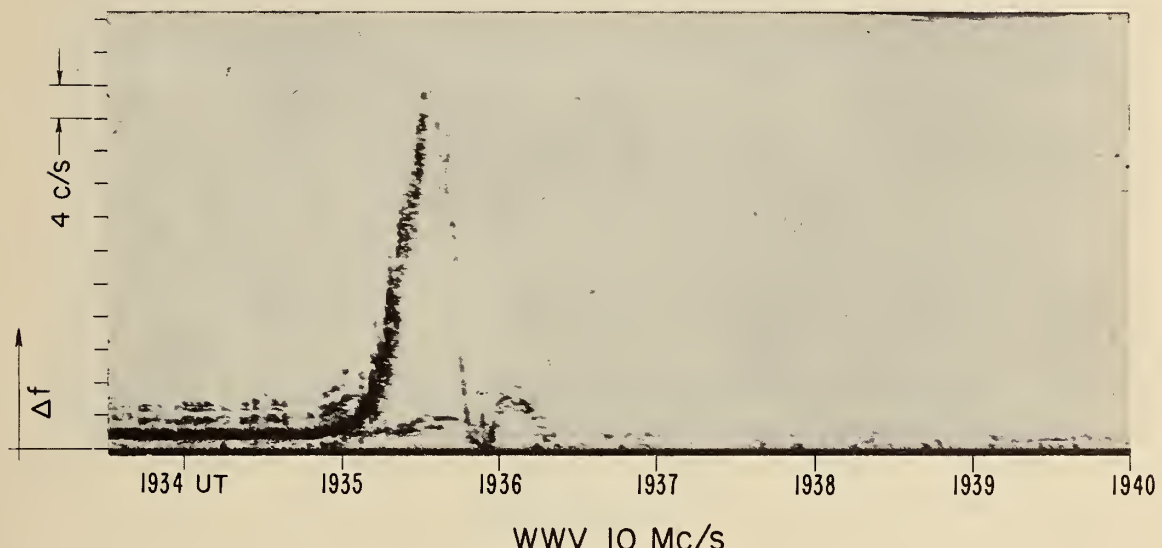
by Davies [1962b] and by Kanellakos and Villard [1962].

The largest sudden frequency deviation yet observed at Boulder is shown in figures 4.4 and 4.5. This effect accompanied a flare of optical importance 2 (1935-1937-2031) on 19 April 1962. The maximum frequency deviation on WWV-10 Mc/s received at Boulder (figure 4.4a) exceeded 40 cycles per second. The positive phase of the effect lasted less than a minute; the overall duration of the event was about 3 minutes. Since the Doppler technique detects the rate of change of electron density, the great magnitude of this event indicates only that this flare caused an extremely rapid change in electron density; the change in the total electron content of the ionosphere need not have been very great. The rate of change of electron density caused by this flare has been investigated in section 2.3 of this report.

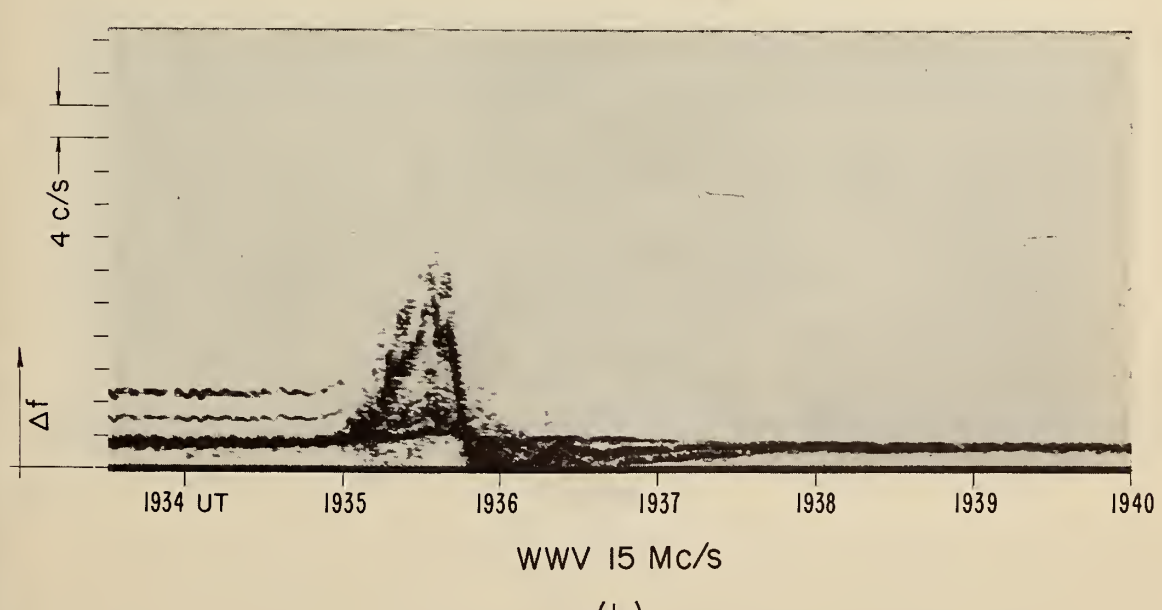
The size of the deviation observed on WWV-10 Mc/s (figure 4.4a) relative to that on WWV-15 Mc/s (figure 4.4b) is partly due to WWV-10 Mc/s being two-hop propagation to Boulder while one-hop propagation was possible on WWV-15 Mc/s. The equivalent vertical-incidence frequencies for F-layer propagation of WWV-10 and -15 Mc/s to Boulder were approximately the same, and, as shown in section 2.1, the frequency deviation per hop depends upon the equivalent vertical-incidence frequency. The deviations observed at near vertical incidence at Boulder on 4 and 5 Mc/s are shown in figure 4.5. The great difference in the magnitudes of the effects observed on 4 and 5 Mc/s is explained by the fact that 5 Mc/s was very close to the critical frequency of the F1 layer as shown in figure 2.8.

Sudden frequency deviation observed during importance 2 flare
on April 19, 1962, WWV-10 and WWV-15 Mc/s received at Boulder

SOLAR FLARE, IMPORTANCE 2, 1935-1937-2031 UT



(a)



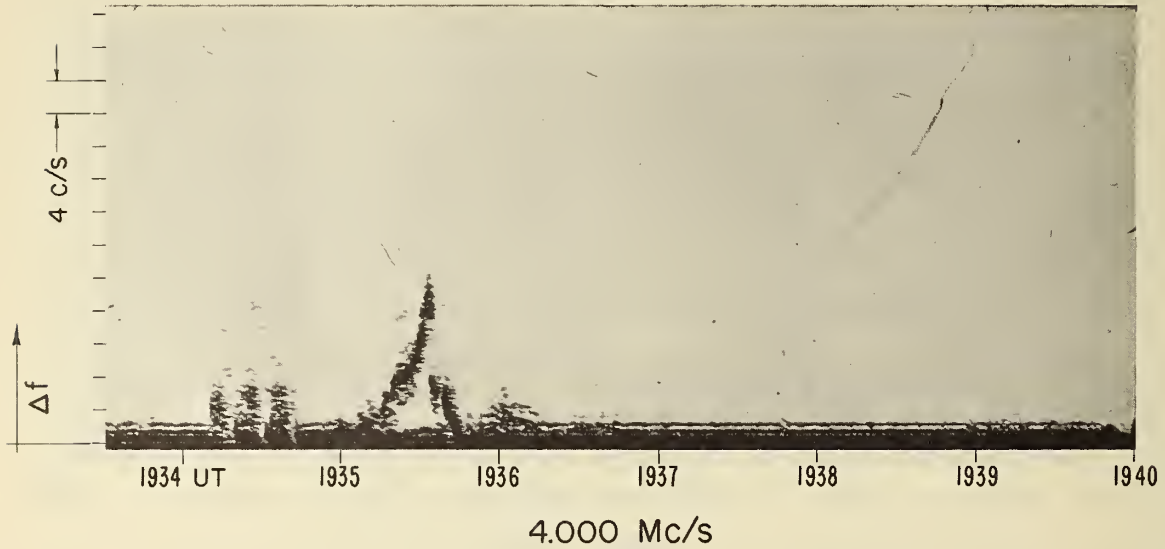
(b)

APRIL 19, 1962
BOULDER, COLORADO

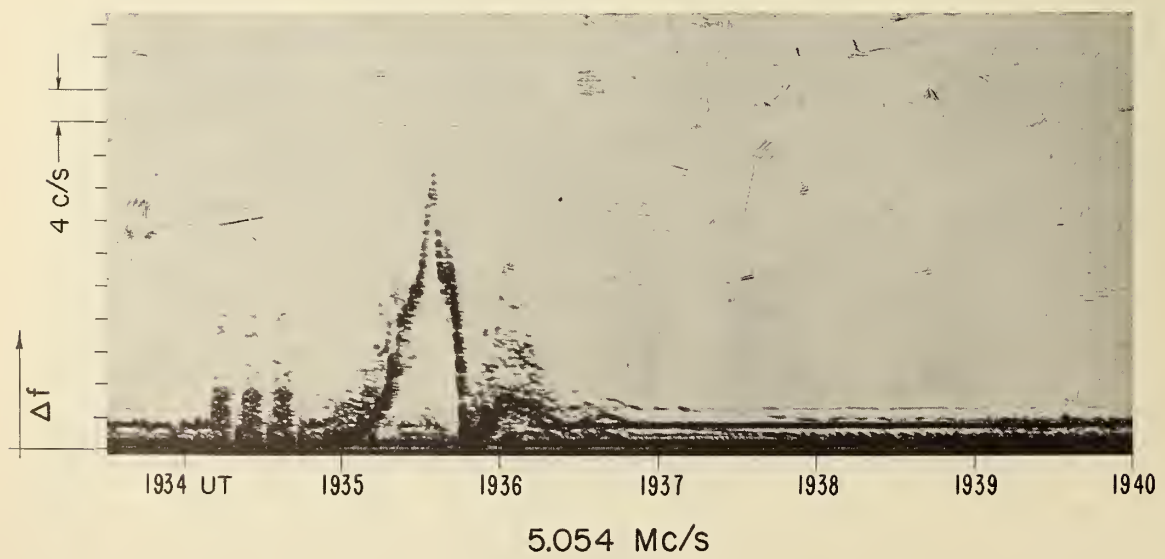
Figure 4.4

Sudden frequency deviation observed during importance 2 flare on
April 19, 1962. 4 and 5 Mc/s vertical incidence at Boulder

SOLAR FLARE, IMPORTANCE 2, 1935 - 1937 - 2031 UT



(a)



(b)

VERTICAL INCIDENCE
APRIL 19, 1962
BOULDER, COLORADO

Figure 4.5

Like the event of 28 September 1961 (figure 4.3), the oblique-incidence records of the 19 April 1962 flare (figure 4.4) show both E- and F-layer traces, the E-layer trace being only slightly deviated. The existence of separate traces for different propagation modes is very helpful in analyzing these events.

4.2. Geomagnetic Variations

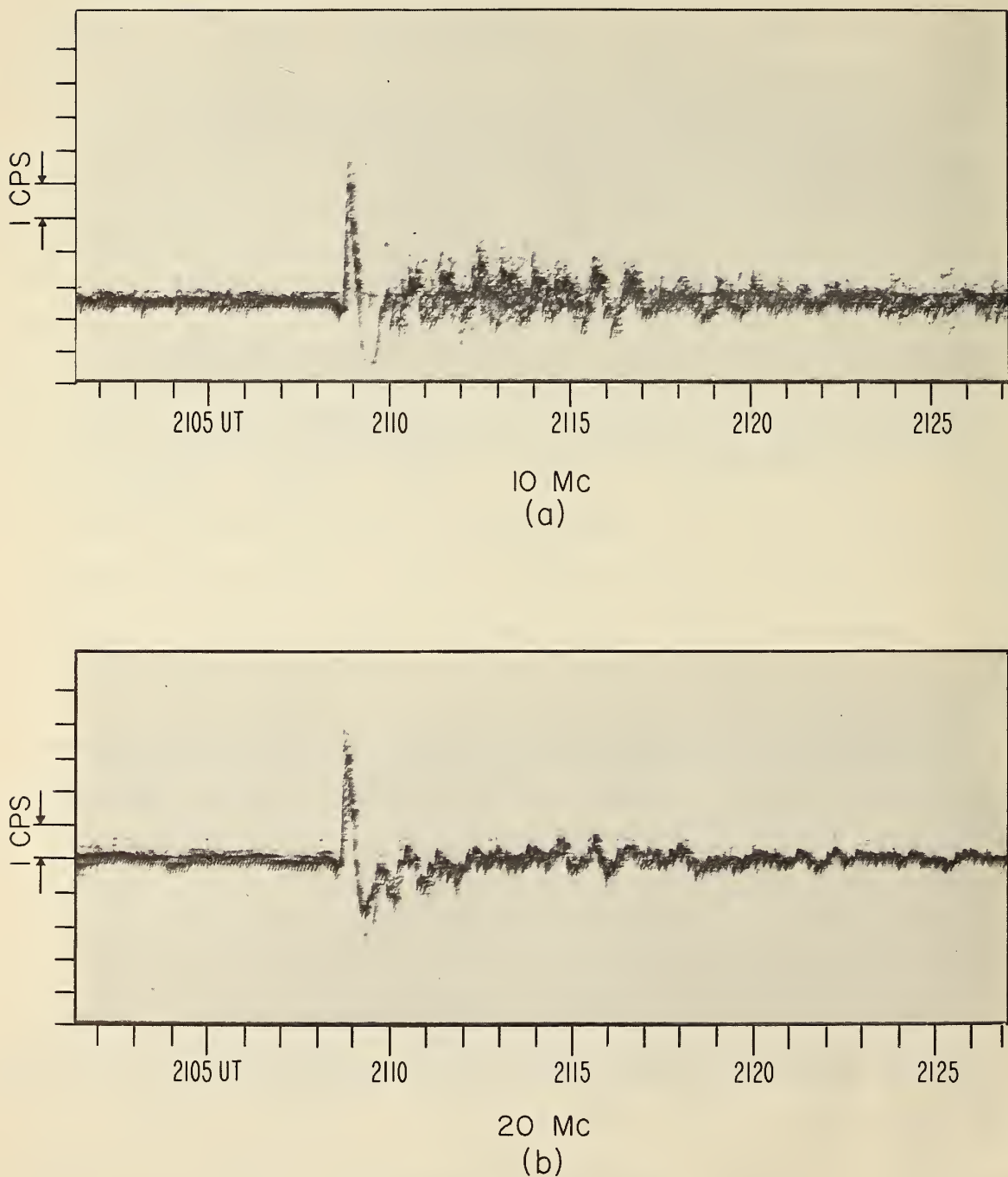
The frequency variations observed during geomagnetic sudden commencements are often very similar to solar flare effects. However, with a little experience, it is usually not difficult to separate the two phenomena. Like solar flare effects, sudden commencement effects show great variation from one event to another. Unlike flare effects, sudden commencement effects can be observed during the night as well as the day.

A lack of data has delayed a statistical study of sudden commencement effects. However, a preliminary investigation indicates that about 47 percent of the sudden commencements reported in the Journal of Geophysical Research (J. Virginia Lincoln, "Geomagnetic and Solar Data") have been accompanied by frequency deviations.

Sudden commencement effects detected by the Doppler technique have been previously discussed by Davies [1962b]; Kanellakos and Villard [1962]; and Chan, Kanellakos, and Villard [1962].

Two examples of frequency deviations related to sudden commencements are shown in figures 4.6 and 4.7. The event of 30 September 1961 (figure 4.6) is characterized by an initial small negative deviation, a

Sudden commencement observed by the Doppler technique at 2108 UT on September 30, 1961. WWV-10 and WWV-20 Mc/s received at Boulder

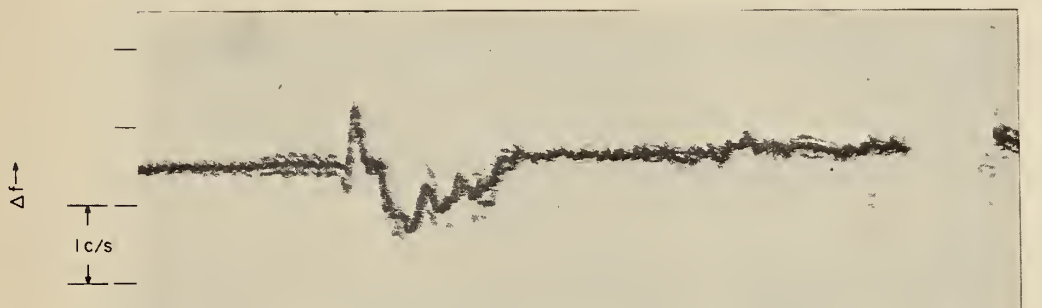


SEPTEMBER 30, 1961
WWV

Figure 4.6

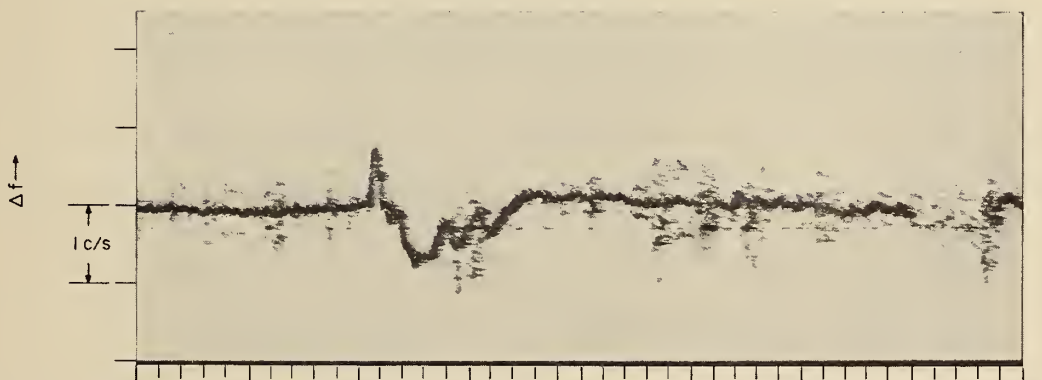
Sudden commencement observed by the Doppler technique at 0219 UT on February 22, 1962. WWV-10 Mc/s received at Shickley, Nebraska, and WWV-10 and WWV-15 Mc/s received at Boulder, Colorado

GEOMAGNETIC SUDDEN COMMENCEMENT - 0220 UT



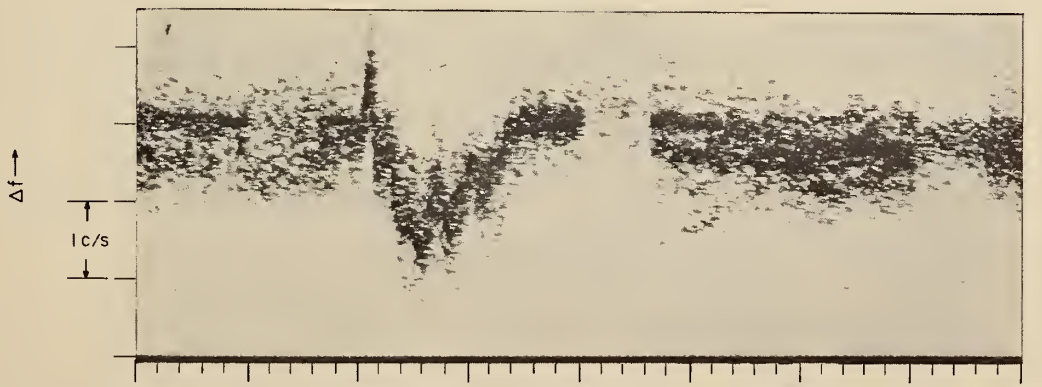
0210 UT 0220 0230 0240 0250

(a) WWV - 10 Mc/s TO SHICKLEY, NEBRASKA



0210 UT 0220 0230 0240 0250

(b) WWV - 10 Mc/s TO BOULDER, COLORADO



0210 UT 0220 0230 0240 0250

(c) WWV - 15 Mc/s TO BOULDER, COLORADO

FEBRUARY 22, 1962

Figure 4.7

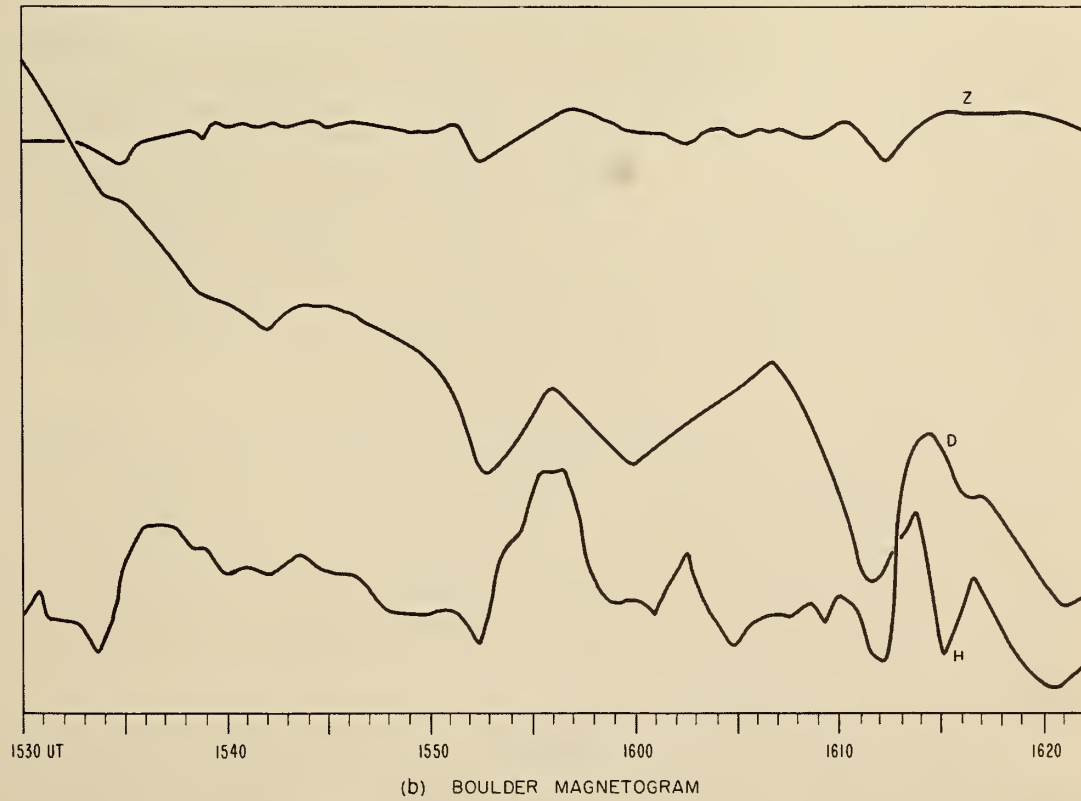
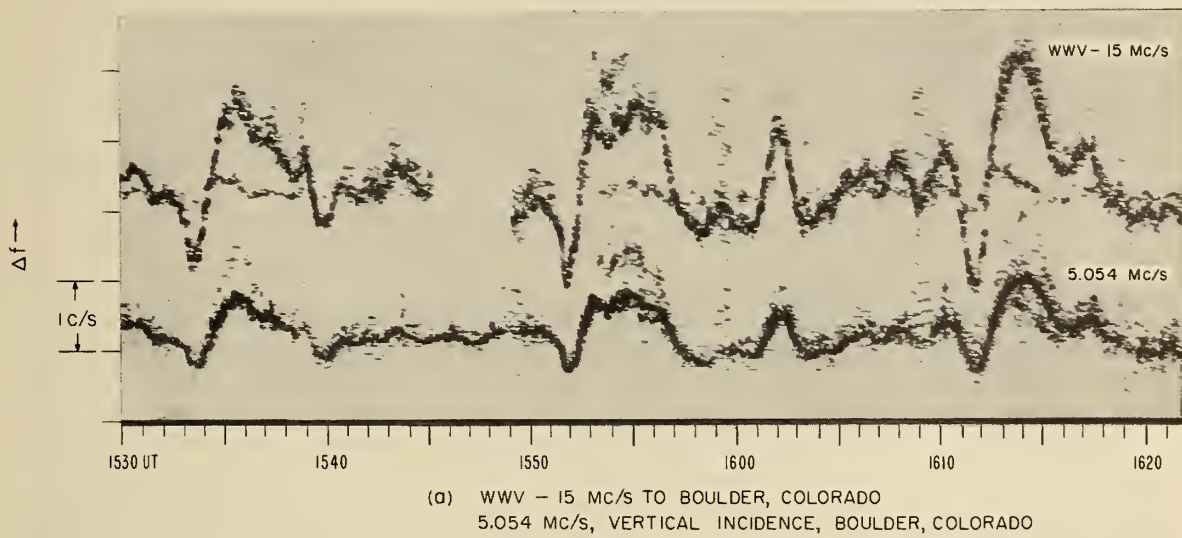
sharp positive spike, and a fifteen minute period of small amplitude oscillations. The sudden commencement at 0220 UT on 22 February 1962 (figure 4.7) was accompanied by a positive deviation of one minute duration followed by a negative frequency shift which lasted about seven minutes. Both of these effects are easily distinguishable from the flare effects shown in figures 4.1 through 4.5: the first by the initial negative shift and the oscillations following the peak and the second by the nature and magnitude of the negative phase relative to the positive phase.

Figure 4.8a shows the Doppler records of WWV-15 and 5.054 Mc/s received at Boulder for a period of about one hour on 26 February 1962 during which three sudden impulses were reported (1533, 1552, and 1611 UT). A tracing of the corresponding portion of the Boulder magnetogram is shown in figure 4.8b. The correlation between the frequency deviations and the variations of the magnetic declination (D trace) is good. The simultaneous frequency variations observed on 5 Mc/s (near vertical incidence) and WWV-15 Mc/s indicate that the disturbances causing these variations occurred simultaneously over a relatively large area. The frequency variations occurring at the times of the reported sudden impulses are very similar to one another.

A brief survey has indicated that approximately 25 percent of the sudden impulses in the geomagnetic field reported in the Journal of Geophysical Research (J. Virginia Lincoln, "Geomagnetic and Solar Data") have been detected by the Doppler technique.

Correlation between frequency variations observed at both oblique and vertical incidence and changes in the magnetic field observed at Boulder

SUDDEN IMPULSES - 1533, 1552, 1611 UT



FEBRUARY 26, 1962

Figure 4.8

5. Discussion

This report has presented some results of ionospheric research done at CRPL with the Doppler technique developed by Watts and Davies [1960]. This technique has proven to be a sensitive method of detecting the effects of solar flares in the E and F regions of the ionosphere, and the major portion of this report has been devoted to these flare effects (sudden frequency deviations).

Theoretically, it has been shown that the Doppler shift, observed on a given frequency propagated over a given path, depends only on the equivalent vertical-incidence frequency. An equivalence theorem has been derived which relates the frequency deviation observed on an oblique path to that which would have been observed with vertical propagation at the equivalent vertical-incidence frequency (neglecting the earth's magnetic field, electronic collisions, and curvature of the ionosphere). This equivalence relation will be useful in comparing Doppler data obtained from different paths or from different parts of the world, and it will provide a convenient means of data interchange.

Two theoretical approaches have been undertaken in an attempt to better understand the Doppler observations. The first approach consists of the calculation of the frequency dependence of the Doppler shifts to be expected from changes in the parameters defining various parabolic layer models of the ionosphere.

The second theoretical treatment has suggested a method for determining the height variation of the time rate of change of electron density during an ionospheric disturbance from a knowledge of the Doppler

shift as a function of frequency. The frequency dependence of Δf during a specific disturbance has not yet been sufficiently well determined to warrant applying this method. However, it has been shown that the frequency deviations observed during several solar flares could have been produced by a $\partial N/\partial t$ which was zero below the E region and constant in the E and F regions.

Statistically it has been found that 13 percent of all the optical flares and subflares reported from October 1960 through December 1962 caused sudden frequency deviations. The percentage of flares detected increases with the optical importance of the flare, shows no pronounced seasonal variation, but does exhibit a diurnal variation with a peak near local noon.

Most sudden frequency deviations have durations of from 2 to 4 minutes; this is much shorter than the duration of the typical optical flare. The sudden frequency deviation almost always occurs between the beginning and maximum phase of the optical flare, with the maximum frequency deviation usually occurring 1 to 2 minutes before the maximum phase of the H α flare.

For long paths, the observed frequency deviations tend to vary directly with the ground path length and inversely with operating frequency. For vertical propagation the observed frequency deviations show no systematic frequency dependence; however, it has been shown that the vertical-incidence data are consistent with the theory which assumes that the time rate of change of ionization during the flare is independent of height.

The CRPL is presently making Doppler measurements over both oblique- and vertical-incidence paths in the United States and oblique paths near the magnetic equator in Africa. In addition, the Battelle Institute of Frankfurt, Germany, supplies oblique-incidence records of MSF (Rugby, England) received at Frankfurt, and workers in England, Hawaii, India, and Japan have shown interest in using the technique. For the immediate future these paths will provide broader coverage for a continuing flare patrol and will be used to study the solar zenith angle and latitude dependences of the ionospheric effects of solar flares.

However, a more sophisticated network of paths is highly desirable if the technique is to be used to best advantage. Although, in principle, the equivalence theorem can be used to assist in the comparison of data obtained from different paths, in practice it becomes difficult to determine the propagation modes for long paths and, hence, it is difficult to apply the equivalence theorem to such paths. On the other hand, vertical propagation emphasizes the local ionospheric variations. Hence it seems that relatively short paths should be the best for study of widespread ionospheric disturbances, such as those caused by solar flares. A worldwide network of such paths is needed in order to conduct a definitive study of the solar zenith angle and latitude dependence of solar flare effects. Such a network would also provide a worldwide monitoring system for flare and geomagnetic disturbance effects. In order to adequately study the height variation of ionospheric disturbances, it will be necessary to use several frequencies over a single path.

So far major attention has been given to the maximum positive frequency deviations induced by solar flares. Some attention should be given to the other characteristics of flare effects (negative phases and recovery rates) to determine whether these can be of assistance in studying the ionospheric response to solar flare radiation. In addition, the effects accompanying geomagnetic disturbances need to be investigated and the mechanism causing them discovered.

Further study should also be made of the relationship between the different ionospheric effects (SWF, SEA, SPA, SFD, etc.) and the various solar phenomena, such as the different types of radio emissions, which accompany visible flares. Such a study would be of assistance in determining the time characteristics and enhancements of the various radiation bands causing the ionospheric disturbances. Another objective of such a study should be to investigate the possibility of predicting the occurrence of solar disturbances which will significantly affect the earth's environment.

The Doppler technique should be capable of detecting any type of rapid ionospheric variation which occurs at heights no greater than the reflection levels for the frequencies used. It should be useful for studying ionospheric effects associated with geomagnetic disturbances as well as those associated with solar flares. In addition, the technique should aid in the study of ionospheric oscillations and the motions of ionospheric irregularities. To be used to best advantage, the Doppler measurements should be made in conjunction with other ionospheric observations (e.g., ionograms, field strength records).

6. Acknowledgments

Partial support for the final stages of preparation of this report was received from the Advanced Research Projects Agency, Nuclear Test Detection Office under Contract No. 183.

7. References

- Budden, K. G. (1955), A method for determining the variation of electron density with height from curves of equivalent height against frequency, Proceedings of the Cambridge Conference on Physics of the Ionosphere, Physical Society, 332.
- Chan, K. L., D. P. Kanellakos, and O. G. Villard, Jr. (1962), Correlation of short-period fluctuations of the earth's magnetic field and instantaneous frequency measurements, J. Geophys. Res. 67, No. 5, 2066-2072.
- Chan, K. L. and O. G. Villard, Jr. (1963), Sudden frequency deviations induced by solar flares, J. Geophys. Res. 68, No. 10, 3197-3224.
- Davies, K. (1962a), Doppler studies of the ionosphere with vertical incidence, Proc. IRE 50, No. 1, 94-95.
- Davies, K. (1962b), Ionospheric effects associated with the solar flare of September 28, 1961, Nature 193, No. 4817, 763-764.
- Davies, K. (1962c), The measurement of ionospheric drifts by means of the Doppler technique, J. Geophys. Res. 67, No. 12, 4909-4913.
- Davies, K. (1962d), Correction to "Doppler studies of the ionosphere with vertical incidence," Proc. IRE 50, No. 6, 1544.
- Davies, K. (1963), Doppler studies of the ionospheric effects of solar flares, Proceedings of the International Conference on the Ionosphere, London, 1962, Institute of Physics and Physical Society.
- Davies, K. (1965), Ionospheric Radio Propagation, NBS Monograph 80, Chapter 4, Section 4.3.1.

Davies, K., J. M. Watts, and D. H. Zacharisen (1962), A study in F2 layer effects as observed with a Doppler technique, J. Geophys. Res. 67, No. 2, 601-609.

Kanellakos, D. P., K. L. Chan, and O. G. Villard, Jr. (1962), On the altitude at which some solar flare induced ionization is released, J. Geophys. Res. 67, No. 5, 1795-1804.

Kanellakos, D. P., and O. G. Villard, Jr. (1962), Ionospheric disturbances associated with the solar flare of September 28, 1961, J. Geophys. Res. 67, No. 6, 2265-2277.

Knecht, R. W., and K. Davies (1961a), Solar flare effects in the F region of the ionosphere, Nature 190, No. 4778, 797-798.

Knecht, R. W., and K. Davies (1961b), Nature 192, No. 4800, 348.

Munro, G. H. (1961), Possible solar flare effects in the F region of the ionosphere, Nature 192, No. 4800, 347.

Smith, N. (1939), The relation of radio sky-wave transmission to ionosphere measurements, Proc. IRE 27, 332-346.

Watts, J. M., and K. Davies (1960), Rapid frequency analysis of fading radio signals, J. Geophys. Res. 65, No. 8, 2295-2301.

Whittaker, E. C., and T. N. Watson (1952), A Course of Modern Analysis, 4th ed., Cambridge University Press, p. 229.

8. Appendix I - The Doppler Shift Written as an Integral

To show:

The Doppler shift is given by

$$\Delta f = -\frac{f}{c} \int_{\text{path}} \frac{\partial u}{\partial t} ds \quad (8.1)$$

for propagation at any angle and by

$$\Delta f = -2 \frac{f}{c} \int_0^h \frac{\partial u}{\partial t} dz \quad (8.2)$$

for vertical propagation.

Restrictions:

- (1) The ionosphere is assumed concentric.
- (2) The effect of the earth's magnetic field is neglected except for vertical propagation.

Proof:

The Doppler shift is given by [Davies, 1962a]

$$\Delta f = -\frac{f}{c} \frac{dP}{dt} . \quad (8.3)$$

In order to calculate the Doppler shift, the time derivative of the phase path must be found. Assuming the ionosphere is horizontally uniform, the time derivative of the phase path is given by:

$$\frac{dP}{dt} = \frac{d}{dt} \int_{\text{path}} \mu ds . \quad (8.4)$$

Substituting $ds = dz/\cos\phi$ in (8.4),

$$\frac{dP}{dt} = \lim_{z \rightarrow h} \frac{d}{dt} 2 \int_0^z \frac{\mu dz}{\cos\phi} . \quad (8.5)$$

Performing the indicated differentiation of the integral in (8.5),

$$\frac{dP}{dt} = \lim_{z \rightarrow h} 2 \int_0^z \frac{\partial \mu}{\partial t} \frac{dz}{\cos\phi} + \lim_{z \rightarrow h} \left[2 \int_0^z \frac{\mu \sin\phi \frac{\partial \phi}{\partial t}}{\cos^2\phi} dz + 2 \frac{\mu}{\cos\phi} \Big|_z \frac{dz}{dt} \right] . \quad (8.6)$$

Using $ds = dz/\cos\phi$ to take the limit of the left term and using Snell's law for curved earth $(a + z) \mu \sin\phi = a \mu_o \sin\phi_o$

$$\begin{aligned} \frac{dP}{dt} &= \int_{\text{path}} \frac{\partial \mu}{\partial t} ds + \lim_{z \rightarrow h} 2 \mu_o \sin\phi_o \left[\int_0^z \frac{a}{a+z} \frac{\frac{\partial \phi}{\partial t} dz}{\cos^2\phi} \right. \\ &\quad \left. + \frac{a}{(a+z) \sin\phi \cos\phi} \Big|_z \frac{dz}{dt} \right] . \end{aligned} \quad (8.7)$$

The term in brackets can be calculated using the criterion that the distance between the transmitter and receiver is constant. Neglecting the effect of the earth's magnetic field,

$$\frac{dD}{dt} = 0 = \lim_{z \rightarrow h} \frac{d}{dt} 2a \int_0^z \frac{\tan\phi}{a+z} dz . \quad (8.8)$$

Performing the differentiation indicated in (8.8),

$$0 = \lim_{z \rightarrow h} \left[2a \int_0^z \frac{\sec^2 \phi}{a+z} \frac{d\phi}{dt} dz + 2a \frac{\tan \phi}{a+z} \Big|_z \frac{dz}{dt} \right]. \quad (8.9)$$

Subtracting $\mu_0 \sin \phi_0$ times (8.9) from (8.7),

$$\frac{dP}{dt} = \int_{\text{path}} \frac{\partial \mu}{\partial t} ds + \lim_{z \rightarrow h} \frac{2a\mu_0 \sin \phi_0}{a+z} \left[-\frac{\sin \phi}{\cos \phi} \Big|_z \frac{dz}{dt} + \frac{1}{\sin \phi \cos \phi} \Big|_z \frac{dz}{dt} \right]. \quad (8.10)$$

The expression in brackets can be manipulated to give

$$\frac{dP}{dt} = \int_{\text{path}} \frac{\partial \mu}{\partial t} ds + \lim_{z \rightarrow h} \frac{2a\mu_0 \sin \phi_0}{a+z} \left[\frac{\cos \phi}{\sin \phi} \Big|_z \frac{dz}{dt} \right]. \quad (8.11)$$

Again using Snell's law,

$$\frac{dP}{dt} = \int_{\text{path}} \frac{\partial \mu}{\partial t} ds + \lim_{z \rightarrow h} \left[2 \mu \cos \phi \Big|_z \frac{dz}{dt} \right] \quad (8.12)$$

The quantity in the brackets is zero when evaluated at the limit, since $\cos \phi$ is zero at reflection for oblique propagation, and μ is zero at reflection for vertical propagation. Therefore, from (8.12)

$$\frac{dP}{dt} = \int_{\text{path}} \frac{\partial \mu}{\partial t} ds. \quad (8.13)$$

Substituting (8.13) into (8.3),

$$\Delta f = -\frac{f}{c} \int_{\text{path}} \frac{\partial \mu}{\partial t} ds. \quad (8.14)$$

It is necessary to neglect the earth's magnetic field because the

proof assumes that the ray direction and the wave normal direction are the same, which is generally not the case when the effects of the magnetic field are included. The step from (8.6) to (8.7) assumes that the angle ϕ gives the wave normal direction, while (8.8) assumes that the angle ϕ gives the ray direction.

If the propagation is vertical, this restriction is not necessary, since equation (8.8) is not necessary for the proof. Combining (8.3) and (8.5), the Doppler shift for vertical propagation is given by

$$\Delta f = -2 \frac{f}{c} \frac{d}{dt} \int_0^h \mu dz . \quad (8.15)$$

Performing the differentiation indicated in (8.15),

$$\Delta f = -2 \frac{f}{c} \int_0^h \frac{\partial \mu}{\partial t} dz - 2 \frac{f}{c} \mu \Big|_h \frac{dh}{dt} . \quad (8.16)$$

The term $-2 \frac{f}{c} \mu \Big|_h \frac{dh}{dt}$ is zero, since the index of refraction is zero at reflection for vertical propagation. Therefore, from (8.16)

$$\Delta f = -2 \frac{f}{c} \int_0^h \frac{\partial \mu}{\partial t} dz . \quad (8.17)$$

Since the derivation of (8.17) from (8.15) does not depend on the coincidence of the wave normal and ray direction (8.17) is correct including the effect of the earth's magnetic field.

The integral form for the Doppler shift as given in (8.14)(for propagation at any angle of incidence neglecting the effect of the earth's

magnetic field) or as given in (8.17) (for vertical propagation including the effect of the earth's magnetic field) is convenient since it can be used in a computer ray tracing program to calculate the Doppler shift by performing a sum approximating the integral along the path as the ray is traced.

9. Appendix II - Equivalence Theorem for Doppler Shifts

To show: $\Delta f(f, \phi_0) = \Delta f(f \cos\phi_0, 0)$,

where the first argument is the wave frequency and the second argument is the angle of incidence of the wave on the ionosphere.

Restrictions:

- (1) The curvature of the ionosphere is neglected.
- (2) The effect of the earth's magnetic field is neglected.
- (3) The effect of collisions is neglected.

Proof:

The Doppler shift is given by (8.1) of Appendix I.

$$\Delta f = - \frac{f}{c} \int_{\text{path}} \frac{\partial u}{\partial t} ds . \quad (9.1)$$

The refractive index is given by

$$n^2 = 1 - \frac{kN}{f^2} . \quad (9.2)$$

Differentiating (9.2) with respect to t and dividing by $2n$,

$$\frac{\partial n}{\partial t} = - \frac{k}{2n f^2} \frac{\partial N}{\partial t} . \quad (9.3)$$

Combining (9.1) and (9.3),

$$\Delta f = \frac{k}{2cf} \int \frac{\frac{\partial N}{\partial t} ds}{\mu} . \quad (9.4)$$

Substituting $ds = dz/\cos\phi$ in (9.4),

$$\Delta f = \frac{k}{2cf} \int \frac{\frac{\partial N}{\partial t} dz}{\mu \cos\phi} . \quad (9.5)$$

Operating on (9.5) with straightforward algebra, using a trigonometric substitution, and applying Snell's law, $\mu \sin\phi = \sin\phi_0$,

$$\Delta f = \Delta f(f, \phi_0) = \frac{k}{2cf \cos\phi_0} \int \frac{\frac{\partial N}{\partial t} dz}{\sqrt{1 - \frac{kN}{f^2 \cos^2 \phi_0}}} . \quad (9.6)$$

Substituting into the function defined by (9.6), it can be seen that

$$\Delta f(f, \phi_0) = \Delta f(f \cos\phi_0, 0) . \quad (9.7)$$

An interpretation of (9.7) is that Δf depends only on the equivalent vertical-incidence frequency, $f \cos\phi_0$.

10. Appendix III - Relationship Between Doppler Shift and Virtual Height

To show:

$$f\Delta f = \frac{k}{c} \frac{\partial N}{\partial t} (h' - h_0) \quad (10.1)$$

if $\partial N/\partial t$ is zero from the ground up to h_0 and constant above h_0 .

Restrictions:

- (1) Only vertical propagation is considered.
- (2) Collisions are neglected.
- (3) Effect of the earth's magnetic field is neglected.

Proof:

The Doppler shift for vertical propagation is given by (8.2) of Appendix I.

$$\Delta f = -2 \frac{f}{c} \int_0^h \frac{\partial \mu}{\partial t} dz \quad (10.2)$$

If the Doppler shift is entirely due to changes in electron density in the ionosphere, then from (10.2),

$$\Delta f = -2 \frac{f}{c} \int_0^h \frac{\partial \mu}{\partial N} \frac{\partial N}{\partial t} dz \quad (10.3)$$

The index of refraction is given by

$$\mu^2 = 1 - \frac{kN}{f^2} \quad (10.4)$$

Differentiating (10.4) with respect to N and dividing by 2μ ,

$$\frac{\partial \mu}{\partial N} = - \frac{k}{2\mu f^2} \quad (10.5)$$

Since $\mu = 1/\mu'$,

$$\frac{\partial \mu}{\partial N} = - \frac{k}{2f^2} \mu' \quad (10.6)$$

Substituting (10.6) into (10.3),

$$\Delta f = \frac{k}{fc} \int_0^h \mu' \frac{\partial N}{\partial t} dz \quad (10.7)$$

For the special case in which $\partial N/\partial t$ is zero from the ground up to a height h_0 , and constant above h_0 ,

$$\Delta f = \frac{k}{fc} \frac{\partial N}{\partial t} \int_{h_0}^h \mu' dz \quad (10.8)$$

Since μ' is one below h_0 for the special case that the region is nondeviative,

$$\Delta f = \frac{k}{fc} \frac{\partial N}{\partial t} \left[\int_0^h \mu' dz - \int_0^{h_0} dz \right] \quad (10.9)$$

Performing the indicated integrations in (10.9),

$$\Delta f = \frac{k}{fc} \frac{\partial N}{\partial t} (h' - h_0) \quad (10.10)$$

Multiplying (10.10) by f ,

$$f\Delta f = \frac{k}{c} \frac{\partial N}{\partial t} (h' - h_0) \quad (10.11)$$

which was to be proved.

A physical interpretation of (10.11) is that the product of the frequency and the Doppler shift for vertical propagation is proportional to the virtual height minus some constant height at all frequencies. Therefore, if $\partial N / \partial t$ is independent of height in the ionosphere, a plot of $f\Delta f$ versus f should look like the ionogram. This relation is approximately valid even if the magnetic field is included as shown by figure 10.1 for conditions at Boulder (dip = 70° , $f_H = 1.47$ Mc/s).

COMPARISON OF THEORETICAL $f\Delta f$ VERSUS f WITH IONOGRAM

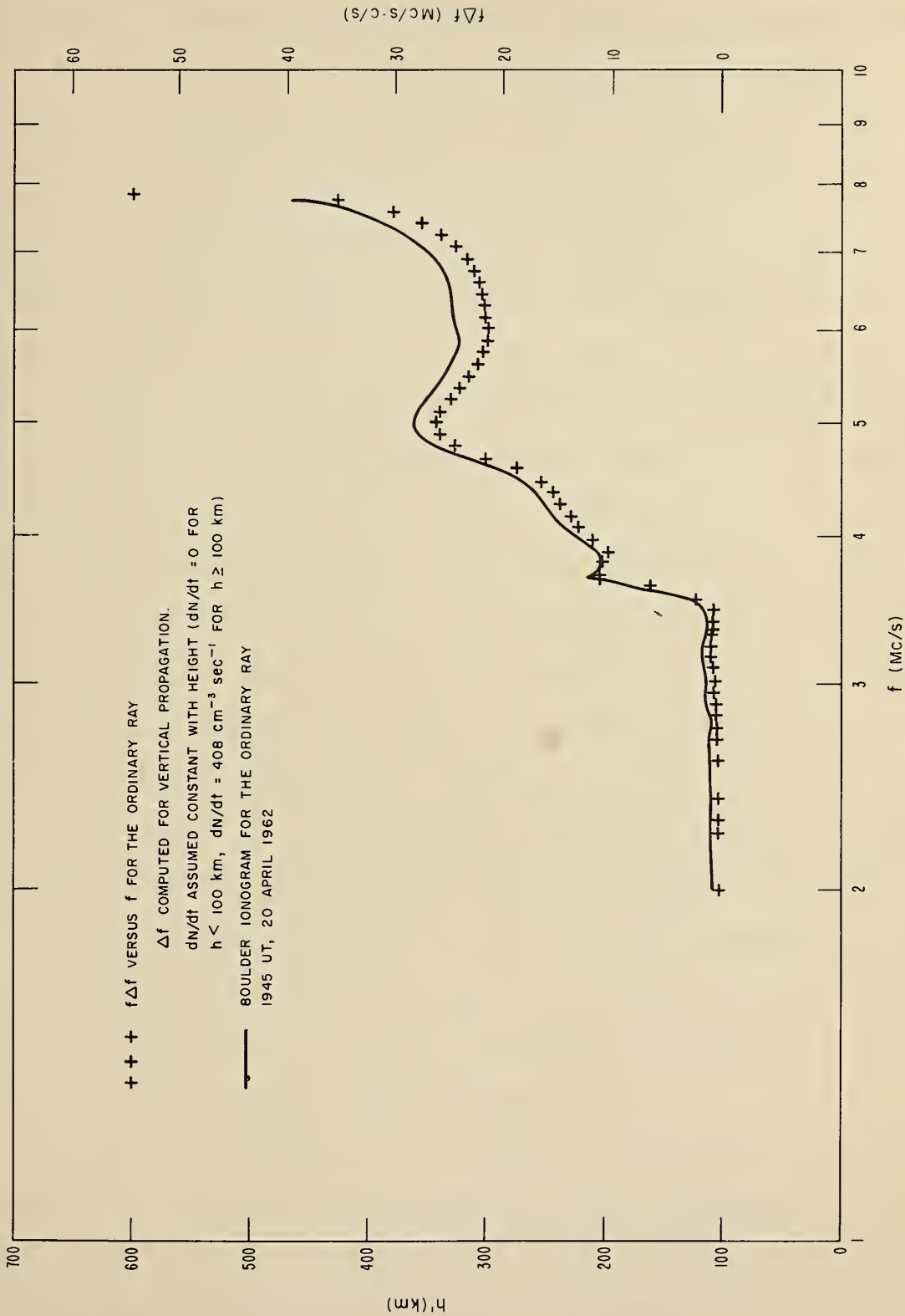


Figure 10.1

11. Appendix IV - Catalog of Sudden Frequency Deviations Observed From October 1, 1960 to December 31, 1962.

The following table lists the sudden frequency deviations observed for the various paths in operation from October 1, 1960, to December 31, 1962. This table also gives the solar flares and solar radio emissions as well as ionospheric effects which were reported to have occurred at the same time that a sudden frequency deviation was observed. Since the paths from WWV to Boulder and the near vertical-incidence paths at Boulder (Sunset to Boulder) were used for flare monitoring during this period, the table includes all SFD's observed on the Boulder records. Consequently there are some entries for which no flares were reported optically. The records for receiving sites other than Boulder have not been examined as closely as have the Boulder records, and only SFD's which could be attributed to reported optical flares have been included in the table for these paths. It should be emphasized that, although all the sudden frequency deviations listed have the characteristics of flare effects, some of the smaller effects, especially those which do not correspond to optically reported flares, may not be due to flare-induced ionization.

A brief description of the method of data reduction may be of assistance in evaluating the information contained in the catalog. The data is recorded on slowly moving magnetic tape (0.02 ips) in the form of the difference frequency between the received frequency and a stable local reference frequency offset from the transmitted frequency by a few cycles per second (typically 2-5 c/s). This magnetic tape is then played back at 30 ips into an audio spectrum analyzer to give a continuous visual

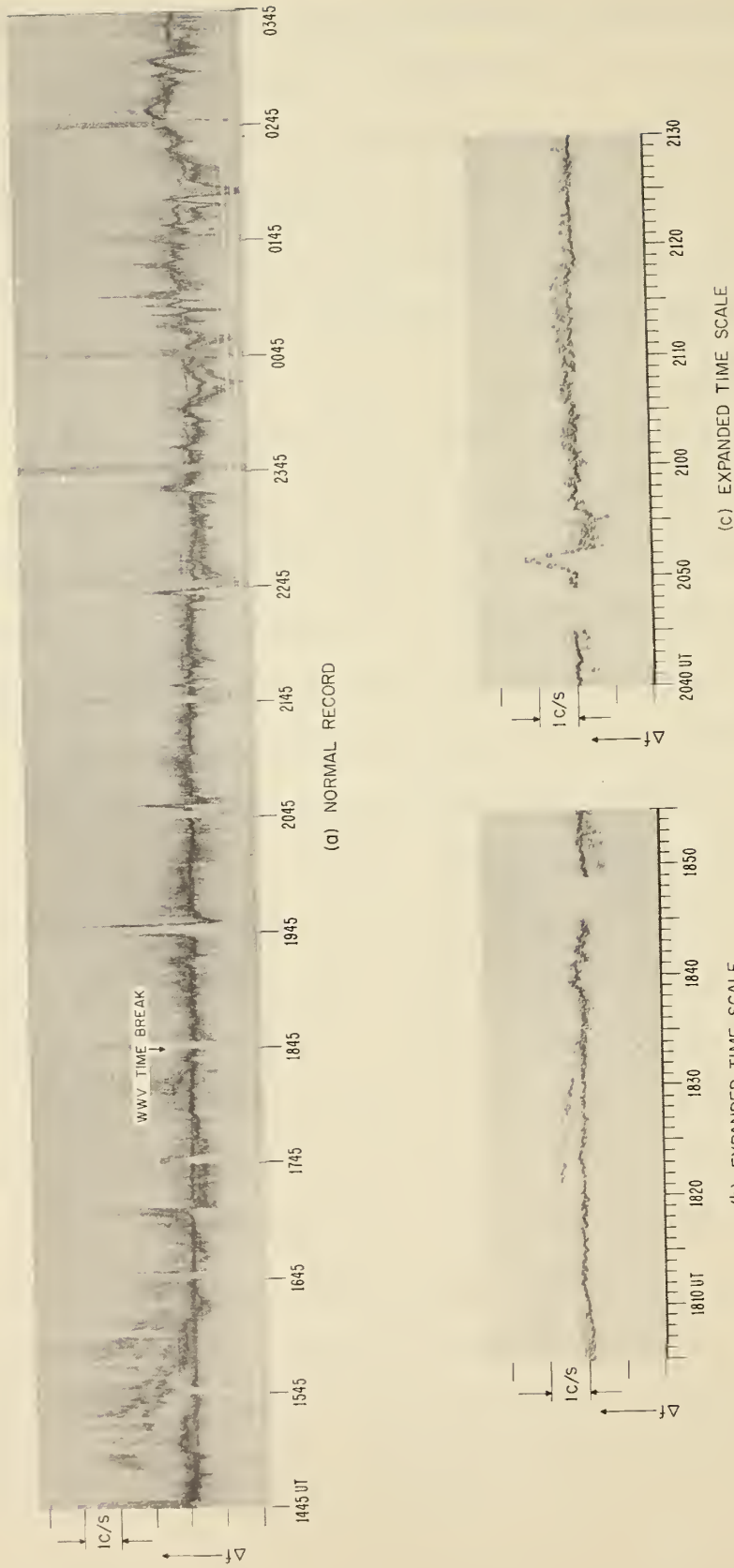
record of the recorded difference frequency versus time. Changes in the received frequency are indicated by the variations of the difference frequency. A sample of such a record is shown in figure 11.1a. Any events of interest can be examined in greater detail by expanding the time scale, as illustrated in figures 11.1b and 11.1c. The times and magnitudes of sudden frequency deviations are determined from the expanded records.

Figure 11.1 illustrates some of the difficulties often encountered in deciding whether an observed effect is, or is not, related to a solar flare. The effects at 1715, 1942, 2050, 2153, and 2240 UT are well defined sudden frequency deviations. The events at 1822, 1837, and 1928 are not as well defined. It is often questionable whether such effects are flare related or arise from some other type of ionospheric disturbance. The effect at 2333 UT, which begins with a negative frequency shift, is definitely not a sudden frequency deviation.

The table gives the times of sudden frequency deviations to the nearest minute with the symbols E (before) and D (later than) being used occasionally for further qualification. D or E used with a beginning or maximum time applies only between successive minutes, whereas a D used with an end time may mean that the end of the effect occurred some undeterminable number of minutes after the given time.

The frequency deviations, Δf , are given in cycles per second. The accuracy with which small frequency variations can be measured from the records is extremely limited so that the smaller events (NM or 0.1 to 0.2 c/s) have no quantitative usefulness. NR has been used to indicate

Sample Doppler record illustrating the range in magnitude of the sudden frequency deviations detected



15 - 16 APRIL, 1962
WWV - 10 Mc/s TO BOULDER, COLORADO

Figure 11.1

that no record exists for the given path and frequency for a given event. The nonexistence of records designated by NR may be due to equipment malfunction or to propagation conditions. An NR has been used when the ground wave has over-powered the sky wave on the vertical-incidence paths. NM (not measurable) indicates that an effect probably exists but that the frequency deviation cannot be measured. This is used for effects too small to measure or for which the quality of the records is not good enough to permit unambiguous interpretation.

The format of the SFD section of the table is as follows:

Time: The times of the beginning, maximum positive frequency deviation, and end of the SFD are given in universal time. If more than one distinct peak exists for a given event, the times of the maxima are listed.

Path and Frequency: The path is given by designating the transmitting and receiving locations. The operating frequency, f , is given to the nearest Mc/s.

Frequency Deviation, Δf : The maximum positive frequency deviation, $\Delta f(+)$, is given in cycles per second. If more than one distinct peak exists the frequency deviation of each maximum is given. For those events which showed a measurable negative frequency deviation, the maximum negative frequency shift, $\Delta f(-)$, is also given.

Change in Absorption, ΔA : The maximum change in absorption, ΔA , is given in decibels for those events for which it was measurable. No signal strength records are available for those events which occurred before September 1961.

Phase Path Change, ΔP : The maximum change in phase path, ΔP , is given in kilometers for selected events. The phase path change is the time integral of the frequency deviation:

$$\Delta P = - \frac{c}{f} \int \Delta f \, dt.$$

The solar flare, solar radio emissions, and the ionospheric effects sections of the table are essentially the same as given in the CRPL-F Series, Solar-Geophysical Data; the descriptive text* for this publication should be consulted for a more complete description of the information contained therein. The order in which the beginning, maximum, and end times, or duration, are given has been changed to be consistent with the SFD section of the table. The radio bursts at 18 Mc/s given in the F-Series under ionospheric effects have been included in the table under solar-radio emissions. An attempt has been made to make the table as complete as space would allow in order that the SFD data available from October 1, 1960, to December 31, 1962, may be brought to the attention of other interested workers.

Abbreviations and Symbols Used

The following list defines the abbreviations used in the table of SFD's. For those portions of the table extracted from the CRPL-F Series, only the notation which differs from that of the F-Series is explained

* "Descriptive Text and Index for CRPL-F, Part B, Solar-Geophysical Data,"

U. S. Department of Commerce, National Bureau of Standards, Central Radio Propagation Laboratory, Boulder, Colorado, November 1961, 1962, 1963.

below. For a full explanation of notation used by the F-Series, reference should be made to the Descriptive Text of the CRPL-F Series, Part B, Solar-Geophysical Data.

Time:

D - greater than

d - duration

E - less than

U - uncertain

Path:

	Transmitters	Receivers
MN	- Monrovia, Liberia	AC - Accra, Ghana
PB	- Point Barrow, Alaska	AN - Anchorage, Alaska
SS	- Sunset, Colorado	BL - Boulder, Colorado
TR	- Tripoli, Libya	FC - Fort Collins, Colorado
WWV	- Beltsville, Maryland	MY - Midway Island, Pacific
WWVH	- Maui, Hawaii	SY - Shickley, Nebraska
		WK - Wake Island, Pacific

Frequency Deviation, Δf :

NM - not measurable

NR - no record

Solar Flares:

NFR - no flare reported

NFP - no flare patrol

Solar Radio Emissions:

2800 Mc/s

1S1 - 1-Simple 1

2S2 - 2-Simple 2

3S3 - 3-Simple

4PI - 4-Post-burst increase

5 Abs - 5-Absorption

6C - 6-Complex

8G - 8-Group

9Pre - 9-Precursor

18 Mc/s

Bur - Burst

Table 11.1
Catalog of Sudden Frequency Deviations
Observed from October 1960 through December 1962

Date	SFD's					Solar Flares					Solar Radio Emissions					Ionospheric Effects			
	UT Beg - Max - End	Path WWV-BL	† Mc/s (+)	Δf, cps Mc/s (-)	ΔA db	-ΔP km	UT Beg - Max - End	UT Beg - Max - End	Imp	UT Beg - Max - End	Type Freq Mc/s	Int or Peak Flux	UT Beg - Max - End	Type Imp					
1960																			
10-05	2023D- 2024	WWV-BL	20	0.1			2022		S										
10-05	2038- 2038D- 2039	WWV-BL	20	0.1			2038		S										
10-08	1802- 1803 - 1805	WWV-BL	20	0.2			1802- 1812- 1830U	1											
10-09	2340- 2341- 2342	WWV-BL	20	0.1			2336		S										
10-11	1609- 1610- 1612	WWV-BL	20	0.1			MFR		1610.2-1610.7-1611.2	181	2800	4							
10-11	1759- 1800- 1802	WWV-BL	20	0.1			1746- 1810- 2007	2	1748 - 1815 - 1834 1759.5-1804.7-1812 1803.4-1804.7-1807	353A 280f 8	2800 2800 108	13 190 3	1800- 1833- 1805-	1850 SEA 1812- 1845	S-SWF SEA SCVA ABS	1+	1+	20	
10-12	1724- 1726- 1731	WWV-BL	20	0.1			1722- 1728- 1820	1	1722 - 1726.5 - 1731 1725 - 1736.5 - 1739 1734 - 1736.5 - 1739 1725.0-1727.5-1730 1726 - -1730 Bar	353A 6cf 6cf 6cf 8 Bar	2800 2800 2800 2800 8 18	8 29 29 29 8 1	1729- SL-SWF	2-					
10-12	1743- 1744- 1745	WWV-BL	20	0.1			1742- 1750- 1852	1	1745.5-1748 - 1752.5 1751.5-1753.0-1753.5 1756.8-1758.9-1801	6cf 3 8	2800 108 108	83 3 3	1744- 1747- 1751-1815	1810 SEA SCVA ABS	1	1	20		
10-12	1856- 1857- 1903	WWV-BL	20	0.1			1856		S										
10-13	1722- 1724- 1726	WWV-BL	20	0.3			1722- 1728- 1820	1											
10-15	1923- 1924D-1927	WWV-BL	20	0.3			1924- 1925- 1943	1	1924 -1924.5- 1926 1928- - 1932	2S2f Bur	2800 18	12 2							
10-26	1836- 1838- 1841	WWV-BL	20	0.1			1834		S										
11-02	1941- 1943- 1945	WWV-BL	20	0.2			1942		S	1941 - 1942 - 1945	6cf	2800	3						
11-03	1821- 1823- 1831	WWV-BL	20	0.5	0.1		1819E		S	1821.5-1824 - 1831.5	6cf	2800	9						
11-05	1536- 1539E-1543	WWV-BL	20	0.3	0.1		NFR												
11-07	1919- 1919D-1921	WWV-BL	20	0.1			1920E		S										

Date	SFD's						Solar Flares						Solar Radio Emissions						Ionospheric Effects			
	UT		Path	f Mc/s	Δf , cps (+)	Δf , cps (-)	ΔA km	$-\Delta P$ km	UT		UT		Type	Freq Mc/s	Int or Peak Flux	UT	UT		Type	Imp		
	Beg -	Max - End							Beg -	Max - End	Beg -	Max - End					Beg -	Max - End				
1960	2110- 2112D-2114	WWV-BL	20	0.2			2110		S													
11-10	1421E-1422 -1425	WWV-BL	20	0.1			1422E		S													
11-11	1508E-1508D-1509	WWV-BL	20	0.6			1510E-1510U-1558U	1	1508.5-1509	-1509.5	1S	2800	6									
11-11	1629 -1630 -1631	WWV-BL	20	0.2			1629E		S													
11-11	1709 -1710 -1717	WWV-BL	20	0.8	0.3		1704		S													
11-11	2054E-2054D-2056	WWV-BL	20	0.2			2052		S													
11-12	1324 -1328E-1339	WWV-BL	20	11.2	0.8		1315 -1330 -1425D	3+	1240E -	-1425D	9Pre Gt Bur 6	2800	11	1325- 5500	1350	SCWA	3					
									1320 -	1345 -1920	6	2800	2	1325- 1326-	1345-1530	SEA	2+					
									1347 -	-2320	108					-1600	S-SWF	3+				
11-12	1657 -1658 -1659	WWV-BL	20	0.2			1657		S													
11-14	1551 -1552 -1554	WWV-BL	20	0.2			1554E-		1													
11-14	2037 -2038 -2040	WWV-BL	20	0.2			2036		S													
11-14	2117 -2119E-2122	WWV-BL	20	0.4			2114 -2120 -2154	2														
11-15	1656 -1657 -1659	WWV-BL	20	0.3			1657		S													
11-15	2101 -2102 -2104	WWV-BL	20	0.1			2100		S													
11-15	2122 -2122D-2124	WWV-BL	20	0.2			2120		S													
11-16	1810 -1811 -1814	WWV-BL	20	0.1			NFR															
11-17	1504 -1506E- -1507D-1510	WWV-BL	20	0.2			1506 -1511 -1538	1	1504.5-1506	-1508.5	6C 4PI	2800	38									
11-17	1751 -1755 -1757	WWV-BL	20	0.2			1754 -1756 -1806	1			S											
11-17	1925 -1926 -1927	WWV-BL	20	0.1			1750		S													
11-18	1507 -1510 -1512	WWV-BL	20	0.2			1920		S													
11-18	1742E-1742 -1744	WWV-BL	20	0.2			1508		S													

Date	SFD's						Solar Flares						Solar Radio Emissions						Ionospheric Effects								
	UT		Path		f Mc/s	Δf , cps (+)	Δf , cps (-)	ΔA	$-\Delta P$	km	Beg -	Max -	End	UT		Beg -	Max -	End	Type	Freq Mc/s	Int or Peak Flux	UT	Type	Imp			
1960	Beg -	Max -	End	WWV-BL	20	NM	0.2			1543	-1551	-1649	2	1554	-1555	1557.5-1557.5-1558.5	1S1	2800	1.08	4							
11-19	1549E-	-1600	WWV-BL	20	NM	0.2				2026	-2045	-2053	1	2017	-2020	-2024	1	1939	-	-2023	9Fre	2800	14	2023-2023-2041-2140	SL-SMF	3-	
11-19	2042	-2043	-2045D	WWV-BL	20	0.2				2017	-2020	-2024	1	2023	-	-2026.5-2110	6cf	2800	2800	2	400	400	14	2028-2028-2033-2340	SEA, SCA, ABS	2+	
11-20	2023E	-2023	-2024	WWV-BL	20	0.1																			3		
11-21	2104	-2106E	-2108	WWV-BL	20	0.2				2035	-2105	-2148	1													80	
11-26	1803	-1805	-1807	WWV-BL	20	0.1				1804																	
12-02	1841	-1841D	-1842	WWV-BL	20	0.1				1840																	
12-02	1904	-1905	-1907	WWV-BL	20	0.1				1904																	
12-03	1637	-1638	-1642	WWV-BL	20	0.2	0.1			1631																	
12-03	1826	-1828	-1831	WWV-BL	20	0.1				1820																	
12-06	1614	-1616	-1618	WWV-BL	20	0.5				1615																	
12-06	1917	-1919	-1920	WWV-BL	20	0.2				1918																	
12-06	2027	-2029	-2031	WWV-BL	20	0.2				2025																	
12-16	1523	-1524	-1528	WWV-BL	20	0.1				1517	-1532	-1630	2	1520	-1550	-1630	8	108	3	3	3S3A	2800	9	1530-	-1605	SL-SMF	1+
12-19	2336	-2337	-2338	WWV-BL	20	0.3				2334																	
12-20	1856	-1858	-1904	WWV-BL	20	0.2				1852	-	-1900D	1														
12-21	1843	-1844	-1845D	WWV-BL	20	0.1				1842E																	
12-26	1622	-1625	-1630	WWV-BL	20	0.4				1624																	

Date 1960	SFD's				Solar Flares				Solar Radio Emissions				Ionospheric Effects			
	UT Beg - Max - End	Path Mc/s	f Mc/s	Δf , cps (+/-)	ΔA , db (+/-)	$-\Delta P$ km	UT Beg - Max - End	UT Beg - Max - End	Type	Freq Mc/s	Int or Peak Flux	UT Beg - Max - End	Type	Imp		
12-27 1960 1536 -1537D-1539	WWI-BL	20 15	NR 0.2				1536 -1539-1544D	1								
12-27 2020 -2021 -2022	WWV-BL	20 15	NR 0.2				2021									
12-27 2040 -2041 -2043	WWV-BL	20 15	NR 0.2				2037									
12-27 2057E-2057 -2059	WWV-BL	20 15	NR 0.1				2046									
12-30 0140 -0141 -0145D	WWVH-BL	15	0.6	0.2			0141 -	-0148	1							
12-30 1700E-1700 -1702	WWV-BL	20 15	0.1				1659									
12-30 1730 -1730D-1732	WWV-BL	20 15	0.2	0.4			1726 -1740 -1757	1	1725 -	-2312	7	108	2			
12-30 1739 -1740 -1742	WWV-BL	20 15	0.1	0.2			1740									
12-30 1806D-1807 -1809	WWV-BL	20 15	0.1	0.2			1806									
12-30 1826 -1831 -1834	WWV-BL	20 15	0.3	0.4			1826 -1833 -1851	1								
12-31 1413 -1414D-1416	WWV-BL	20 15	0.2	0.2			1407 -	-1430	1+							
12-31 2009 -2009D-2010	WWV-BL	20 15	0.2	0.2			2008									
1961 01-01 1538 -1539 -1541	WWV-BL	20 15	0.1	0.1						NFR						
01-01 1640 -1641 -1643	WWV-BL	20 15	0.1	0.2						NFR						
01-03 1518 -1520 -1524	WWV-BL	20 15	0.1	0.1						1520	S					

Date	SFD's						Solar Flares						Solar Radio Emissions						Ionospheric Effects			
	UT		Path	f Mc/s	Δf , cps (+)	ΔA , db (-)	$-\Delta P$ km	UT			UT			Type	Freq Mc/s	Int or Peak Flux	Beg - Max - End	UT		Type	Imp	
	Beg -	Max -						Beg -	Max -	End	Beg -	Max -	End					Beg -	Max -			
1961	01-03	1907 -1908 -1914	WWV-BL	20 15	0.7 NR	0.2		1900										1910-	-1925	SL-SMF	1-	
	01-03	1952 -1953 -1954	WWV-BL	20 15	0.2 NR		1952															
	01-04	0206 -0208 -0223	WWVH-BL	15	1.0	0.2		0206	-0208	-0220	2							0207- 0206-0210-0223	-0230	S-SMF SCNA ABS SEA	1 1 25 1+	
	01-04	1623 -1624 -1627	WWV-BL	20 15	0.3 0.1		1621											0207-0225-0304				
	01-04	1710E-1710D-1724	WWV-BL	20 15	0.6 0.3		1729E-1729E-1747U	1	1710	-1711 at:10	-1719						2800 2800	40 17	1712- 1707-1720-1803 1713-1721-1800	SL-SMF SEA SCNA ABS	1+ 2 1 20	
	01-08	1827 -1828 -1830	WWV-BL	20 15	0.1 0.1																	
	01-18	1727 -1728 -1729	WWV-BL	20 15	0.1 NR																	
	01-27	1638E-1639E-1641	WWV-BL	20 15	0.2 NR		1636															
	01-29	2133 -2134 -2136	WWV-BL	20 15	0.1 0.3		2133															
	01-29	2148E-2149E-2150D	WWVH-BL	15	1.2		2146															
	01-30	1423E-1423D-1435	WWV-BL	20 15	1.8 1.8	0.2 0.3	1420	-1425	-1440	1	1423.8-1424.7-1430.8 1412E-1508 1424.0-1425.5-1426.0 1426.0-1428.0-1429.5						2800 2 108 3	160 2 108 3	1423- 1425- -1440 -1445	S-SMF SEA	1	
	01-30	1856 -1858E-1859	WWV-BL	20 10	0.2 NM		1842															
	01-30	2002 -2004 -2010D	WWV-BL	20 10	3.0 6.6	1.2 NM	2000	-2004	-2013	1	2003 2004 2010	-2006 -	-2011				282f Bur Bur	2800 18 18	70 1 1	2005-2011-2033 2006E-2009-2010D SEA SCNA ABS	1 1 10	

Date	SFD's						Solar Flares			Solar Radio Emissions			Ionospheric Effects		
	UT Beg - Max - End	UT Path	f Mc/s (+)	Δf , cps (+)	ΔA , db (-)	$-\Delta P$ km	UT Beg - Max - End	UT Beg - Max - End	Type	Freq Mc/s	Int or Peak Flux Beg - Max - End	UT Beg - Max - End	Type	Imp	
01-31 1511 -1514 -1526	WWV-BL	20 1.0 10 2.4	0.4 0.7			1509 -1514 -1535	1	1511.5-1514.3-1516.5 1512.0-1513.2-1514.6 1517.0-1518.3-1518.9	2S2f 4PI 8 3	2800 2800 1.08 1.08	350 1512- 2 3	-1526	S-SMF	1	
01-31 1724D-1726 -1727	WWV-BL	20 0.2 10 NM				1717									
01-31 2109 -2110 -2113	WWV-BL	20 0.2 10 0.2				2108									
01-31 2134E-2135E-2137	WWV-BL	20 0.5 10 1.0				2131 -2137 -2155	1	2133.5-2135 -2139 2131.0-2131.9-2132.5 2133.0-2135.5-2136 2134 - -2137	2S2 3 8 Bur 18	2800 1.08 1.08 18	14 2 3 1	2137-2140-2153 2 2137-2145-2200	SCNA, ABS, SEA	1 1	
02-02 1432 -1433D-1435	WWV-BL	20 0.1 10 NM													
02-02 1852 -1854 -1856	WWV-BL	20 0.1 10 0.1													
02-03 1853 -1854 -1856	WWV-BL	20 0.1 10 0.2													
02-03 1908 -1910D-1914	WWV-BL	20 0.2 10 NM													
02-04 1702 -1703 -1705	WWV-BL	20 0.2 10 0.2													
02-06 1411 -1414 -1416	WWV-BL	20 NR 10 0.3				1410 -1416 -1425	1+								
02-12 1506 -1508D-1510	WWV-BL	20 0.1 10 0.3													
02-14 1355 -1357 -1359	WWV-BL	20 NR 10 0.2													
02-17 2203E-2205 -2210	WWV-BL WWVH-BL	20 0.3 10 0.4													

Date 1961	SFD's					Solar Flares			Solar Radio Emissions			Ionospheric Effects			
	UT Beg - Max - End	Path Mc/s	f Mc/s	Δf , cps (+)	Δf , cps (-)	ΔA km	$-\Delta P$ km	UT Beg - Max - End	UT Beg - Max - End	Type	Freq Mc/s	Int or Peak Flux	UT Beg - Max - End	Type	Imp
02-17	2213 -2214 -2216	WWV-BL WWVH-BL	20 10	0.1 0.1				NFR							
02-25	0008 -0009 -0011	WWV-BL	20	0.1				0008							
02-25	0025 -0025D-0028	WWV-BL	20	0.2				NFR							
03-14	1728 -1728D-1730	WWV-BL	20	NR				1722							
03-14	2041 -2042 -2044	WWV-BL	20	NR				2040							
03-16	1641 -1643E-1644	WWV-BL	20	0.2				1640E-	-1700D	1	1642.8-1643.6-1645	3	108	2	
03-18	1738 -1739D-1758	WWV-BL	20	0.5	0.2			1738 -1742 -1810	1+	1738.5-1741.5-1747	7 Irreg Act	2800	15	1740-1743-1755	SEA 1
			10	0.1					1642 -	-1644	IIIG	450-30	2		
			10	0.9	0.4						IIIG	420-25	3		
			10	0.9	0.4						IIIG	420-25	3		
											II	115-70	1		
											II	115-70	1		
											Bur.	80-25	2		
											Bur.	18	1		
03-23	1300 -1304 -1314	WWV-BL	20	NR				1217E-	-1236D	1	1315 -1618 -1825	7	108	3	
03-26	1831 -1832 -1843	WWV-BL	20	0.6	0.1			1830			1320 -	-2040	1	400-25	1-3
03-26	2215 -2217 -2220	WWV-BL	20	0.1	0.2			2215E							
03-27	1417 -1419 -1427	WWV-BL	20	0.1	0.3			1416E-	1450D	1	1428.4-1429.0-1429.6	3	108	2	
03-27	1718 -1721 -1724	WWV-BL	20	0.2	0.4			1714							
03-28	1716 -1717 -1720	WWV-BL	20	0.1	0.3			1715							

Date	SFD's					Solar Flares					Solar Radio Emissions					Ionospheric Effects			
	UT		Path	f Mc/s	Δf , cps (+)	Δf , cps (-)	ΔA	$-\Delta P$ km	UT		UT		Type	Freq Mc/s	Int or Peak Flux	UT		Type	Imp
	Beg -	Max - End		Mc/s	(+)	(-)	db	km	Beg -	Max -	End	Beg -	Max -	End	Beg -	Max -	End		
1961 03-28	1908 -1909 -1911	WWV-BL	20	0.1					1908										
03-28	2214 -2214D-2216	WWV-BL	10	0.1					2214										
03-29	1643E-1643D-1645D	WWV-BL	20	0.2					1641										
03-29	1832E-1833E-1835	WWV-BL	10	0.1					1831										
03-29	2253 -2256 -2259	WWV-BL	20	0.1					2253	-2259	-2323	1							
03-30	0028 -0029 -0031	WWV-BL	20	0.1					0023										
03-30	1437 -1438 -1441	WWV-BL	20	0.1					MFR										
03-30	1902 -1903 -1906	WWV-BL	10	0.3					1848	-1910	-1930	1	1902	-1903	-1906	2800	13		
03-30	2135 -2136 -2138	WWV-BL	20	0.3					2134							2800	2		
04-03	1710 -1712E-1716	WWV-BL	20	NR	0.6				1711	-	-1725D	1+	1711	-1711.8-1712.5	282f	2800	35		
04-04	1411 -1413 -1415	WWV-BL	10	NR	0.2				1411										
04-04	1920D-1923E-1926	WWV-BL	20	0.1					1921										
04-04	2233 -2234D -2237 -2239	WWV-BL	20	0.1					2233	-2240	-2306	1	2232.5-2237.7-2244	6cf	2800	25			
			10	0.3												580-90	2		
			20	0.2												130-50	2		
			10	0.4															

Date	SFD's								Solar Flares				Solar Radio Emissions				Ionospheric Effects				
	UT		Path	f Mc/s	Δf , cps		ΔA	$-\Delta P$ km	UT		Imp	UT		Type	Freq Mc/s	Int or Peak Flux		UT	Beg - Max - End	Type	Imp
	Beg -	Max -			(+)	(-)			Beg -	Max -		Beg -	Max -			Beg -	Max -				
04-05 1551 -1554	WWV-BL	20	NR	0.4				1545			S										
04-05 -1555D-1558	WWV-BL	10	NR	0.5				1555	-1629	-1647	1+	1603.7-1604.2-1604.4	3	108	2						
04-05 1621 -1624 -1640D	WWV-BL	20	2.1	0.2				1555	-1629	-1647	1+	1623.5-1625.5-1627.5	6C	2800	14	1623-	1623-1626-1641	S-SMF	1+		
		10	0.7	0.5				1556	-1625	-1635	1	1624	IIIg	975-600	1-	1623-1626-1641		SCVA	25		
04-05 1814 -1815 -1817	WWV-BL	20	0.1	0.2				1800			1625	-	-1628	540-950	1-	1624-1629-1717		SEA			
04-05 2055 -2057E-2100	WWV-BL	20	0.2	0.3				2051	-2059	-2149	1	1815.2-1816.2	3	108	2						
04-06 1749E-1751 -1753	WWV-BL	20	0.2	0.3				2056			2056	-2141	3S3A	2800	3						
04-06 1835 -1836D-1838	WWV-BL	20	0.1	0.3				2059	-2059.9-2108		2056	-	2056	108	2						
04-06 2129 -2132 -2136	WWV-BL	20	0.1	0.3				2104	-		2056	-2104	2	540-950	3						
04-08 1557 -1559 -1601	WWV-BL	20	NR	0.2				2131	-2140	-2223	1	2130	-2230	3S3A	2800	3					
04-09 1533 -1534D-1537	WWV-BL	20	NR	0.7				2132	-	-2132.7-2133.5	2132	-	-2132.7-2133.5	1S1	2900	4					
04-10 1828E-1830 -1833	WWV-BL	20	0.2	0.6				1532	-	-1541	1										
04-10 1924 -1925D-1928	WWV-BL	20	0.2	0.5				1827			1829	-1831	-1834	282f	2800	14					
		10	0.4	0.4				1924			1825	-1925.8-1926.5	4PI	2800	1.8						
04-10 2232E-2233 -2235	WWV-BL	20	0.2	0.4									NFR	1S1	2800	3					
04-11 1717 -1718D-1720	WWV-BL	20	NR	0.2				1720	-	-1724	Bur					108	3				
		10	0.2	0.2									NFR	3	108	3					

Date 1961	SFD's							Solar Flares			Solar Radio Emissions			Ionospheric Effects		
	UT		Path	f Mc/s	Δf , cps		ΔA km db	UT		UT	Type	Freq Mc/s	Int or Peak Flux	UT	Type	Imp
	Beg	Max - End			(+)	(-)		Beg - Max - End	Imp							
04-15 1616 - 1617D - 1619	WWV-BL	20 10	WWV-BL	20 0.3	0.1	0.2	1604	S								
04-18 2355E-2355D-2357	WWV-BL	20 10	WWV-BL	20 0.2	2356			S								
04-19 1859 - 1900D-1906	WWV-BL	20 10	WWV-BL	20 0.7			1900	S								
04-24 0042 - 0043 - 0045	WWV-BL	20 10	WWV-BL	20 0.3			0035 -0050 -0145	1								
04-25 2007 - 2008D-2022	WWV-BL	20 10	WWV-BL	20 0.6	0.1	0.6	2003 -2010 -2030	1	2007.3-2008.2-2009.7	282	2800	10.7				
04-26 1652 - 1700E-1720D	WWV-BL	20 10	WWV-BL	20 1.2	0.3	1.2	1648 -1718 -1945	3	1640 -Indet -2037 1656.8-1702 -1704.8 1647.5-1648 -1648.1	353A 6C 3	2800 2800 108	32 18.3 2	1650- 1652-1707-1825 ABS	3 2 30		
04-26 1730E-1730D-1734	WWV-BL	20 10	WWV-BL	20 0.5			1755E-1758 -1834D	2+								
04-26 2352 - 2353 - 2355	WWV-BL	20 10	WWV-BL	20 0.1			2353	S								
04-27 1611 - 1613 - 1615	WWV-BL	20 10	WWV-BL	20 0.2			1607E	S								
04-27 1617 - 1618 - 1620	WWV-BL	20 10	WWV-BL	20 0.2			1612	S								
04-27 1709 - 1710 - 1715	WWV-BL	20 10	WWV-BL	20 0.3			1708	S								
04-27 1740 - 1741 - 1743	WWV-BL	20 10	WWV-BL	20 0.2			1738	S								
04-27 1835E-1836D-1840	WWV-BL	20 10	WWV-BL	20 0.5			1836	S								
04-27 1933 - 1936 - 1940	WWV-BL	20 10	WWV-BL	20 0.3			1933	S	1934.3-1934.7-1935.3	1S1	2800	3.8				
04-27 2205 - 2207E-2211	WWV-BL	20 10	WWV-BL	20 0.6			2202	S								

Date 1961	SFD's				Solar Flares				Radio Emissions				Ionospheric Effects			
	UT Beg - Max - End	Path	f Mc/s	Δf , cps (+)	Δf , cps (-)	ΔA dB	$-\Delta P$ km	UT Beg - Max - End	UT Beg - Max - End	Type	Freq Mc/s	Int or Peak Flux	UT Beg - Max - End	Type	Imp	
04-28	1212 -1213 -1216	WWV-BL	20 10	NR 0.4				1201 -	-1239D	1	1205 -Indet -1235 1211.7-1212.9-1214	333A 282	2800 2800	5.3 8.9		
04-28	1622 -1624 -1628	WWV-BL	20 10	MM 0.4				1622		S						
04-28	1904 -190bD-1905	WWV-BL	20 10	NR 0.1				1905		S						
04-28	1940 -1941 -1943	WWV-BL	20 10	NR 0.2						MFR						
04-28	2010 -2012 -2014	WWV-BL	20 10	MM 0.4				2011		S						
04-28	2049E-2051D-2054	WWV-BL	20 10	MM 0.3				2047		S						
04-29	1406 -1407 -1408	WWV-BL	20 10	MM 0.2					1406	S						
04-29	1451 -1452D-1455	WWV-BL	20 10	MM 0.1					1451	S						
04-29	1537 -1538 -1539	WWV-BL	20 10	MM 0.2					1540E	S						
05-03	1549E-1550 -1551	WWV-BL	20 10	0.1 MM						MFR						
05-03	2330 -2331 -2333	WWV-BL	20 10	0.1 0.3						MFR						
05-04	1309E-1310E-1313	WWV-BL	20 10	MM 0.6					1309 -1313 -1323	1	1309.5-1310.3-1312.5	1S1	2800	4		
05-04	1614 -1615D-1617	WWV-BL	20 10	0.2 MM					1615 -1617 -1637	1						

Date	SFD's					Solar Flares					Solar Radio Emissions					Ionospheric Effects		
	UT Beg - Max - End	Path	f Mc/s	Δf , cps (+)	Δf , cps (-)	ΔA km	ΔP km	UT Beg - Max - End	UT Beg - Max - End	Imp	Type	Freq Mc/s	Int or Peak Flux	UT Beg - Max - End	Type	Imp		
1961-05-01	2204 -2207 -2211 -2240	WWV-BL WWV-BL	20 20 10	NR 1.4 0.4	NR 2.2 2.2	2145 -2212 -2333D	3	2145 -Indet 2205 -2208.8-2214. 2207.5-2208.6-2210.5 2202 - 2209 - 2207.5 - -2210	2205 - -2208.8-2214. 2207.5-2208.6-2210.5 -2205 - -2212 -2210	3S3A 2S2f 3 Bur Bur IV	2800 2800 108 18 18 2100	10 95 2 2 2 2	2205- 2203-2225-2308 2205-2220-2300U	SL-SWF SEA SCNA ABS	1+ 2 2 50			
1961-05-05	1622 -1624 -1625	WWV-BL	20 10	NR 0.2	NR 0.4	1609 -	1	-1627D	1									
1961-05-05	1725 -1726 -1728	WWV-BL	20 10	NR 0.4	NR 0.2	1724 -1726 -1731	1											
1961-05-05	1733 -1735 -1738	WWV-BL	20 10	NR 0.2	NR 0.4	MFR												
1961-05-05	1929 -1930 - -1932 - -1942E-1950	WWV-BL WWV-BL WWV-BL	20 20 20	MM 0.6 0.5	MM 0.6 0.5	1928 -1933 -1949 1928 -1945 -1949	1 1	1929 -1930 -1949 -1930	1929 - -1949 -1930	3 IIIG 250-25	108 3	108 3	250-25	IIIIG	3			
1961-05-05	2231 -2232 -2242	WWV-BL	20 10	NR 0.8	NR 0.7	2231	S	2230.0-2232.0-2232.0 2230 -	-2232	3 IIIG 300-25	108 3	108 3	2236-2248-2335	SEA	2			
1961-05-09	1543 -1544D-1545D	WWV-BL	20 10	1.6 2.4	MM 0.3	1540 -1552 -1942	2	1540 -Indet 1543 -1544.8-1546.3 1551 -	-1830 -1544.8-1546.3 -1621	3S3A 2S2f Bur	2800 2800 18	6 9 4						
1961-05-10	1858 -1859E-1902	WWV-BL	20 10	0.2 1.8	MM 0.3	1858	S	1858.3-1859.6-1900.1	2		108	2						
1961-05-11	1927 -1929 -1931	WWV-BL	20 10	0.1 0.3	MM 0.3	1927	S											
1961-05-12	1355 -1356 -1357	WWV-BL	20 10	NR 0.6	NR 0.6	1354	S	1250 -Indet -1515 1355.2-1355.8-1356.9 1355.2-1356.8-1356.9	3S3A 2S2 3	2800 2800 108	5 12 3							
1961-05-12	1757 -1758D-1801	WWV-BL	20 10	NR 0.3	NR 0.3	1758	S	1803.2-1803.8-1803.8	3		108	3						

Date	SFD's						Solar Flares			Solar Radio Emissions			Ionospheric Effects		
	UT Beg - Max - End	Path	f Mc/s (+)	Δf , cps (-)	ΔA db	$-\Delta P$ km	UT Beg - Max - End	UT Beg - Max - End	Type	Freq Mc/s	Int or Peak Flux	UT Beg - Max - End	Type	Imp	
1961															
05-12	1825 -1826D-1829	WWV-BL	20 10	NR 0.2			1825 -1828 -1838	1							
05-13	0000 -0000D-0001	WWV-BL	20 10	NR 0.4			0002E- -0006	1							
05-13	1131 -1131D-1132	WWV-BL	20 10	NR 0.1					MFR						
05-15	1940 -1940D-1942	WWV-BL	20 10	MM 0.3			1938		S						
05-24	2203 -2204 -2206	WWV-BL	20 10	NR 0.1			2200		S						
05-25	1553 -1555E-1559	WWV-BL WWVH-BL	20 10	MM 0.6			1555E- -1606D	1							
05-28	1413 -1414 -1417	WWV-BL	20 10	0.1 0.2			1412		S						
05-28	1906 -1907E-1909	WWV-BL	20 10	0.4 1.6	0.2		1904		S						
05-28	2023 -2025 -	WWV-BL	20 10	0.1 0.4	0.6		2024		S						
05-28	-2028 -2032	WWV-BL	20 10	0.1 0.3			2340		S						
05-28	2341 -2342D-2344	WWV-BL	20 10	MM 0.1			1928		S						
05-29	1930 -1931 -1932	WWV-BL	20 10	MM 0.2											
06-05	1521 -1525 -1536	WWV-BL WWVH-BL	10 10	MM MM			1520 -1538 -1604	1	1520 -1528 -1532.5	6C 4PI Uncl	2800 2800 125	1525- 1525-1535-1610	S-SWF SPA	1+	
06-06	2328 -2329 -2332	WWV-BL	10 10	MM 0.4			2328		1523 -	-1531					
06-09	1436E-1436D-1445D	WWV-BL	10				1436 -1440 -1508	1							
															1438- -1452

Date 1961	SFD's						Solar Flares			Solar Emissions			Ionospheric Effects			
	UT		Path	Δf , cps Mc/s	ΔA dB (+)	$-\Delta P$ km (-)	UT		Type	Freq Mc/s	Int or Peak Flux	UT		Type	Imp	
	Beg -	Max - End					Beg -	Max - End				Beg - Max - End	Type			
06-09	1510 -1511	-1513	WWV-BL	1.0	NN		1511 -	-1526	1	1510 -1511.1-1512.7	1s1	2800	4			
06-09	1736 -1736D	-1738	WWV-BL	1.0	0.5											
06-09	1751 -1751D	-1753	WWV-BL	1.0	0.6		1750 -1752 -1756	1							2+	
06-09	2103D-2104	-2107	WWV-BL	1.0	0.8		2100 -2103 -2110	1							1+	
06-09	2249E-	-2259	WWV-BL	1.0	NN		2248 -2254 -2306	2							22	
06-10	1516 -1517E-	-1518 -1522	WWV-BL	1.0	0.6		1509 -1514 -1526	1							1+	
06-11	1501 -1507	-1530	WWV-BL	1.0	NN		1502 -1518 -1612	2	1500	-1507 -1527	6cf	2800	365	1503-1600	S-SWF	
			WWVH-BL	1.0	NN				1d:21	4PI	4PI	2800	10	1505-1513-1520	SCNA	
									1505.0-1506.0-1509.5	9a	9a	108	3	1505-1519-1600	ABS	
									1509.5-1513 -1529.5	9b	9b	108	3		SEA	
									1505 -	-1511	Bur	18	2+			
									1515 -	-1519	Bur	18	2			
06-14	1629B-1630	-1633	WWV-BL	1.0	NN	0.8	1618 -1631 -1650		1611 -Indet -1651	3834	2800	2	1625 -	-1650	SL-SWF	
									1612 -1614.5-1618	1S1f	2800	6			1+	
									1627 -1629.5-1635	2S2f	2800	30				
									1618 8-1620.0-1620.8	3	108	3				
									1633.0-1634.2-1637.5	8	108	2				
									1629 5-	IIIIS	380-850	1-				
									1629 5-	IIIB	780-750	1-				
06-15	1635 -1641	-1645D	WWV-BL	1.0	3.2		1622 -1636 -1705	1+	1630 -Indet -1725	383fa	2800	5	1640-1650-1705	SCNA	1	
									1638 -1642 -1647	2S2f	2800	185			20	
									1638.7-1640.5-1641.5	2	108	2	1640-1655-1710	ABS	1	
									1643.0-1645.0-1646.5	8	108	3	1640- -1715	SEA	1+	
									1651.7-1653.5-1656.0	9a	108	3		S-SWF		
									1700.0-1708.0-1849.0	9b	108	2				
									1635 -	-1638	Bur	18	1+			
									1638 -	-1643	Bur	18	2			
									1644 -	-1653	Bur	18	1+			
06-15	1702 -1706	-1708	WWV-BL	1.0	0.6		1702 -	-1730	1	1717.5-1718.5-1723.5	2S2f	2800	95	1720 -	-1735	S-SWF
06-15	1718E-1718D	-1723	WWV-BL	1.0	5.0	1.0	1718E-1720U-1728U	1	1717 -	-1722	Bur	108	2			1-
06-15	1833 -1834	-1835	WWV-BL	1.0	0.2		1833									

Date 1961	SFD's						Solar Flares						Solar Radio Emissions						Ionospheric Effects								
	UT		Path		f Mc/s	Δf, cps (+)	ΔA db (-)	-ΔP km	UT		UT		UT		UT		UT		UT		UT		Type	Freq Mc/s	Int or Peak Flux	Type	Imp
Beg - Max - End	Beg - Max - End	WWV-BL	WWV-BL	10	0.3			Beg - Max - End	Beg - Max - End	Beg - Max - End	Beg - Max - End	Beg - Max - End	Beg - Max - End	Beg - Max - End	Beg - Max - End	Beg - Max - End	Type	Imp	Beg - Max - End	Type	Imp						
06-15 1840 -1842 -1845D	WWV-BL	10	0.3					1840																			
06-15 2203 -2204 -2210	WWV-BL	10	0.7					2200																			
06-16 1754 -1755 -1757	WWV-BL	10	0.4					2202																			
06-16 2009 -2010 -2015	WWV-BL	10	0.2					1755																			
06-23 2319 -2320 -2331	WWV-BL	10	0.7	0.3				2009																			
06-24 1859 -1902 -1911	WWV-BL	10	0.6					2318																			
06-24 1927 -1928 -1933	WWV-BL	10	0.2					1854E																			
06-24 1950 -1951 -1953	WWV-BL	10	0.3					NFR																			
06-25 1500 -1502 -1506	WWV-BL	10	0.3					1455																			
06-25 1515 -1516 -1517	WWV-BL	10	0.3					NFR																			
06-28 2053 -2054 -2059	WWV-BL	10	0.3	0.2				2051																			
06-29 1917 -1918 -1928	WWV-BL	10	0.2					1917																			
06-29 1953E-1953D-1956	WWV-BL	10	0.5	0.4				1947																			
06-29 2100 -2101 -2103	WWV-BL	10	0.4					2057																			
06-29 2105 -2109 -2112	WWV-BL	10	0.3																								
06-29 2109 -2112	WWV-BL	10	0.2																								
06-29 2109 -2112	WWV-BL	10	0.8	0.4																							
07-01 2132 -2133 -2137	WWV-BL	10	1.2	0.4				2132																			
07-02 1325 -1327D-1333	WWV-BL	10	0.4					1335E-																			
07-05 2042 -2043 -2045D	WWV-BL	10	0.2					2042																			
07-09 1507 -1507D-1509	WWV-BL	10	0.3					1506																			

Date 1961	SFD's						Solar Flares						Solar Emissions						Ionospheric Effects		
	UT		Path	Δf , cps (+)	ΔA , db (-)	$-\Delta P$ km	UT		UT		Type	Freq Mc/s	Int or Peak Flux	UT		UT		Type	Imp		
	Beg	Max - End					Beg	Max - End	Beg	Max - End				Beg	Max - End	Beg	Max - End				
07-10	1315	-1315D-1317	WWV-BL	1.0	3.1				1312	-	-1450	1						1313-	-1335	S-SWF	
07-10	1732	-1733D-1738	WWV-BL	1.0	1.6	0.6														1+	
07-10	1743	-1743D-1745D	WWV-BL	1.0	0.4	0.4			1741	-	1753	-1800	1								
07-10	1828	-1830 -1832	WWV-BL	1.0	0.4																
07-11	2313	-2313D-2315	WWV-BL	1.0	1.4				2313												
07-12	1934	-1935 -1937	WWV-BL	1.0	0.2				1940E												
07-12	1955	-1956 -1959	WWV-BL	1.0	0.4				1955												
07-12	2136	-2138 -2143	WWV-BL	1.0	0.8	0.5			2135												
07-12	2249E-	-2252	WWV-BL	1.0	NM	0.5			2248	-	2254	-2318	1								
07-13	2212	-2214E-2216	WWV-BL	1.0	1.4	0.3			2211												
07-14	1216E	-1216 -1217	WWV-BL	1.0	0.8																
07-14	1218	-1218D-1220	WWV-BL	1.0	1.0																
07-14	1222E	-1225 -1225D	WWV-BL	1.0	1.0				1227												
07-14	1314	-1314D-1316	WWV-BL	1.0	0.4				1314												
07-14	1800	-1801 -1803	WWV-BL	1.0	0.4																
07-15	1510	-1512 -	WWVH-BL	1.0	4.2				1434	-1508	-1857U	3	1510.5-1512	-1517	76	1512-1517-1530					
		-1514 -	WWVH-BL	1.0	2.8				1508	-1512	-1530	2	1536	-1610	6cf	2800	1.11	SCWA	1		
		-1520 -1530D	WWVH-BL	1.0	2.0							1505	-1616	-1845	9	1512-	3	ABS	21		
																		S-SWF	3		
																		SEA	1		
07-16	1259	-1300 -1310	WWV-BL	1.0	3.0				1258	-1300	-1316	1									
07-16	1507	-1509 -1511	WWV-BL	1.0	0.2				1507E-		-1525D	1									
07-16	1557	-1557D- -1558D-1559	WWV-BL	1.0	1.3				1556												
			WWV-BL	1.0	0.6																

Date 1961	SF'D's						Solar Flares						Solar Radio Emissions						Ionospheric Effects			
	UT Beg - Max	UT End	Path Mc/s	f Mc/s	Δf , cps (+)	Δf , cps (-)	ΔA km	$-\Delta P$ km	UT Beg - Max	UT End	Imp	UT Beg - Max	UT End	Type	Freq Mc/s	Int Peak Flux	UT Beg - Max - End	Type	Imp			
07-16 1961	1630 -1631 -1642	WWV-BL	1.0	1.4	0.8		1625		S	1620 -1628	-1650	3S3	2800	4								
07-16 1961	1650E-1651 -1653	WWV-BL	1.0	0.8			1650		S													
07-16 1961	1659 -1700 -1701	WWV-BL	1.0	0.6					NFR													
07-16 1961	1856E-1856 -1857	WWV-BL	1.0	0.3			1856E		S													
07-16 1961	1911E-1911D-1912	WWV-BL	1.0	0.5			1910		S													
07-16 1961	1920 -1923E-1929	WWV-BL	1.0	0.8			1909 -1922	-1935	1													
07-16 1961	1939 -1940D-1943	WWV-BL	1.0	1.2	0.3		1938 -1943	-2055	1+	1933 -1955	-2125	3S3A	2800	16								
	1957 -1958E-1959	WWV-BL	1.0	0.2			1938 -2040	-2055	1-	1950 -1952	-1955.3	2S2	2800	14								
	2001 -2001D-2003	WWV-BL	1.0	0.4																		
	2009 -2009D-2011	WWV-BL	1.0	0.3																		
	2030 -2020E-2022	WWV-BL	1.0	0.5																		
	2030 -2031 -	WWV-BL	1.0	0.6																		
	-2037 -2043D	WWV-BL	1.0	2.4	0.6																	
07-16 1961	2059 -2100 -2105	WWV-BL	1.0	0.6	0.4		2057		S													
07-17 1961	1435 -1436D-1438	WWV-BL	1.0	1.0					NFR													
07-17 1961	1610 -1611 -1613	WWV-BL	1.0	0.4			1610E-	-1804D	1													
07-17 1961	1649E-1649D-	WWV-BL	1.0	0.6			1645 -1657	-1711	1	1640 -1657	-1720	3S3A	2800	4								
	-1653 -	WWV-BL	1.0	0.5						1657 -1657.5-1659		6C	2800	7								
	-1655 -	WWV-BL	1.0	0.6																		
	-1658 -1700	WWV-BL	1.0	0.6																		
07-17 1961	1820 -1820D-1842	WWV-BL	1.0	0.8			1817		S	1830 -1850	-1915	3S3	2800	4								
07-17 1961	1913 -1915E-	WWV-BL	1.0	3.4	1.0		1907 -1916	-1935	1													
	-1928 -1930	WWV-BL	1.0	0.6																		
07-17 1961	2034E-2034 -2036	WWV-BL	1.0	0.3			2033		S													
07-17 1961	2132 -2133E-	WWV-BL	1.0	0.6			2138 -2255		1	2140 -2141.8-2202	d1:17	6CF	2800	54								
	-2135D-																					
	-2138 -																					
	-2140 -																					
	-2141 -																					
	-2143D-2145D																					

SCNA
2
ABS
35
S-SMF
2+
SPA
SEA
2+
2141-2142-2230
2140-2144-2300
2141-2152-2230

Date 1961	SFD's						Solar Flares			Solar Emissions			Ionospheric Effects		
	UT		Path	Δf , cps Mc/s	ΔA , db (+)	$-\Delta P$ km (-)	UT			Type	Freq Mc/s	Int or Peak Flux	UT		
	Beg	Max - End					Beg	Max - End	Imp				Beg - Max - End	Type	Imp
07-18	1441	-1441D-1443	WWV-BL	1.0	0.4		1436	S							
07-18	1917	-1917D- -1915D- -1915D-	WWV-BL	1.0	1.0 0.6 0.6		1916	S							
07-18	2051	-2052 -2057	WWV-BL	1.0	0.2		2046	S							
07-18	2103	-2104 -2106	WWV-BL	1.0	0.2		2102	S	2106 -2112 -2140						
07-18	2257	-2259 -2301	WWV-BL	1.0	0.5		2258	S							
07-19	1501	-1502 -1504	WWV-BL	1.0	0.2		1501E- -1510D	1	1452 -1454 -1550						
07-19	1806	-1808 -1810	WWV-BL	1.0	0.3		1801	S							
07-19	1906	-1910 -1922	WWV-BL	1.0	0.8		1903 -1912 -1945	1							
07-19	2055	-2059D-2110D	WWV-BL	1.0	2.0	2.4	2051 -2102 -2120	1	2100 -Indet -2114 2103-3-2105 -2109-3	3S3A 6C	2800 2800	2800 2800	2	2055-2110-2200 2100- -2125	SPA SL-SNT
07-20	1551	-	WWV-BL SS-BL	1.0 2.1	NN NN		1553	3	1552 -1553.5- -1621.3-1634 d7:30	6cf 4PI 9A	2800 2800 1.08	1200 1800 3	1550- 1551- 80	-2200 -1600 -1752- -2140	S-SNT SPA SEA SCNA ABS
07-21	1714	-1717 -1728	WWV-BL	1.0	2.6	1.4	1714 -1718 -1734	2	1655 -1827 -2330 1701 -1703.5-1721	3S3A 6cf	2800 2800	10 59	1702-1710-1900 1703-1708- 1703-1710-	S-SNT SPA SCNA ABS	
07-22	1634	-1634D-1635	WWV-BL	1.0	0.3		1636	S	1635 -Indet -1750	3S3	2800	5			
07-23	1835	-1835D-1839	WWV-BL	1.0	0.7		1835	S							
07-23	2130	-2131 -2133	WWV-BL	1.0	0.4		2130	S							
07-23	2227	-2228 -2233	WWV-BL	1.0	0.3		2227	S	2227 -	-2231	Bur	18	2		
07-24	1813	-1814 -1820	WWV-BL	1.0	0.6		1722 -1827D-2214	2+	1730 -1802 -2330D 1816 -	3S3f Bur	2800 18	16 1	1748-1810-1900 1755- -1930	SPA SL-SNT	

Date 1961	SFD's						Solar Flares						Solar Radio Emissions						Ionospheric Effects			
	UT Beg - Max - End	Path	f Mc/s	Δf, cps (+)	ΔA db (-)	-ΔP km	UT Beg - Max - End	UT Beg - Max - End	Imp Beg - Max - End	UT Beg - Max - End	Type	Freq Mc/s	Int or Peak Flux	UT Beg - Max - End	Type	Imp	UT Beg - Max - End	Type	UT Beg - Max - End	Type		
07-24	1830 -1831 -1833	WWV-BL	10	0.3			NFR															
07-25	1219 -1220 -1223	WWV-BL	10	0.3			1219		S 1224 -1224.8-1228		6C	2800	7									
07-25	1356 -1357D-1403	WWV-BL	10	0.8			1354		S 1220 -1226 -1231		Bur	18	1+									
07-25	1441 -1442 -1443	WWV-BL	10	0.9			1441		S 1335 -1357.5-1407		333f	2800	5									
07-25	2241 -2241D-2245	WWV-BL	10	0.6			2242E-2244	-2316	1 2239.5-2241.5-2243.5	d20	282f 4PI	2800	13									
07-26	1940 -1941 -1942	WWV-BL	10	0.4			1940		S 1947 -1947.8-1952		2S2	2800	45									
07-26	1946D-1947D- -1948D-1949D	? -BL ? -BL	10	4.0	1.0		1947		S 1947 -1947.8-1952		2S2	2800	45									
07-28	1956 -1957E-1959	WWV-BL	10	0.4	0.4		1954		S 2223 -2223.5-2224		1S1	2800	5									
07-28	2223 -2224 -2227	WWV-BL	10	0.3	0.4		2222		S 2223 -2223.5-2224		1S1	2800	5									
07-28	2338E-2339 -2341	WWV-BL	10	0.4			2338		S 1436 -1440 -1448	1 1438.3-1439.2-1441.8	1S1	2800	3.5									
08-10	1438 -1439 -1441	WWV-BL	10	0.6			1436	-1440 -1448	1 1438.3-1439.2-1441.8	1432 -	-1443	Bur	18	2								
08-10	1505E-1505 -1506	WWV-BL	10	0.5			1502 -	-1510D	1 1505.2-1505.5-1506	1505 -	-1510	1S1	2800	6								
08-10	2314 -2318 -2323	WWV-BL SS-BL	10	0.5	0.6		2309	-2320 -2353	1 2315.5-2316.8-2318		2S2	2800	22									
08-11	1705 -1709 -1716	WWV-BL	10	0.5			1708		S 1614 -1618 -1635D	1 1611 -Indet -1656	333A	2800	2									
08-12	1614 -1615 -1617	WWV-BL	10	0.2			1614	-1618 -1635D	1 1613.5-1616 -1618	1614 -	-1635	1S1	2800	7								
08-12	1628 -1629 - -1633 -1636	WWV-BL WWV-BL	10	0.5	0.5		1628		S 1629 -1630.3-1633	1620.5-1622.5-1625	282f 8	2800	12									
08-12	1711 -1713 -1717	WWV-BL SS-BL	10	0.6	0.6		1705	-1714 -1736	1 1712.5-1713.2-1713.5	1711.2-1714.0-1716.7	1S1	2800	3									
										1711 -	-1717			18								

Date 1961	SFD's						Solar Flares						Solar Radio Emissions						Ionospheric Effects			
	UT		Path	f Mc/s	Δf , cps (+)	ΔA , db (-)	$-\Delta P$ km	UT			Imp	UT			Type	Freq Mc/s	Int or Peak Flux	UT		Type	Imp	
	Beg -	Max - End						Beg -	Max -	End		Beg -	Max -	End				Beg - Max - End	Beg - Max - End			
08-12	2048 -2049 -	WWV-BL SS-BL WWV-BL SS-BL WWV-BL SS-BL	1.0 5 1.0 5 1.0 5	2.2 1.4 1.4 0.8 2.4 1.0	2050 -2052 -2115	1	2048.5-2051.3-2052.5 2048.9-2049.0-2053.9	6cf 4PI 8	2800 2800 108	60 4 3	2052- -2105	S-SWF	1-									
08-13	1906 -1908 -1914	WWV-BL	10	2.2	0.3	1906 -1910 -1931	1	1907.5-1909 -1919.5 1907.0-1907.5-1913 1907 -1914	2.52 2 Bur.	2800 108 18	10 2	1907-										
08-14	2214E-2214 -2216	WWV-BL	10	0.2	2213																	
08-15	1646 -1647 -1648D	? -BL	10	2.8	1640 -1647 -1710	1	1645 -1705 -1735 1646.5-1648.3-1651.5	3.3A 6cf	2800 2800	3 13	1643-1652-1720 1647-1655-1708	SPA SEA	1+									
08-18	2041D- -2054 - -2056 -2100	WWV-BL WWV-BL WWV-BL	10 10 10	0.6 0.2 0.3	2038 -2048 -2103	2	2036 -2052 -2115 2039 -2044 -2050 2054.2-2056.3-2058 2047.5-2049.3-2054 2036 - -2050	3.3A 2S2f 6C 8 Bur.	2800 2800 6C 8 108 18	12 43 28 3 3	2040- -2120 2045-2107-2135 2049E- -2200U	S-SWF SPA SEA SCNA	1+									
08-25	1608 -1611 -1612	WWV-BL	10	0.2	1608																	
08-25	1624 -1625 -1629	WWV-BL	10	0.3	1625E																	
08-25	2007 -2008 -2010	WWV-BL	10	0.6	2006																	
08-25	2356 -2356D-2357	WWV-BL SS-BL	10 4	0.1	2357																	
08-25	2358 -2358D-2400	WWV-BL SS-BL	10 4	0.3	2359 -	-	-0.018	1														
08-26	1617 -1618 -1621	WWV-BL	10	0.2	1616E- -1630D	1																
08-29	1714 -1715 -1718	WWV-BL	10	0.3	1715																	
08-29	1849E-1851 -1855	WWV-BL	10	0.5	1846																	
08-29	2020 -2021 -2024	WWV-BL	10	0.2	2021																	
08-30	1618 -1621 -1624	WWV-BL	10	0.3	1617 -1623 -1634	1																
08-31	1459 -1502 -1506	WWV-BL	10	0.4	1458 -1506 -1520	1																

Date 1961	SFD's						Solar Flares						Solar Radio Emissions						Ionospheric Effects			
	UT		Path		f Mc/s	Δf, cps (+)	ΔA db (-)	-ΔP km	UT		UT		Type	Freq Mc/s	Int or Peak Flux	UT		Type	Imp			
Beg - Max - End	Beg - Max - End	WWV-BL	WWV-BL	10	0.3				Beg - Max - End	Type	Beg - Max - End	Beg - Max - End	Beg - Max - End	Beg - Max - End	Type	Imp						
08-31 1512 -1513 -1516	WWV-BL	WWV-BL	10	0.3																		
08-31 1758 -1759 -1802	WWV-BL	WWV-BL	10	0.1																		
08-31 2109 -2110 -2111	WWV-BL	WWV-BL	10	0.2																		
08-31 2121D-2122 -2123	WWV-BL	WWV-BL	10	0.1																		
09-01 1413 -1414 -1417	WWV-BL	WWV-SY	10	MM	0.7																	
	SS-BL	SS-BL	5	MM	0.7																	
	4	MM	0.6	MM																		
09-01 1423 -1423D-1425	WWV-BL	WWV-SY	10	MM	0.3																	
	SS-BL	SS-BL	5	MM	0.3																	
	4	MM		MM																		
09-02 0320 -0322 -0324	WWVH-SY	WWVH-SY	10	3.5																		
09-02 1413 -1417 -1419	WWV-BL	WWV-SY	10	0.4																		
	SS-BL	SS-BL	5	MM	0.2																	
	4	MM		MM																		
09-02 1431 -1432 -1436	WWV-BL	WWV-SY	10	1.3																		
	SS-BL	SS-BL	5	MM	1.4																	
	4	MM	0.4	MM	0.4																	
09-02 1509 -1510 -1512	WWV-BL	WWV-SY	10	0.3																		
	SS-BL	SS-BL	5	MM	0.2																	
	4	MM	0.2	MM																		
09-02 1645D-1646 -1649	WWVH-SY	WWVH-SY	10	1.4																		
	SS-BL	SS-BL	4	MM	0.3																	

Date	SFD's						Solar Flares						Solar Radio Emissions						Ionospheric Effects			
	UT	Path	f Mc/s	Δf, cps (+)	Δf, cps (-)	ΔA dB	-ΔP km	UT	UT	Beg -	Max -	End	Imp	Beg -	Max -	End	Type	Freq Mc/s	Int or Peak Flux	UT Beg - Max - End	Type	Imp
1961	UT	Max - End																				
09-02	2235 -2238 -2240D	WWV-BL WWV-SY SS-BL	10 5 4	0.4 0.2 NM	0.3 0.2 0.2			2230 -22350	1+	2238 -	-	-2241										
09-02	2319 -2320 -2324	WWV-BL WWV-SY SS-BL	10 5 4	0.3 0.2 0.2																		
09-02	2333 -2334 -2336	WWV-BL WWV-SY SS-BL	10 5 4	0.3 0.2 0.2																		
09-03	1625 -1626 -1628	WWV-BL WWV-SY SS-BL	10 5 4	0.1 NR NM																		
09-03	1834 -1835 -1839	WWV-BL WWV-SY SS-BL	10 5 4	0.2 NR NM																		
09-03	2019 -2024 -2030	WWV-BL WWV-SY SS-BL	10 5 4	0.4 1.0 1.0																		
09-03	2040 -2045D-2100	WWV-BL WWV-SY SS-BL	10 5 4	NM 4.2 1.2																		
09-04	1430 -1432 -1434	WWV-BL WWV-SY SS-BL	10 5 4	12 NM 6	2.4 0.8	8		1425 -1435 -1512	1	1425 -	-1435	-1512										
								1431.5-1432.3-1433.5		1431.5-1432.3-1433.5	-1433.5	-1433.5										
								d14.5		d14.5	-1437.15	-1437.15										
								1435.15-		1435.15-	-1446.30	-1446.30										
								1446.15-		1446.15-	-1458	-1458										

Date	SFD's						Solar Flares						Solar Radio Emissions						Ionospheric Effects			
	UT Beg - Max - End	UT Beg - Max - End	Path	f Mc/s	Δf , cps (+)	Δf , cps (-)	ΔA km	ΔP km	UT Beg - Max - End	UT Beg - Max - End	Type	Freq Mc/s	Int or Peak Flux	UT Beg - Max - End	UT Beg - Max - End	Type	Imp					
1961-09-04	1513E-1513D- -1514 -1516	WWV-BL WWV-SY SS-BL	10 10 5 4	6.0 4.0 1.8 1.6	0.8 0.6 0.2 0.4	0.8 0.6 0.2 0.4	1512 10 5 4	-1520 -1540U -1540	1 1 1	1513.7 -1514 d42.8	-1516.2	2S2f 4PI	2800 2800	85 4	1510-1518-1600 1512-1518-1542 1515- 1515-	SPA SCIA ABS SEA S-SMF	39 1+ 30 1 1+					
09-04	1530 -1532 -1540	WWV-BL WWV-SY SS-BL	10 10 5 4	3.0 2.0 0.9 0.8	0.3 0.3 0.3 0.3	0.3 0.3 0.3 0.3	1538E		S													
09-04	1807 -1808 -1810	WWV-BL WWV-SY SS-BL	10 10 5 4	1.0 0.6 0.6 0.2	0.4 NM NM NM	0.4 NM NM NM	1807		S													
09-04	1834 -1835 -1837	WWV-BL WWV-SY SS-BL	10 10 5 4	1.1 0.8 0.8 0.2	0.4 0.4 0.4 NM	0.4 NM NM NM	1834 -1846 -2010	1+	1842.45- -1843.15		III		21-32	1	1833-1840-1910U	SPA	26					
09-04	1853 -1854 -1855	WWV-BL WWV-SY SS-BL	10 10 5 4	0.4 0.2 0.2 0.1	0.2 NM NM NM	0.2 NM NM NM	MFR															
09-04	1902 -1903D- -1905 -1909	WWV-BL WWV-SY SS-BL	10 10 5 4	2.6 1.8 1.0 0.5	0.8 0.5 0.4 0.7	0.8 0.5 0.4 NM	1902 -1905 -1919U	1	1902.8 -1903.2-1905.0		2S2f		2800	16								
09-04	1911 -1915 -1920	WWV-BL WWV-SY SS-BL	10 10 5 4	6.6 4.6 3.0 1.1	3.0 1.8 1.1 NM	3.0 1.8 1.1 NM	1911 -1924U-2018	2	1911 -1914.8 -1919		6cf 4PI		2800 2800	143 8	1913- 1914-1919-1950	SPA SCIA ABS	1+ 2 30					

Date	SFD's						Solar Flares						Solar Radio Emissions						Ionospheric Effects					
	UT Beg -	UT Max -	Path Mc/s	f (+)	Δf , cps db	ΔA , km	UT Beg -	UT Max -	UT End	Imp	UT Beg -	UT Max -	UT End	Type	Freq Mc/s	Int or Peak Flux	UT Beg - Max - End	Type	Imp					
1961																								
09-05	1415 -1418 -1420	WWV-BL WWV-SY SS-BL	10 NR 4	1.5 0.8 0.4			1415 -	-	-1510D	1	1415 -	1415.5-1417.2-1422.5	-2155	353A 6cf	2800 2800	12 88	1418-1441-1600	SEA	1					
09-05	1427 -1431 -1435	WWV-BL WWV-SY SS-BL	10 NR 4	0.8 0.5 0.4			1428E-	-	-1514D	1+	1428.3- 1432 - 1439	6cf		2800	50	1430-	-1450	S-SWF	1					
09-05	1514 -1515 -1518	WWV-BL WWV-SY SS-BL	10 NR 4	1.0 0.3 0.4			1514 -	-	-1514D	1	1509.9-1510.3-1512	1S1		2800	6									
09-05	1649E-1652 -1655	WWV-BL WWV-SY SS-BL	10 NR 4	0.5 0.6 0.4			1644 -1658 -1734	1	1647 -	1652 - 1655	2S2 4PTI	2800	20	1640- 1649-1650- 1653-1702-1730	SL-SWF SPA SEA	2+ 32 2								
09-05	1811 -1816 -	WWV-BL WWV-SY SS-BL	10 NR 4	0.3 0.6 0.4			1812																	
09-05	1822 -1825 -1829	WWV-BL WWV-SY SS-BL	10 NR 4	0.3 0.3 0.2			1817																	
09-08	1330 -1331 -1334	WWV-BL WWV-SY SS-BL	20 NR 5 4	NR NR 0.2			1331 -1335 -1350	1																
09-08	1628 -1629 -1632	WWV-BL WWV-SY SS-BL	20 NR 5	NR 0.4 0.2			1628																	

Date	SFD's						Solar Flares						Solar Radio Emissions						Ionospheric Effects			
	UT Beg - Max - End	Path	f Mc/s	Δf, cps (+)	Δf, cps (-)	ΔA db	-ΔP km	UT Beg - Max - End	UT Beg - Max - End	UT Beg - Max - End	Type	Freq Mc/s	Int or Peak Flux	UT Beg - Max - End	Type	Imp						
1961																						
09-17	1749 -1752 -1756	WWV-BL WWV-SY SS-BL	20 10 5	0.2 0.7 0.4				1748 -1756 -1808	1	1741.5-1742.5-1742.6 1750.2-1752.4-1757.9	3 2S2f d47	108 2800 4PI	2800 2800	2 2								
09-18	2041 -2044 -2045D	WWV-BL WWV-SY SS-BL	20 10 5	0.2 0.3 0.1				2042	S													
09-20	1021 -	TR-AC	20	.25				1021 -1022 -1026	1													
09-22	2050 -2051D-2054	WWV-BL WWV-SY SS-BL	20 10 5	0.1 0.2 NR				2052	S													
09-23	1103 -	TR-AC	20	.25				1101E-		-1113D	1											
09-23	1323 -	TR-AC	20	.25				1323 -		-1407	1											
09-24	0705 -	TR-AC	20	.25				0700E- 0708E-		-0900D -0850	1											
09-24	1352 -	TR-AC	20	.67				1350 -		-1431D	1											
09-25	0640 -	TR-AC	20	.5				0641 -		-0720	1											
09-25	1015 -	TR-AC	20	1.33				1016 -		-1030D	1											
09-25	1838 -1839D-1843	WWV-BL WWV-SY SS-BL	20 10 5	NR 0.7 0.2				1838 -	S	1839.5-1840.3-1841.5	2S2	2800	2800	12								
09-26	0620 -	TR-AC	20	.25				0620E-		-0903D	2											
09-26	0911 -	TR-AC	20	.25				0909E-			1											
09-26	1015 -	TR-AC	20	.25				1016E-		-1108D	2											

Date	SFD's				Solar Flares				Radio Emissions				Ionospheric Effects			
	UT Beg - Max - End	Path Mc/s	f Mc/s (+)	Δf , cps (-)	ΔA db	$-\Delta P$ km	UT Beg - Max - End	Imp	UT Beg - Max - End	Type	Freq Mc/s	Int or Peak Flux	UT Beg - Max - End	Type	Imp	
1961-11-10 1526 -1528 -1534	WWV-BL WWV-SY SS-BL	20 10 5 4	0.2 0.4 0.3 0.1			1510E- 10 NR 5 NM 4 NM	-1530D	1	1440 - -1543	IV	21-41	3				
1961-11-11 1541 -1543 -1545D	WWV-BL WWV-SY SS-BL	20 10 5 4	0.2 0.4 0.3 0.1			1540		S	1541.5-1542.5-1544.3 1542 -1543.45	III	8	108 23-41	3 1+			
1961-11-11 1915 -1918 -1922	WWV-BL WWV-SY SS-BL	20 10 5 4	0.1 0.2 0.1 0.1			NER		S								
1961-11-19 1608 -1612 -1617	WWV-BL WWV-SY SS-BL	20 10 5 4	0.1 0.2 0.1 0.1			1615E		S								
1961-11-21 1819 -1821 -1825	WWV-BL WWV-SY SS-BL	20 10 5 4	0.1 0.2 0.1 0.1			1818		S								
1961-11-22 2014 -2016 -2024	WWV-BL WWV-SY SS-BL	20 10 5 4	0.6 1.6 0.9 0.8			NM NR NM NM	10 10 10 10	0.09 0.57	2012 -2016 -2044	2			2015-2018-2045			
1961-11-24 1852 -1854 -1857	WWV-BL WWV-SY SS-BL	20 10 5 4	0.1 0.1 0.1 0.1			NM NR NM NM			1853E	S			2016-2025-2115			
														SCNA ABS SEA	1+ 25	

Date	SFD's					Solar Flares			Solar Emissions			Ionospheric Effects		
	UT		Path	f Mc/s	Δf , cps (+)	ΔA db (-)	UT		UT		Type	Freq Mc/s	Int or Peak Flux	UT
	Beg -	Max -					Beg -	Max -	End	Beg - Max - End				Type
1961														
12-01	1633	-1634D-1637	WWV-BL	20	NR	-0.4								
			WWV-SY	10	0.3									
			SS-BL	5	NR									
				4	NR									
12-01	1817	-1818 -1820	WWV-BL	20	NR	0.5								
			WWV-SY	10	0.5									
			SS-BL	5	NR	0.6								
				4	NR	0.6								
12-01	1910	-1911D-1915	WWV-BL	20	NR									
			WWV-SY	10	0.5									
			SS-SY	5	NR	0.4								
				4	NR	0.4								
12-01	2132	-2133 -2137	WWV-BL	20	NR									
			WWV-SY	10	0.5									
			SS-BL	5	NR	0.4								
				4	NR	0.2								
12-02	1920	-1922 -1926	WWV-BL	20	0.3									
			WWV-SY	10	1.0									
			SS-BL	5	NR	0.8								
				4	NR	0.5								
					NR	0.6								
12-05	1357	-1359 -1402	WWV-BL	20	NR									
			WWV-SY	10	NR	1.5								
			SS-BL	5	NR									
				4	NR									
12-06	1758	-1801 -1805	WWV-BL	20	0.2									
			WWV-SY	10	NR	0.2								
			SS-BL	5	NR									
				4	NR									

Date 1961	SFD's					Solar Flares			Solar Radio Emissions			Ionospheric Effects		
	UT Beg - Max - End	Path Mc/s	f Mc/s (+)	Δf , cps (-)	ΔA km db	UT Beg - Max - End	UT Beg - Max - End	Type	Freq Mc/s	Int or Peak Flux	UT Beg - Max - End	Type	Imp	
12-21 1820 -1821D-1824	WWV-BL WWV-SX SS-BL	20 10 5 4	0.1 0.2 NR NR			1820		S						
12-27 1657 -1701 -1706	WWV-BL WWV-SY SS-BL	20 10 5 4	0.1 0.2 NR NR			1656 -1703 -1838	1	1657 -1702 -1800	3S3	2800	5			
12-28 2134 -2135 -2137	WWV-BL WWV-SY SS-BL	20 10 5 4	0.2 0.3 NR NR			2130	S							

Date	SFD's						Solar Flares			Solar Radio Emissions			Ionospheric Effects		
	UT		Path	f Mc/s	Δf, cps	ΔA km	-ΔP db	UT		UT		Freq Mc/s	Int or Peak Flux	UT	
	Beg -	Max -		(+)	(-)	MM	MM	Beg -	Max -	End	Beg -	Max -	End	Type	Type
1962			WWV-BL WW WWV-SY SS-BL	15 10 10 5	0.2 0.1 0.1 0.1	MM MM MM MM	MM	1841.		S					
01-26	1841 - 1842	-1845D	WWV-BL WW WWV-SY SS-BL	15 10 10 5	0.3 0.4 0.6 0.15	MM MM MM MM	MM	1613 - 1614 - 1618	1-	1618 -	- 1618.3	III	22-41	1	
01-27	1613D-1614E-1615		WWV-BL WWV-SY SS-BL	15 10 10	0.3 0.4 0.6	MM MM MM	MM	1920U-1936U-1945U	1	1915 - indet - 1959	383A 6C	2800 2800	1.3 6		
01-28	1930E-1932	-1935	WWV-BL WWV-SY SS-BL	15 10 10	0.25 0.3 0.3	MM MM MM	MM	1441 - 1443 - 1454D	1	1441.3-1442 - 1444.1	151f 151L	2800 2800	4 3		
01-31	1441 - 1441D-1444		WWV-BL WWV-SY SS-BL	15 10 10	0.35 0.65 0.45	MM MM MM	MM	1533 - 1539 - 1551	1	1447 - 1447.7-1450.5					
01-31	1537 - 1538D-1541		WWV-BL WWV-SY SS-BL	15 10 10	0.2 0.35 0.40	MM MM MM	MM	1902 - 1906 - 1940	1	1902 - 1904 - 1908	151 4PI	2800	6 2		
01-31	1903E-1904	-1906	WWV-BL WWV-SY SS-BL	15 10 10	0.5 0.4 0.1	MM MM MM	MM	2111 - 2112 - 2114		2110					
01-31			WWV-BL WWV-SY SS-BL	15 10 10	0.15 0.3 0.15	MM MM MM	MM								

Date	SFD's						Solar Flares						Radio Emissions						Ionospheric Effects			
	UT Beg	Max - End	Path	f Mc/s	Δf , cps (+)	ΔA , db	$-\Delta P$ km	UT Beg -	Max - End	UT Beg -	Max - End	Type	Freq Mc/s	Int or Peak Flux	UT Beg - Max - End	Type	Imp					
1962 02-01	1509 -1509 -1511	WWV-BL WWV-SY SS-BL	15 10 5	0.1 0.1 NM	0.1 NM NM	0.1 NM 4	NM	1508 -1510 -1518	1-	1414E 1410	- 1509 - 2320	0003D	6	108 21-41	2 1-							
02-01	1551 -1552 -1554	WWV-BL WWV-SY SS-BL	15 10 5	0.2 0.2 0.2	0.2 NM 4	0.2 NM NM	NM	1552 - 1555 - 1622	1-	1550 1552 1410	- 1554 - 1552 - 2320	- 1610 - 3-1553 - 2320	353A 1SL cont	2800 2800 21-41	3 1.5 1-							
02-01	1635E-1635 -1636	WWV-BL WWV-SY SS-BL	15 10 5	0.2 0.3 0.2	0.2 0.3 0.2	0.2 NM 4	NM	1635 - 1644 - 1738	1				1634-1642-1735U	SEA	2							
02-01	1639 -1640E -1643	WWV-BL WWV-SY SS-BL	15 10 5	0.9 1.5 0.7	0.9 1.4 0.7	0.9 1.4 0.7	NM	1636 - 1640 - 1653	1	1636 - 1640	- 1641	252	2800	8	1640- S-SWF	1						
02-01	1654 -1656 -1659	WWV-BL WWV-SY SS-BL	15 10 5	0.5 0.8 0.7	0.5 0.8 0.7	0.5 0.8 0.7	NM	1655 - 1659 - 1706	1	1654 1654	- 1723 - 1657	- 1705	353A 252f	2800 2800	3 7	1656-1704-1738 1657- -1720	SEA S-SWF	1+				
02-01	1818D-1819 -1822	WWV-BL WWV-SY SS-BL	15 10 5	0.2 0.8 0.4	0.2 0.8 0.4	0.2 0.8 0.4	NM	1818 - 1824 - 1832	1-	1829 -	- 1829.3	III	1941	1+	1815-1830U-1850U	SEA	2					
02-02	2215D-2217D -2222	WWV-BL WWV-SY SS-BL SS-FC	15 10 5 4	0.2 0.4 0.3 0.3	0.2 0.4 0.3 0.3	0.2 0.4 0.3 0.3	NM	2215 - 2220 - 2300	2													

Date	SFD's						Solar Flares			Solar Emissions			Ionospheric Effects			
	UT		Path	f Mc/s	Δf , cps (+)	ΔA , dB (-)	UT		Type	Freq Mc/s	Int or Peak Flux	UT		Type	Imp	
	Beg -	Max - End					Beg -	Max - End				Beg -	Max - End			
1962																
02-04	1730	-1731D-1735	WWV-BL	15	0.1	1.0	0.2	1.0	0.1	NR	1726- 1732 - 1746	1-	1400 - 1550 - 1845	383f	2800	8
			WWV-SY	10	0.1											
			SS-BL	5												
			SS-FC	4												
02-06	1624	-1625 -1629	WWV-BL	15	0.1	1.0	0.3	WWV-SY	10	0.1	1624- 1628 - 1634	1-				
			SS-BL	5				SS-FC	4	0.2						
			SS-FC	4												
02-06	1837	-1839 -1842	WWV-BL	15	0.1	1.0	0.1	WWV-SY	10	0.1						
			SS-BL	5				SS-FC	4	0.2						
			SS-FC	4												
02-07	0426D-0427D-0430		WWVH-BL	10	1.5											
02-07	2127	-2128 -2130	WWV-BL	15	0.1	1.0	0.3	WWV-SY	10	0.2						
			SS-BL	5				SS-FC	4	0.1						
			SS-FC	4												
02-10	2124	-2125E-2126	WWV-BL	15	0.1	1.0	0.1	WWV-SY	10	0.1	2124 - 2128 - 2154	1				
			SS-BL	5				SS-FC	4	0.1						
			SS-FC	4												
02-15	2054	-2055D-2058	WWV-BL	15	0.1	1.0	0.2	WWV-SY	10	0.3						
			SS-BL	5				SS-FC	4	0.1						
			SS-FC	4												

Date	SFD's						Solar Flares			Radio Emissions			Ionospheric Effects		
	UT Beg - Max	UT Max - End	Path Mc/s	f Mc/s	Δf , cps (+)	Δf , cps (-)	$-\Delta P$ km	UT Beg - Max	UT Max - End	Imp	UT Beg - Max	UT Max - End	Init or Peak Flux	Type	Imp
1962 02-16	0142 -0142D-0145	WWV-BL WWV-SY SS-BL SS-FC	15 10 5 4	NM 0.3 0.2 NM	NM NR NM NM	NM 0.2 0.2 NM	NFR								
02-19	2134 -2136 -2146	WWV-BL WWV-SY SS-BL SS-FC	15 10 5 4	0.3 0.3 0.5 NR	10 NR 4 NR	15 0.5 0.7 0.4	2134E-2144 - 2202	2	1230E - 1319 - 2025D	rec inc	2800	39			
02-21	1829 -1830 -1833	WWV-BL WWV-SY SS-BL SS-FC	15 10 5 4	1.3 2.3 1.6 NR	10 NR 4 NR	10 2.3 1.4 0.6	1835E-1835U-1855	1-	1805 - 1841.5 - 1928 1831.8 - 1833.2 - 1835.1 1832 - - 1834	3634f 181f III	2800 2800 16-41	3 3 1+			
02-21	2033 -2034 -2036	WWV-BL WWV-SY SS-BL SS-FC	15 10 5 4	0.2 0.3 0.1 0.1	10 NR 4 NR	15 0.4 0.1 0.1	NFR		2048 - 2040 -	2048.3 cont	III	21-41	1+		
02-22	2014 -2015E-2018	WWV-BL WWV-SY SS-BL SS-FC	15 10 5 4	0.7 1.3 1.0 0.5	10 NR 4 NR	10 1.3 1.0 0.5	2013 - 2015 - 2033	1-	2000 - 2030 - 2055 2002 - - 2003.3	353 III	2800 23-41	4 1			
02-23	1416 -1417E-1420	WWV-BL WWV-SY SS-BL SS-FC	15 10 5 4	0.1 0.2 0.2 0.1	10 NR 4 NR	1416 -	- 1419	1-	1348E - 1424 - 1614	6	108	1			

Date	SFD's						Solar Flares						Solar Radio Emissions						Ionospheric Effects			
	UT		Path	f Mc/s	Δf , cps		ΔA km	$-\Delta P$ km	UT		Imp	UT		Type	Freq Mc/s	Int or Peak Flux	UT		Max - End	Type	Imp	
	Beg -	Max -			(+)	(-)			Beg -	Max -		Beg -	Max -				Beg -					
02-23 1865 -1856 -1859	WW-BL	15	0.8	WW-SY SS-BL SS-FC	10	1.8	1654 - 1656 - 1700U	1- 1823 - 1848 - 1902	1- 1750 - 1913 - 2200	- 1659.2	III	21-41	1-	2800	28	353Af	2800	28	28	28	28	
	WW-SY	10	1.1		5	0.5																
	SS-BL	5	0.5		4	0.5																
02-23 1888 -1890 -1832	WW-BL	15	0.4	WW-SY SS-BL SS-FC	10	0.5	1823 - 1848 - 1902	1+ 1750 - 1913 - 2200	1+ 353Af	- 1659.2	III	21-41	1-	2800	28	28	28	28	28	28	28	
	WW-SY	10	0.4		5	0.3																
	SS-BL	5	0.3		4	0.2																
02-23 1841 -1843D-1848	WW-BL	15	1.3	WW-SY SS-BL SS-FC	10	2.8	1823 - 1848 - 1902	1+ 1750 - 1913 - 2200	1+ 353Af	- 1659.2	III	21-41	1-	2800	28	28	28	28	28	28	28	
	WW-SY	10	1.5		5	1.0																
	SS-BL	5	1.0		4	0.8																
02-23 1900 -1901 -1903	WW-BL	15	0.7	WW-SY SS-BL SS-FC	10	1.2	1823 - 1848 - 1902	1+ 1750 - 1913 - 2200	1+ 353Af	- 1659.2	III	21-41	1-	2800	28	28	28	28	28	28	28	
	WW-SY	10	0.8		5	0.2																
	SS-BL	5	0.2		4	0.2																
02-23 1950D-1951 -1955	WW-BL	15	MM	WW-SY SS-BL SS-FC	10	MM	1823 - 1848 - 1902	1+ 1750 - 1913 - 2200	1+ 353Af	- 1659.2	III	21-41	1-	2800	28	28	28	28	28	28	28	
	WW-SY	10	MM		5	0.3																
	SS-BL	5	0.2		4	0.2																
02-23 2155D-2156D-2157	WW-BL	15	0.7	WW-SY SS-BL SS-FC	10	0.8	1823 - 1848 - 1902	1+ 1750 - 1913 - 2200	1+ 353Af	- 1659.2	III	21-41	1-	2800	28	28	28	28	28	28	28	
	WW-SY	10	0.6		5	0.5																
	SS-BL	5	0.5		4	0.5																
02-23	WW-FC	4	0.7	WW-SY SS-BL SS-FC	4	0.7	1823 - 1848 - 1902	1+ 1750 - 1913 - 2200	1+ 353Af	- 1659.2	III	21-41	1-	2800	28	28	28	28	28	28	28	
	WW-SY	10	0.8		5	0.6																
	SS-BL	5	0.5		4	0.5																
02-23	WW-FC	4	0.7	WW-SY SS-BL SS-FC	4	0.7	1823 - 1848 - 1902	1+ 1750 - 1913 - 2200	1+ 353Af	- 1659.2	III	21-41	1-	2800	28	28	28	28	28	28	28	
	WW-SY	10	0.8		5	0.6																
	SS-BL	5	0.5		4	0.5																
02-23	WW-FC	4	0.7	WW-SY SS-BL SS-FC	4	0.7	1823 - 1848 - 1902	1+ 1750 - 1913 - 2200	1+ 353Af	- 1659.2	III	21-41	1-	2800	28	28	28	28	28	28	28	
	WW-SY	10	0.8		5	0.6																
	SS-BL	5	0.5		4	0.5																
02-23	WW-FC	4	0.7	WW-SY SS-BL SS-FC	4	0.7	1823 - 1848 - 1902	1+ 1750 - 1913 - 2200	1+ 353Af	- 1659.2	III	21-41	1-	2800	28	28	28	28	28	28	28	
	WW-SY	10	0.8		5	0.6																
	SS-BL	5	0.5		4	0.5																
02-23	WW-FC	4	0.7	WW-SY SS-BL SS-FC	4	0.7	1823 - 1848 - 1902	1+ 1750 - 1913 - 2200	1+ 353Af	- 1659.2	III	21-41	1-	2800	28	28	28	28	28	28	28	
	WW-SY	10	0.8		5	0.6																
	SS-BL	5	0.5		4	0.5																
02-23	WW-FC	4	0.7	WW-SY SS-BL SS-FC	4	0.7	1823 - 1848 - 1902	1+ 1750 - 1913 - 2200	1+ 353Af	- 1659.2	III	21-41	1-	2800	28	28	28	28	28	28	28	
	WW-SY	10	0.8		5	0.6																
	SS-BL	5	0.5		4	0.5																
02-23	WW-FC	4	0.7	WW-SY SS-BL SS-FC	4	0.7	1823 - 1848 - 1902	1+ 1750 - 1913 - 2200	1+ 353Af	- 1659.2	III	21-41	1-	2800	28	28	28	28	28	28	28	
	WW-SY	10	0.8		5	0.6																
	SS-BL	5	0.5		4	0.5																
02-23	WW-FC	4	0.7	WW-SY SS-BL SS-FC	4	0.7	1823 - 1848 - 1902	1+ 1750 - 1913 - 2200	1+ 353Af	- 1659.2	III	21-41	1-	2800	28	28	28	28	28	28	28	
	WW-SY	10	0.8		5	0.6																
	SS-BL	5	0.5		4	0.5																
02-23	WW-FC	4	0.7	WW-SY SS-BL SS-FC	4	0.7	1823 - 1848 - 1902	1+ 1750 - 1913 - 2200	1+ 353Af	- 1659.2	III	21-41	1-	2800	28	28	28	28	28	28	28	
	WW-SY	10	0.8																			

Date 1962	SFD's						Solar Flares						Solar Radio Emissions						Ionospheric Effects			
	UT Beg - Max	UT Max - End	Path	f Mc/s	Δf , cps (+)	Δf , cps (-)	ΔA	$-\Delta P$ km	UT Beg - Max	UT Max - End	Imp	UT Beg - Max	UT Max - End	Type	Freq Mc/s	Int or Peak Flux	UT Beg - Max - End	Type	Imp			
02-24 1341 -1342 -1345D	WW-BL WW-SY SS-BL SS-FC	15 10 5 4	0.1 0.3 0.2 0.1	1341 -1342 -1349	1-	1346E 1400E	-	0030 - 1800	6	108 22-41	3											
02-24 14425-1443 -1444	WW-BL WW-SY SS-BL SS-FC	15 10 5 4	0.4 0.5 0.2 0.1	1430E - 1506D	1+	1400E	-	- 1800	cont	22-41	1-											
02-24 1450 -1453 -1500	WW-BL WW-SY SS-BL SS-FC	15 10 5 4	1.0 1.4 0.3 0.1	1455E-1454 - 1456	1																	
02-24 1621 -1623 -1625	WW-BL WW-SY SS-BL SS-FC	15 10 5 4	0.3 1.0 0.3 0.2	1620 - 1625 - 1635	1-	1631 - 1632 - 1640	- 1626.3	- 1627.2	III	353 16-41	2800 16-41	2										
02-25 1612 -1614 -1620D	WW-BL WW-SY SS-BL SS-FC	15 10 5 4	0.1 0.4 0.2 0.1	1612 - 1614 - 1620	1-	1415 - 1513 - 2030	- 1345E 1400E	- 0031 - 2400	352Af 6 cont	2800 108 21-41	5 3 1-											
02-25 1815E-1815 -1817	WW-BL WW-SY SS-BL SS-FC	15 10 5 4	0.3 0.2 0.2 0.2	1814 - 1817 - 1831	1-																	

Date	SFD's						Solar Flares						Solar Radio Emissions						Ionospheric Effects			
	UT		Path	f Mc/s (+)	Δf , cps Mc/s (+)	ΔA db (-)	$-\Delta P$ km		UT		UT		Type	Freq Mc/s	Int or Peak Flux	UT		UT		Type	Imp	
	Beg	Max					-	End	Beg	Max	-	End				Beg	Max	-	End			
1962 02-25	1823 - 1824 - 1825	WW-BL WW-SY SS-BL SS-FC	15 10 5 4	0.3 0.4 0.2 0.2	NM NM NM NM	10 10 4 4	1814 - 1824 - 1831	1-														
02-25	1835 - 1837E - 1839	WW-BL WW-SY SS-BL	15 10 5	0.2 0.3 0.3	NM NM NM	10 10 4	1825 - 1828 - 1836	1-														
02-25	1912 - 1912D - 1915	WW-BL WW-SY SS-BL SS-FC	15 10 5 4	0.1 0.1 0.2 0.2	NM NM NM NM	10 10 4 4	1912 - 1920 - 1935	1-	1918 - 1918.5 - 1920.3 1911 - 1914.15						1SLf III	2800 16-41	3 2					
02-25	1941 - 1942 - 1944	WW-BL WW-SY SS-BL SS-FC	15 10 5 4	0.5 0.8 0.5 0.3	NR NR NR NR	10 10 5 4	1940 - 1943 - 1955	1-	1942.2 -						III	21-41	1+					
02-26	1940 - 1941D-1944	WW-BL WW-SY SS-BL SS-FC	15 10 5 4	0.5 0.7 0.3 0.3	NR NR NR NR	10 10 5 4	MFP		1343E -						6 cont	108 23-41	2 1-					
02-27	1959 - 1962 - 1965	WW-BL WW-SY SS-BL SS-FC	15 10 5 4	0.5 0.2 0.1 0.2	NR NR NM NM	10 10 5 4	1358 -	-	1402	1-	1342E - 1552 - 2108D 1356E - - 2400				6 cont	108 23-41	2 1-					

Date 1962	SFD's						Solar Flares			Solar Radio Emissions			Ionospheric Effects		
	UT		Path	Δf , cps (+)	Δf , cps (-)	UT		UT		Type	Freq Mc/s	Int or Peak Flux	UT	Type	Imp
	Beg -	Max -				End	Beg -	Max -	End				Beg -	Max -	End
02-27 1420 -1421D -1424	WW-BL	15	NR	0.2	-	1422E -	-	1435D	1-	1426 - 1434.2 - 1442	353	2800	2		
02-27 1732 -1733D-1735	WW-SY SS-BL SS-FC	10 5 4	NR NM NM	0.2 0.1 0.1	-										
02-27 2048 -2051D-2059	WW-BL	15	NR	0.5	-	1745 - 1755 - 1750	1-	1731 - 1734 - 1740	1-	1517 - 1625 - 1917	353AF	2800	8		
02-28 1806 -1808 -1813	WW-SY SS-BL SS-FC	10 5 4	NR NM NR	0.5 0.2 0.6	-	2050 - 2055 - 2120	1	2050 - 2058 - 2200	1	2050 - 2051.8-2053	353A 282	2800	8		
02-28 1936 -1938E -1946	WW-BL	15	NR	0.8	-	1806 - 1812 - 1930	1	1804 - 1815 - 1825	1	1810.1 - 1811.6	66F 4PT	2800	29		
02-28	WW-SY SS-BL SS-FC	10 5 4	NR NM NR	0.7 0.4 0.5	-	1934 - 1941 - 2028	1	1937 - 1938.5 - 1940	1	1855 - - 2000	282 4PT cont	2800	10		
												24-41	8		
													1		

Date	SFD's						Solar Flares			Solar Emissions			Ionospheric Effects		
	UT Beg - Max - End	UT Path	f Mc/s	Δf, cps (+)	ΔA dB	-ΔP km	UT Beg - Max - End	UT Beg - Max - End	UT Beg - Max - End	Type	Freq Mc/s	Int or Peak Flux	UT Beg - Max - End	Type	Imp
03-01 1636 -1637	WWV-BL WWV-SY SS-BL SS-FC	15 10 5 4	NR 4.8 1.4 1.4				1635 - 1643 - 1723	2	1634.3 - 1635 - 1642.5 - d28 1636.5-1645U - 1648.5 1637.2D- 1639 - 1645 - 1646.5 - 1654 -	III 6CF 4PI 9a II BUR BUR BUR BUR	24-41 2800 2800 108 21-41 18 18 108 18	1634- 1636-1648-1720 1638-1644-1720 SCNA ABS SEA	S-SWF SPA SCNA ABS SEA	2+ 83 2 50 2	
- 1638 -	WWV-BL WWV-SY SS-BL SS-FC	15 10 5 4	NR 7.0 1.6 1.4												
- 1640D -	WWV-BL WWV-SY SS-BL SS-FC	15 10 5 4	NR 7.0 2.0 1.4												
- 1641D-1705	WWV-BL WWV-SY SS-BL SS-FC	15 10 5 4	NR NM 2.8 1.8												
03-01 1842 - 1844D-1845D	WWV-BL WWV-SY SS-BL SS-FC	15 10 5 4	NR 1.2 0.6 2.8				1842 - 1844 - 1849	1-	1844 - 1844.3 - 1844.9 1845.2-1845.5-1846.1	1S1 1S1	2800 2800	1			
03-13 1849E-1450	WWV-BL WWV-SY SS-BL	15 10 5	4.7 7.6 0.6	0.6 1.2 35			1448 - 1451 - 1640D	2+	1447.5-1450.5-1507 d6:23	6CF 4PI	2800 2800	470 12	1445-1505-1640 1448- 1450-1500-1545 ABS SEA	SPA S-SWF SCNA ABS SEA	99 3 1 20 2

Date 1962	SFD's						Solar Flares						Solar Radio Emissions						Ionospheric Effects			
	UT Beg - Max - End	UT Path	f Mc/s	Δf , cps (+)	Δf , cps (-)	ΔA	$-\Delta P$ km	UT Beg - Max - End	UT Beg - Max - End	UT Beg - Max - End	Type	Freq Mc/s	Int or Peak Flux Beg - Max - End	UT Beg - Max - End	Type	Imp						
03-13 -1452D-1500	WWN-BL WWN-SY SS-BL	15 10 5	1.4 1.8 0.4					1450 - 1452.3 - 1512 1517.3-1520 - 1521.2	8 6cf	108 2800	2 3											
03-17 1938 -1940B-1943	WWN-BL WWN-SY SS-BL	15 10 5	1.4 1.6 0.9			15		1939 - 1941 - 1959	1	1939 - 2000 - 2120 1939-1940.2 - 1942 1940 - 1949 - 2155	3S3A 1S1 BUR	2800 2800 18	2 6 2	1933-1944-1953 1940- 1940-1944-2015	SEA S-SWRF SCNA ABS	1 1 1 20						
03-19 0100 -0101 -0105	WWN-BL WWN-SY SS-BL	15 10 5	NR 0.6 0.4					0100 - 0107 - 0125D	1													
03-19 2119 -2120 -2122	WWN-BL WWN-SY SS-BL	15 10 5	NR 0.9 0.6							MFR	1338 - 2120 - 2120.7 - 2121	RiseA 252	2800 2800	13 20								
03-19 2126D-2127 -2129	WWN-BL WWN-SY SS-BL	15 10 5	NR 0.4 0.2							MFR												
03-22 1558 -1600 -1603	WWN-BL WWN-SY SS-BL	15 10 5	0.3 0.4 0.2					1558 - 1602 - 1610	1	1505E - 1559.6-1600.5-1600.6 1605.0-1605.0-1606.0	cont 3	24-41 3	1- 2 3									
03-22 2136 -2137D-2140	WWN-BL WWN-SY SS-BL	15 10 5	0.3 0.3 0.1					2136 - 2140 - 2154U	1-	2132 - 2145 - 2158 2136 - 2138 - 2143	3S3A 2S2	2800 2800	6 18									

Date	SFD's				Solar Flares				Solar Radio Emissions				Ionospheric Effects				
	UT Beg - Max	UT Max - End	Path	f Mc/s	Δf , cps (+)	Δf , cps (-)	ΔA km	$-\Delta P$ km	UT Beg - Max	UT Max - End	Imp Beg - Max	UT Max - End	Type	Freq Mc/s	Int or Peak Flux	UT Beg - Max - End	Type
1962 03-22	2227 -2230 -2234	WWV-BL	15 10 WWV-SY SS-BL	NM NR 0.3 0.1 NR	2220U-2241-2310U	3	2214 - 2230 - 2250D	rec inc	2800	35							
03-24	1354 -1355 -1357	WWV-BL	15 10 WWV-SY SS-BL	0.2 0.3 0.1 0.1													
03-25	1234 -1236 -1238	WWV-BL	15 10 WWV-SY SS-BL	NR 1.1 1.0 NR 0.1	1254E- -1325D	1	1208E- 1425 - 1648D 1208E-1209.5-1212D 1223 - 1224 - 1227 1234 - 1237 - 1246	353AF 252 15 252	2800 2800 2800 2800	16 9 4 90	1237- -1306- 1238- 1238-1242-1334	SP4 S-SWF SEA	2 2 1+				
03-25	1358 -1359 -1401	WWV-BL	15 10 WWV-SY SS-BL	0.2 0.4 0.2 0.1 0.1	1405E-1436 - 1506	1+	1357 - 1358.5 - 1402	1SELf	2800	5							
03-25	1904 -1905 -1909	WWV-BL	15 10 WWV-SY SS-BL	0.4 0.6 0.4 0.4 0.3													
03-27	2107 -2107D-2110	WWV-BL	15 10 WWV-SY SS-BL	NM NM 0.1 NM NM	1902 -1908 -1924 1903 -1909 -1940 1902.3- 1905.15- 1909.45	1-	1901 - 1907 - 1930 1906.1-1906.2-1907.9 1904.3- -1909.45	353f 3 III III	2800 3 108 8.5-41 7.6-41	3 2 2 2+							
03-30	1436 -1437 -1439	WWV-BL	15 10 WWV-SY SS-BL	0.2 0.6 0.4 NR NR	2107 -2108 -2117	1-											
					1431 -1438 -1446	1-											

Date	SFD's						Solar Flares			Solar Radio Emissions			Ionospheric Effects		
	UT Beg - Max - End	UT Max - End	Path	f Mc/s (+)	Δf , cps · (-)	ΔA km db	$-\Delta P$ km	UT Beg - Max - End	UT Beg - Max - End	Type	Freq Mc/s	Int Peak Flux	UT Beg - Max - End	Type	Imp
1962 03-30	1459 -1500 -1503	WWV-BL WWV-SY SS-BL	15 10 5 4	0.2 0.3 0.2 NM	NM	NM	1458 - 1505 - 1516	1-							
03-31	1900 -1903 -1912	WWV-BL WWV-SY SS-BL	15 10 5 4	0.7 1.4 0.9 0.5	0.7	0.3	1858 - 1905 - 1954	1+							
03-31	2135 -2138 -2143	WWV-BL WWV-SY SS-BL	15 10 5 4	0.3 0.8 0.5 0.2	0.2	0.4	2130 - 2139 - 2152	1							
04-07	1732 -1733D-1736	WWV-BL WWV-SY SS-BL	15 10 5 4	NR 0.6 0.3 NR	NR	0.2	NFR								
04-07	1818 -1820D-1823	WWV-BL WWV-SY SS-BL	15 10 5 4	0.3 0.2 0.2 NM	0.2	0.2	1819E-1822 - 1906	1+							
04-12	2149E-2150 -2152	WWV-BL WWV-SY SS-BL	15 10 5 4	0.4 0.6 0.4 0.2	0.41 0.73	0.4	2149 - 2213 - 2244	1-	2134 - 2147.8 - 2148 - 2148.15 -	BUR 9a 6cf cont	18 108 2800 8.5 hr	2134- 2212- 2215-2218-2227	-2216 -2400 150 2+	BUR G-SWF SEA	3 1+ 1

Date	SFD's						Solar Flares			Solar Emissions			Ionospheric Effects		
	UT		Path	Δf , cps		ΔA db	$-\Delta P$ km		UT		Type	Freq Mc/s	Int or Peak Flux	UT	
	Beg -	Max -		Mc/s	(+)		(-)	Beg -	Max -	Beg -				Max -	
04-13 1962	21117	-2118D-2121	WWV-BL	15	0.2			0.23	21117-2121	-2130	1-				
04-13	2254	-2256D	WWV-BL	15	0.4			0.61	2253-2302	-2320	1-	2301.3 -	- 2304.3	III	20-41
04-13	-2300	-2302	WWV-BL	15	0.2			1.29							1+
04-14	1301	-1302	WWV-SY	10	0.4										
04-14	1304	-1306D-1309	SS-BL	5	0.2										
04-14	1311	-1313	WWV-BL	15	0.8			0.52	1300E-1302	-1320	1-				
			WWV-SY	10	1.1			1.28							
			SS-BL	5	0.7										
			WWV-BL	15	0.4										
			WWV-SY	10	0.7			1.07							
			SS-BL	5	0.3			1.13							
			WWV-BL	15	0.4										
			WWV-SY	10	0.4			0.6	1300E-1307	-1320	1-				
			SS-BL	5	0.2			1.21							
			WWV-BL	15	0.1										
			WWV-SY	10	0.3			0.94							
			SS-BL	5	0.2			0.98							
			WWV-BL	15	0.1										
			WWV-SY	10	0.1										
			SS-BL	5	0.1										
			WWV-BL	15	0.1										

Date 1962	SFD's						Solar Flares						Solar Radio Emissions				Ionospheric Effects			
	UT		Path		f Mc/s	Δf, cps (+)	ΔA db (-)	-ΔP km	UT		UT		Type	Freq Mc/s	Int or Peak Flux	UT	Type	Imp		
Beg - Max - End	Beg - Max - End	Beg - Max - End	Beg - Max - End	Beg - Max - End	Beg - Max - End	Beg - Max - End	Beg - Max - End	Beg - Max - End	Beg - Max - End	Beg - Max - End	Beg - Max - End	Beg - Max - End	Beg - Max - End	Beg - Max - End	Beg - Max - End	Beg - Max - End	Beg - Max - End			
04-14	1915 -1918 -1920	WW-BL 15 10 WW-SY 10 SS-BL 5	WW-BL 15 0.8 0.2 WW-SY 10 1.5 SS-BL 5	12 25	0.16 0.42	1910E-1924 - 2005	1	1902 - 1933 1913 - 1919 1917 - 1917.5-	2050 - 1930 - 1920 - 1921	353A 2S2f BUR III	2800 2800 18 7.6-41	7 59 2 2+	1903-1930-2030 1917-1924-2100U 1918- 1920-1926-2030	SPA SEA SCNA ABS	75 2 2+ 2	T5 2 2+ 30				
04-15	1715 -1718 -1725	WW-BL 15 10 WW-SY 10 SS-BL 5	WW-BL 15 0.3 1.1 WW-SY 10 0.5 SS-BL 5 0.3	3 8	1715 - 1720 - 1731	1-	1640 - 1716.5-1719.3-1732.5	1810 - 1810 -	cont 6cf	1841 2800	1- 10	1715-1720-1800 1715-1721-1800 1720- -1755	SPA SEA	12 1+ 1-	S-SWF					
04-15	1837 -1840 -1845D	WW-BL 15 10 WW-SY 10 SS-BL 5	WW-BL 15 0.2 0.2 WW-SY 10 0.1 SS-BL 5 0.1	10 10 4	1835 - 1845 - 1854	1-	1810 -	- 2500	cont	2141	1	/	/	/	/	/				
04-15	1928 -1930D-1933	WW-BL 15 10 WW-SY 10 SS-BL 5	WW-BL 15 0.4 0.6 WW-SY 10 0.4 SS-BL 5 0.4	10 10 4	1929 - 1951 - 2007	1	1942 - 1950 - 1956D	1-	1943 - 1944.3 - 1947	1S1	2800	5								
04-15	1942 -1949D-1955	WW-BL 15 10 WW-SY 10 SS-BL 5	WW-BL 15 1.3 2.2 WW-SY 10 1.5 0.9 SS-BL 5 0.5	10 10 4	0.6 0.2 0.2	0.93 0.2 0.2	2051 - 2053 - 2058	1-												
04-15	2050 -2052E-2058	WW-BL 15 10 WW-SY 10 SS-BL 5	WW-BL 15 0.6 1.1 WW-SY 10 0.8 0.4 SS-BL 5 0.4	10 10 4	0.2 0.4 0.4	0.93 0.2 0.2	2051 - 2053 - 2058	1-												
04-15	2153 -2154 -2158	WW-BL 15 10 WW-SY 10 SS-BL 5	WW-BL 15 0.2 0.4 WW-SY 10 0.3 SS-BL 5 0.2	10 10 4	0.25 0.63 0.98 0.2	0.25 0.63 0.98 0.2	2153 - 2155 - 2158	1-												

Date	SFD's						Solar Flares						Solar Radio Emissions						Ionospheric Effects			
	UT		Path	f Mc/s (+)	Δf , cps (+)	ΔA db (-)	UT		Imp	UT		Type	Freq Mc/s	Int or Peak Flux	UT		Type	Imp				
	Beg	Max - End					Beg - Max	End		Beg	Max - End				Beg - Max	End						
1962																						
04-15	2240 -2242 -2249	WW-BL WW-SY SS-BL	15 10 5	0.6 1.1 0.8 0.5 0.5	1.30 3.69 3.80 5.75	2241 - 2245 - 2252	1	2241 - 2243.8 - 2246	1S1F	2800	4											
04-16	0234 -0235 -0244	FB-AN WW-BL WW-SY SS-BL	10 15 10 5	0.3 NR NR 0.4 0.4		0233 - 0236 - 0249 2145 - 2147 - 2153	1-	1500E -	-	2524	6	108	2									
04-16	2146E-2156D-2148																					
04-17	0100 -0102 -0105	WW-BL WW-SY SS-BL	15 10 5	0.3 0.7 0.4																		
04-17	1444 - 1445D-1447	WW-BL WW-SY SS-BL	15 10 5	NR NR 0.2		1444 - 1446 - 1513	1	1438E - 1445.7-1445.9-1447.3 1455E -	1 2S2 cont	2800	10	108	2	1445-1450-1510					SEA			
04-17	2252 -2253D-2256	WW-BL WW-SY SS-BL	15 10 5	1.0 1.9 1.0	0.65 2.14 2.10	2252 - 2256 - 2313	1-	2252.5-2253.2-2300	2S2	2800	55											
04-18	1801 -1803 -1805	WW-BL WW-SY SS-BL	15 10 5	0.3 0.5 0.4	2.11 2.89															SCWA G-SWF	2 3	
04-18																						

Date	SFD's				Solar Flares				Solar Radio Emissions				Ionospheric Effects			
	UT Beg - Max - End	Path Mc/s	f (+)	Δf, cps (-)	ΔA km	-ΔP km	UT Beg - Max - End	UT Beg - Max - End	Type	Freq Mc/s	Int or Peak Flux	UT Beg - Max - End	Type	Imp		
04-19 1962	1736 -1738 -1740	WW-BL SS-BL	15 10 5 4	0.2 0.3 NM			1734 -1743 -1818	1- 1710 - 1746 1735-15 -	3S3A III	2800 7.6-4.1	3					
04-19 1974 1-1742D-1744	WW-BL SS-BL	15 10 5 4	0.8 1.4 NM				1742-3-1742-7-1744 1743-1-1743-7-1744-6	1S1 3	2800 108	5						
04-19 1935 -1935D -1938II	WW-BL PB-AN SS-BL	15 10 5 4	18 43+ 0.3 32	3.2 7.2 5.6 11	15 24 18 18	7 34 14 14	1935 - 1937 - 2031	2 1935 - 1936-3 - 1943 d2:32	2S2 4PT	2800 2800	165 5	1934-1937-2040 1935-1938-1950	SEA SCWA ABS S-SWF SPA	1+ 1 20 1+ 60		
04-19 1954E-1955D-1957	WW-BL SS-BL	15 10 5	1.2 1.6 1.0				1942 - 1947 - 2000	2 1955 - 1955-3 - 1957	1S1	2800	3					
04-19 2035 -2037E-2040	WW-BL SS-PL	15 10 5 4	0.4 0.9 0.4 0.3	0.1 0.2 0.2 0.2			2035E-2038U-2053 2036 -2039 -2042	1- 1								
04-20 1322 -1323 -1325	WW-BL SS-BL	15 10 5 4	0.6 1.0 1.0 0.3				1314 - 1332 - 1432	1 1220E - 1328 - 1335	6 - 1344	353	108 2800	2				
04-20 1534 -1535 -1538	WW-BL SS-BL	15 10 5 4	0.3 0.3 0.2 0.1				1536E- - 1547	1- 1220E - 1534-45 -	6 - 1535.15		108 23-4.1	2				
04-20 1626 -1628 -1633	WW-BL SS-BL	15 10 5 4	0.1 0.2 0.1 NM				1625 - - 1629D	1- 1220E -	- 0128	6	108	2				

Date	SFD's						Solar Flares						Solar Emissions						Ionospheric Effects									
	UT	Path	f Mc/s	Δf , cps (+)	Δf , cps (-)	ΔA db	$-\Delta P$ km	UT	UT	Beg -	Max -	End	Imp	UT	UT	Beg -	Max -	End	Type	Freq Mc/s	Int or Peak Flux	UT	Beg -	Max -	End	Type	Imp	
1962	UT																											
04-20	1734 -1736 -1740	WW-BL	15	0.2				NFR																				
04-20	1959 -2001E-2010D	WW-BL	15	0.3	0.1	NM																						
04-21	1316 -1317 -1319	WW-BL	15	3.8	25	6.3	1958 -2002	-2038	2	1957.3 -	1959 -	2009	2800	72	2000-	-2030	S-SWT	2										
04-21	1450 -1451 -1455	WW-BL	15	9.0	50	22	2000 -	-2003		-	-	2004	7.6-41	2+	2000-2004-2035	SCWA	2											
04-21	1920 -1920D-1932	WW-BL	15	0.2	NM	15	1307 -1321	-1353	1	1219E -	-	0.129	6	108	2	2000-2007-2050	ABS	30										
04-26	0536 -0538 -0542	PB-AN	10	1.2																								
04-26	1833 -1835 -1837	WW-BL	15	NM	NM	NM																						
04-27	1410 -1412D-1425	WW-BL	15	6	1.2	30	5.04	-1350	-1440	2	1344 -	1356 -	1451	3834F	4	1410-1426-1520	SPA	85										
		SS-BL	10	10	4.4	30	10.8				1405 -	1413 -	1429	2800	175	1410-1420-1526	SEA	2										
			5	NR	NR	NR					1412.15-	-	1415	11-41	2+	1413- -1414-1417-1430	S-SWT	1+										
											1412.3-	-	1503	9	108	3	1414-1417-1430	SCWA	30									
											1415.15-	-	1416.3	11-41	2+	1415-1417-1430	ABS	2										
											1418 -	-	1426	11-41	2	1418-1426-1430	SEA	2										
											1420 -	-	1635	22-41	2	1420-1426-1430	SEA	2										

Date	SFD's						Solar Flares						Radio Emissions						Ionospheric Effects			
	UT Beg - Max - End	UT Path	f Mc/s (+)	Δf , cps (-)	ΔA db	$-\Delta P$ km	UT Beg - Max - End	UT Beg - Max - End	UT Beg - Max - End	UT Beg - Max - End	Type	Freq Mc/s	Int or Peak Flux	UT Beg - Max - End	UT Beg - Max - End	Type	Imp					
04-27 1962	2300 -2302E-2306	WWV-BL SS-BL	15 10 4	0.2 0.4 NR	NR	NR	2300 -2305 -2315	1-	2300 - 2300.3 - 2300.5 -2304.3-2306.6	- 2305 -2305.5 -2306.6	BUR III	1.8 12.4I 2.	3 2 2									
04-28 1962	1718 -1719D-1721	WWV-BL SS-BL	15 10 4	0.3 0.6 NR	NR	NR			1556.5-1557.1-1758.5	4		1.08	2									
04-28 2025	-2027 -2029	WWV-BL SS-BL	15 10 4	0.5 0.6 NR	NR	NR	2023 -2029 -2041	1-	2021 - 2030 - 2044 2023 - 2023.45- 2023.5-2027.2-2031 2026.8-2027.3-2027.8 2028 -	- 2032 - 2028 2 2 - 2029	353AF EUR III	2800 18 7.6I 2 1.08 2800 21.4I	3 1 2 2 7 1+									
04-29 1980	-1801 -1804	WWV-BL SS-BL	15 10 4	0.1 0.2 NR	NR	NR	1801 - 1803 - 1806	1-														
05-01 1985	-1839E-1842	WWV-BL SS-BL	15 10 4	0.3 0.7 NR	NR	NR																
05-01 1914	-1916 -1927	WWV-BL FB-AN SS-BL	15 10 4	1.5 2.0 0.3	0.5 0.6 NR	15 NR NR	1915- 1920 - 1928	1	1915 - 1920.5 - 2105 1918.3- 1918.5-1922.5-1936.5 1919 - - 1955	Irrig Act III 9 BUR	2800 7.6I 108 18	60 3 3 3										
05-01 2024	-2026 -2028	WWV-BL SS-BL	15 10 4	0.2 0.2 NR	NR	NR			1935 -	- 2130	IV	23.4I	1									
05-02 1927	-1928 -1930	WWV-BL SS-BL	15 10 4	0.3 0.4 NR	NR	NR	1927 - 1930 - 1932	1-	1927.3-1928.4-1931.0 d50	282f 4PI	2800 2800	12 1										

Date 1962	SFD's						Solar Flares						Solar Radio Emissions						Ionospheric Effects			
	UT		Path	f Mc/s	Δf , cps (+)	ΔA , db (-)	$-\Delta P$ km	UT		UT		Type	Freq Mc/s	Int or Peak Flux	UT		Type	Imp				
	Beg -	Max - End						Beg -	Max - End	Beg -	Max - End				Beg - Max - End	UT Beg - Max - End						
05-04	1616 -1617D-1619	WW-BL SS-BL	WW-BL SS-BL	15 10 5 4	0.1 NM NR NR	0.1 0.2 0.1 NR	1617 - 1619- 1621	1-	1619.15-	-1620.4	III	20-41	1									
05-09	2117 -2118D-2119	WW-BL SS-BL	WW-BL SS-BL	15 10 5 4	0.2 0.1 NR																	
05-10	1807 -1809 -1811	WW-BL SS-BL	WW-BL SS-BL	15 10 5 4	0.4 0.6 0.1 NM																	
05-10	1906 -1908 -1913	WW-BL SS-BL	WW-BL SS-BL	15 10 5 4	0.4 0.6 0.1 NM																	
05-11	1332 -1333 -1335	WW-BL SS-BL	WW-BL SS-BL	15 10 5 4	0.2 0.4 0.2 0.1																	
05-11	1618 -1619 -1622	WW-BL SS-BL	WW-BL SS-BL	15 10 5 4	0.3 0.4 0.1 NR																	
05-11	2101 -2102 -2104	WW-BL SS-BL	WW-BL SS-BL	15 10 5 4	0.1 0.3 0.1 NR																	
05-12	1352 -1354 -1357	WW-BL SS-BL	WW-BL SS-BL	15 10 5 4	0.3 0.6 0.2 0.1																	
05-13	2117 -2121 -2123	WW-BL SS-BL	WW-BL SS-BL	15 10 5 4	0.2 0.3 0.3 NM																	

Date	SFD's				Solar Flares				Solar Radio Emissions				Ionospheric Effects			
	UT	Path	f Mc/s	Δf, cps (+)	ΔA km (-)	-ΔP db	UT Beg - Max - End	UT Beg - Max - End	UT Beg - Max - End	UT Beg - Max - End	Freq Mc/s 8 2800	Int or Peak Flux 8 2800	UT Beg - Max - End	Type	Imp	
1962	UT															
05-18	1530 -1531D -	WW-BL SS-BL	15 10 5 4	0.7 1.1 NM NM			1530 -1534- 1546	1	1531 - 1531.5 - 1531.7 - 1532.4 - 1536.7	BUR BUR 282f	18 108 2800	1 3 56				
	-1533D-1536	WW-BL SS-BL	15 10 5 4	0.9 1.5 NM NM												
05-18	2002 -2004 -2007	WW-BL SS-BL	15 10 5 4	0.4 0.5 NM NM			1958 -2005 - 2015	1-								
05-20	2033 -2035 -2038	WW-BL SS-BL	15 10 5 4	0.1 0.3 NM NM			2035 - 2040 - 2048	1-								
05-23	1753 -1754 -	WW-BL SS-BL	15 10 5 4	0.4 1.1 0.1 NM			NFR									
05-25	1158 -1200 -1204	WW-BL SS-BL	15 10 5 4	0.1 0.2 0.2 0.1			NFR		1142E -	- 0156	6	108	2			
05-27	1516 -1516D	WW-BL SS-BL	15 10 5 4	1.3 1.7 0.7 NM	0.3		1511 -1518 -1522	1-	1516 - 1516.5 - 1516.45 - 1517 - 1517.2 - 1517 - 1520	III III 282 BUR	3 7.6-41 2800 18	108 7.6-41 2800 11				
05-27	-1517D-1521	WW-BL SS-BL	15 10 5 4	0.5 0.9 NM NM												
05-29	1759 -1800D-1804	WW-BL SS-BL	15 10 5 4	0.2 1.0 0.3 0.2			1759 -1804 - 1830	1	1800 - 1802 - 1803 - 1822	181 4PI	2800 2800	5				

Date	SFD's						Solar Flares						Solar Radio Emissions						Ionospheric Effects							
	UT		Path		f Mc/s	Δf , cps (+)	ΔA , db (+)	$-\Delta P$ km	UT		UT		UT		UT		Freq Mc/s		Int or Peak Flux		UT		Type		Imp	
Beg - Max - End	Beg - Max - End	WWV-BL	15 10 5	0.8 1.8 NM				Beg - Max - End	Beg - Max - End	Beg - Max - End	Beg - Max - End	Beg - Max - End	Beg - Max - End	Beg - Max - End	Beg - Max - End	Freq Mc/s	Freq Mc/s	Int or Peak Flux	Beg - Max - End	Beg - Max - End	Type	Type	Type	Type	Type	Type
05-30 1359 -1359D-1401E	SS-BL	WWV-BL	15 10 5	0.8 1.8 NM				1358E-	-1408D	1- 1359 - 1359.15-	-1400	-1400	-1400	-1400	III	III	16-41 16-41	1- 1- 1-								
05-30 1636 -1637 -1639	SS-BL	WWV-BL	15 10 5	0.2 0.3 NM				1627 - 1632 - 1645	1- 1633.45- 1637 -	-1634.2 -1637.2 -1640	III	III	III	III	27-41 27-41 BUR	27-41 27-41 BUR	1+ 2 1									
05-30 1657 -1658D-1700	SS-BL	WWV-BL	15 10 5	0.2 0.4 NM																						
05-31 0028 -0030 -0033	SS-BL	WWV-BL	15 10 5	0.2 0.1 0.2				0030E -	- 0050D	1																
06-01 1204 -1205D-1207	SS-BL	WWV-BL	15 10 5	NR 0.5 0.1				1203 - 1213 - 1238	1	1204.6-1205.3-1206.2 1205.15- -1206.3	III	III	III	III	108 17-41	108 17-41	3 1+									
06-01 1955 -1956 -2000	SS-BL	WWV-BL	15 10 5	0.4 0.6 0.1				1954 - 1958 - 2010	1- 1956 -	1950 - 2013 - 2110 - 1957					353 2800 21-41	353 2800 21-41	6 1									
06-01 2006 - □ - □	SS-BL	WWV-BL	15 10 5	0.5 0.2 0.2				2006 - 2019 - 2043	2	2005 - 2006.3- 2009 -	- 2015 - 2010 - 2015					II III BUR	II III BUR	19-41 21-41 18								
06-19 2254 -2256 -2300D	WWH-AN FB-AN	WWH-AN FB-AN	15 10	0.5 0.2				2250 - 2301 - 2320	1-																	
06-27 2039 -2041D-2045D	WWV-BL	WWV-BL	15 10 5	0.7 0.2 0.2				2035 - 2042 - 2049	1-																	

Date	SFD's						Solar Flares						Solar Radio Emissions				Ionospheric Effects			
	UT Beg - Max - End	UT Path	f Mc/s (+)	Δf , cps (-)	ΔA	$-\Delta P$ km	UT Beg - Max - End	UT Beg - Max - End	Type	Freq Mc/s	Int or Peak Flux	UT Beg - Max - End	Type	UT Beg - Max - End	Imp					
1962 07-05	1715 -1719 -1725	WWV-BL SS-BL	15 10 5 4	0.3 0.8 NM NM		1716 -1722 -1728	1- 1711 - 1714 - 1744	3S3f	2800	1.4	1708-1716-1745 1715-1720-1730 1716-1721-1726	SEA SPA SCWA ABS S-SWF	3 22 10 2 1							
1936 07-05	-1939E	WWV-BL WWH-AN -MX	15 15 15	1.3 2.3 0.9	0.3		1935- 1942 - 1957	1+ 1954 -	3S3f 5Abs	2800	3	1930-1940-1955 1935- -2005 1932-1944-2030 1938-1943-2000	SEA SL-SWF SPA SCWA ABS SEA S-SWF	3+ 1 35 1 20 1 2+						
-1940E-195D																				
08-13	2038 -2039D-2044	WWH-AN WWV-BL	15 10	1.3 2.0	0.2 0.3			2037- 2045 - 2118	1- 2039.5- 2041 - 2042.1 2039.5-2040.3-2041 2040 - 2047 -	cont 2S2f 4PI 3 III II I	12.41 2800 2800 108 7.641 18 1	2040-2046-2110 2040- -2140 2045-2050-2130U	SL-SWF SEA	5 1 3						
		PB-AN SS-BL	10 5	0.5 0.4				2304 - 2322 - 2344	1- 2305 - 2305.5 - 2307.5 - 2308.5-2310.5	2041 BUR BUR BUR BUR BUR BUR	18 18 18 18 18 18 1	2307 2310.5 2306 - 2307 2307.5-2308.5-2310.5								
08-13	2307 -2308 -2313	WWH-AN	15	0.7				0226 - 0235 - 0300	1											
08-14	0226 -0227 -0230	WWH-AN	15	0.7																

Date 1962	SFD's						Solar Flares			Solar Radio Emissions			Ionospheric Effects		
	UT		Path	Δf , cps Mc/s (+)	ΔA db (-)	$-\Delta P$ km	UT			Type	Freq Mc/s	Int or Peak Flux	UT Beg - Max - End	Type	Imp
	Beg - Max	End					Beg	-	Max						
08-14 0244 -0246 -0251	WWH-AN PB-AN	15 0.4 10 0.3	0244 -0247 -0310	1	0246 -	-	0252	BUR	18	2	0245- 0247-	-0300	S-SWF SCNA	1+ 2	
08-14 1836 -1837D-1842	WWH-AN WWV-BL	15 0.4 10 0.5	1829 - 1839 - 1912	1-											
08-14 2259 -2300D-2302	SS-BL WWH-AN WWV-BL	15 0.2 10 0.5 10 0.6 NR 4 NM	2256 - 2302 - 2337	1-											
08-15 2306 -2309 -2315	WWH-AN WWV-BL SS-BL	15 0.8 10 0.5 10 0.1	2606 - 2309 - 2313	1-	2305 - 2305.3 - 2305.5 - 2305.5 - 2307.5 - 2308.5 - 2310.5	-	2310 2310 2310.5 2307 2310.5	BUR III III III III	18 1 2800 2800 6C	1 2 2800 2800 9	2305- 2310	-2310	BUR	1	
08-16 1450 -1451 -1454	PB-AN	10 1.6	1440 - 1446 - 1452	1-											
08-18 2048 -2050 -2055	WWH-AN	15 0.4	2048 - 2051 - 2101	1-	2049 -	-	2055	BUR	18	1					
08-21 1714 -1715 -1717	WWV-BL SS-BL	15 0.5 10 0.5 10 0.1	1718 - 1720 - 1726	1-	1716.15- 1718.30-	-	-1718.45 -1720.45	III III	7.6-41 7.6-41	1 1+					
08-24 2139 -2140D-2144	WWH-AN WWV-BL SS-BL	15 0.9 15 0.2 10 0.4 5 NM 4 NM	2128 - 2140 - 2158	1-	2136.45-	-	-2137.30	III	12-41	1+					
08-24 2232 -2235 -2240	WWH-AN WWV-BL SS-BL	15 0.8 15 0.1 10 0.3 5 NM 4 NM	2225 - 2234 - 2247	1-											

Date 1962	SFD's				Solar Flares				Solar Radio Emissions				Ionospheric Effects			
	UT Beg - Max - End	Path	f Mc/s	Δf , cps (+)	Δf , cps (-)	ΔA km	$-\Delta P$ km	UT Beg - Max - End	UT Beg - Max - End	Type	Freq Mc/s	Int or Peak Flux	UT Beg - Max - End	Type	Imp	
09-01 1200 -1201 -1205	WW-BL SS-BL	15 10 5 4	NR MM NR NR				1155E-	-1210	1-							
09-01 1341 -1342D-1344	WW-BL SS-BI	15 10 5 4	NR 0.3 MM NR				1341 - 1346 - 1353	1								
09-01 2040 -2041 -2044	WW-BL SS-BL	15 10 5 4	0.2 0.4 0.1 0.2				2040 - 2043 - 2048	1-	2039.15-	-2039.3	III	23-37	1-			
09-01 2142 -2144E-2147	WW-BL SS-BL	15 10 5 4	0.2 0.3 0.3 0.2				2142 - 2146 - 2157	1-	2143 - 2144 - 2148	1S1	2800	4				
09-01 2236 -2237 -2240	WW-BL SS-BL	15 10 5 4	0.1 0.1 0.1 0.1				MFR									
09-02 1436 -1437D-1442	WW-BL SS-BL	15 10 5 4	0.1 0.3 NR MM				1435E-1443 - 1515	1-								
09-02 1620 -1622E-1625	WW-BL SS-BL	15 10 5 4	0.3 0.6 NR MM				1619 - 1624 - 1730	1	1618 - 1637 - 1728	3S3	2800	5	1624-1633-1700	SPA		
09-03 1828 -1830 -1836	WW-BL SS-BL	15 10 5 4	0.7 0.9 0.7 0.4	0.2 0.3 0.3 0.3			1830 - 1837 - 1921	1,2	1825 - 1846 - 2030	3S3F	2800	8				
09-04 1237 -1239 -1241	WW-BL SS-BL	15 10 5 4	NR 0.2 NR NR				1829 -	1831 - 1836	8 cont	108	3					
							1829 -	- 1925	BUR	18	3					
							1829 -	- 1835								
							1237 - 1243 - 1306	1-	1235E-2324 - 0110	6	108	2				
							1239 - 1240 - 1244			4PI	2800	2				
							d1:45	- 2000		cont	7.6-41	2				
							1357E-	-								

Date	SFD's						Solar Flares						Solar Radio Emissions						Ionospheric Effects			
	UT		Path	f Mc/s	Δf , cps		ΔA km	$-\Delta P$ db	UT		UT		Imp	Type	Freq Mc/s	Int or Peak Flux	UT		Type	Imp		
	Beg	Max			(+)	(-)			Beg	Max	-	End					Beg	Max	-	End		
1962 09-04	1709 -1711D-1716	WWV-BL	15 10 5 4	0 0.4 0.1 0.1					1711 -1715 -1724	1-	1705 -1808 -2045	-	353A 2	2800 108	4 2							
09-04	2151 -2152 -2155	WWV-BL	15 10 5 4	0.1 0.2 0.1 0.1					2136 -	-2142D	1-	2000 -	-	2400	cont	1541	1					
09-06	1709 -1711 -1714	WWV-BL	15 10 5 4	0.2 0.4 0.3 NM					1706 -1712 -1724	1-												
09-07	2154 -2155D-2200	WWV-BL	15 10 5 4	0.3 0.5 NR 0.2					2152 -2157 -2223	1-	2149 -2156 -2300D	-	353A 2S2f III	2800 2800 12-41	6 8 1+							
09-09	1912 -1913 -1915	WWV-BL	15 10 5 4	0.4 0.6 NR 0.2					1913 -1914 -1922	1-	2155.2- 2156 -2158.9	-										
09-10	2313 -2315 -2319	WWV-BL	15 10 5 4	0.2 0.4 NR 0.4					2312 -2321 -2406	1-	1912.7-1913.4-1914.7	-	1S1	2800	3.5							
09-11	1954 -1955D-1957	WWV-BL	15 10 5 4	NM 0.2 NR 0.1									NFR									
09-13	1229 -1230D-1237	WWV-BL	15 10 5 4	0.6 NR NM 0.1					1213 -	-	-1235D	1-										
09-13	1730 -1732 -1736	WWV-BL	15 10 5 4	0 0.4 NR NR									1729 -1733 -1739	1-								

Date	SFD's				Solar Flares				Solar Radio Emissions				Ionospheric Effects			
	UT Beg - End	UT Max - End	Path	f Mc/s (+)	Δf , cps (-)	ΔA db	$-\Delta P$ km	UT Beg - Max - End	UT Beg - Max - End	Type	Freq Mc/s	Int or Peak Flux	UT Beg - Max - End	Type	Imp	
09-14 1962	1739 -1741 -1743	WW-BL SS-BL	15 10 5 4	NM 0.1 NR 0.1				1721 -1728 -1739	1-							
09-14 1825	1826D-1829	WW-BL SS-BL	15 10 5 4	0.1 0.1 NR NM												
09-14 1857	1858 -1904	WW-BL SS-BL	15 10 5 4	NM 0.2 NR 0.1				1858 -1858 -1912	1-							
09-14 2010	-2011 -2014	WW-BL SS-BL	15 10 5 4	0.1 0.2 NR 0.1				2006 -2010 -2015	1-							
09-15 1249	-1250 -1254	WW-BL SS-BL	15 10 5 4	NR NM NR NR				1248 -1302 -1346	1-	1257 - 1259 - 1300 d10	151 4PI	2800 2800	6 3			
09-15 1432	-1433D-1437	WW-BL SS-BL	15 10 5 4	0.1 0.5 NR NR				1432E-1434 -1528D	1-							
09-15 1501	-1503 -1508	WW-BL SS-BL	15 10 5 4	0.4 NM NR NR				1442E-1504 -1545D	1-							
09-16 1428	-1429D -1431	WW-BL SS-BL	15 10 5 4	0.3 0.5 NR NM				1429 -1430 -1440	1-	1407E -	- 2425D	cont	20-41	1+		
09-16 1437	-1439 -1442	WW-BL SS-BL	15 10 5 4	0.2 0.3 NR 0.1				1438 -1440 -1442	1-	1407E -	- 2425E	cont	20-41	1+		

Date 1962	SFD's					Solar Flares					Radio Emissions					Ionospheric Effects			
	UT		Path	f Mc/s (+)	Δf , cps (+)	ΔA db (+)	$-\Delta P$ km (+)	UT		UT		Type	Freq Mc/s	Int or Peak Flux	UT		Type	Imp	
	Beg -	Max - End						Beg -	Max - End	Beg -	Max - End				Beg -	Max - End			
09-16	1701	-1702	-1704	WW-BL	15	0.2	NR			NFR					20-41	1+			
				SS-BL	10	0.4	NR												
					5		NR												
					4		NR												
09-20	1808	-1809D	-1813	WW-BL	15	0.8	NR			1809	-1811	-1825	1-	1809.5-1810.3-1812	151 4PI	2800 2800	7		
				SS-BL	10	1.0	NR												
					5		NR												
					4		NR												
09-21	1314	-1315D	-1318	WW-BL	15	0.2	NR			1314	-1314	-1321	1-						
				SS-BL	10	0.3	NR												
					5		NR												
					4		NR												
09-22	2057	-2059	-2101	WWH-AN WW-BL	15	1.0	NR			2055	-2101	-2117	1-						
				SS-BL	10	0.3	NR												
					5		NR												
					4		NR												
09-24	1531	-1532D	-1536	WW-BL	15	NR	0.1			1522	-1532	-1545	1-						
				SS-BL	10	0.7	NR												
					5		NR												
					4		NR												
09-26	1628	-1631	-1635	WW-BL	15	NR	0.5			NFR					22-41	1-			
				SS-BL	10	0.3	NR												
					5		NR												
					4		NR												
09-26	1721	-1722	-1725	WW-BL	15	NR	0.2			1722	-1723	-1727	1-	1414E -	- 2100	cont	22-41	1-	
				SS-BL	10	0.3	NR												
					5		NR												
					4		NR												
09-29	1625	-1628D	-1635	WW-BL	15	NR	0.2			1620	-1626	-1638	1-						
				SS-BL	10	0.2	NR												
					5		NR												
					4		NR												

Date	SFD's						Solar Flares			Solar Radio Emissions			Ionospheric Effects		
	UT Beg - Max - End	Path	f Mc/s	Δf , cps (+)	Δf , cps (-)	ΔA km	$-\Delta P$ km	UT Beg - Max - End	UT Beg - Max - End	Type	Freq Mc/s	Int or Peak Flux	UT Beg - Max - End	Type	Imp
1962 09-29	1753 -1755 -1758	WW-BL SS-BL	15 10 5 4	0.5 0.9 NR NR				1753 -1757 -1810	1-						
09-30 09-30	1816 -1818 -1821	WW-BL SS-BL	15 10 5 4	0.1 0.2 NR NR				1815 -1820 -1829	1-						
09-30 09-30	1925 -1926E-1929	WW-BL SS-BL	15 10 5 4	0.1 0.1 NR NR				1924 -1930 -2037	1-						
09-30 10-02	2006 -2008 -2013	WW-BL SS-BL	15 10 5 4	0.2 0.4 NR NR				2002 -2011 -2019	1-						
10-02 10-07	1252 -1253 -1256	WW-BL SS-BL	15 10 5 4	0.2 0.3 NR NR				1313E- -1342D	1						
10-08	2342 -2343 -2345D	WW-BL SS-BL	15 10 5 4	0.1 0.4 NR NR						MFR					
10-09	1658 -1701E-1704	WW-BL SS-BL	15 10 5 4	0.3 0.4 NR NR						MFR					
10-10	2127 -2128D-2131	WW-BL SS-BL	15 10 5 4	0.2 0.3 NM NM				2128 -2132 -2155	1-						
	1320 -1325 -1330	WW-BL SS-BL	15 10 5 4	0.2 0.3 NM NM						MFR					

Date	SFD's						Solar Flares			Solar Radio Emissions						Ionospheric Effects				
	UT		Path	f Mc/s	Δf , c/s (+)	Δf , c/s (-)	UT			UT			Type	Freq Mc/s	Int or Peak Flux	UT		Type	Imp	
	Beg	Max - End					Beg	Max - End	Beg	Beg	Max - End	Beg	Max - End			Beg - Max - End				
1962-10-12	2300	-2301D-2304	WW-BL	15	0.2		2300	-2303	-2317	1-	2251 -	- 2252	III	22-36	1-					
			SS-BL	10	0.3					2251.9-2252.1-2253	3	108	3							
			SS-BL	5	0.3					2300 -	- 2304	III	19-41	3						
			SS-BL	4	0.3					2304.15-	- 2305	III	22-41	1						
										2304.2-2305.3-2309.2	8	108	3							
1962-10-13	1440	-1441D-1445D	WW-BL	15	NM															
			SS-BL	10	0.1															
			SS-BL	5	NM															
			SS-BL	4	0.1															
1962-10-13	1750E-1750D-1751	WW-BL	15	1.0			1750	-1754	-1803	1-	1748.3-	- 1749.45	III	22-38	1-					
		SS-BL	10	1.3						1748.3 -	- 1749.45	BUR	18	1						
		SS-BL	5	1.2																
		SS-BL	4	NM																
1962-10-13	1805	-1806E-1808	WW-BL	15	8.4	1.6	1805	-1808	-1825	1-	1808.3 -	- 1809.15-	III	23-41	1-					
			SS-BL	10	10.0	1.8				1808.3 -	- 1809.15-	BUR	10-41	2-						
			SS-BL	5	3.2	0.3					- 1810	- 1810	BUR	18	1					
			SS-BL	4	3.6	0.4														
1962-10-13	2033	-2034D-2037	WWH-AN	15	0.4		2033	-2035	-2038	1-	2029.45-	- 2033.3	III	22-41	1-					
			WW-BL	15	0.2					2029.3 -	- 2034.15	III	13-41	2						
			SS-BL	10	0.3					2034.45-	- 2037.15	III	13-41	2						
			SS-BL	5	NM					2038.9 -	- 2039.9	III	108	2						
			SS-BL	4	NM					2039.9 -	- 2039.9	BUR	18	1						
1962-10-16	2030	-2032D-2037	WW-BL	15	NM		2032E-2034	-2042D	-2042D	1-	2028.30-	- 2029.30	III	22-41	1-					
			SS-BL	10	0.2					2029.45-	- 2030.3	III	20-41	1+						
			SS-BL	5	NM					2030.30-	- 2033.15	III	16-41	1+						
			SS-BL	4	NM					2034 -	- 2034.15	III	21-41	1						
										2034.15 -	- 2034.15	BUR	18	1						
1962-10-17	1803	-1804D-1807	WW-BL	15	NM	0.2	1803	-1806	-1815	1-	1758 -	- 1758.3	III	26-39	1-					
			SS-BL	10	0.2															
			SS-BL	5	0.1															
			SS-BL	4	NM															
1962-10-18	1705	-1706D-1709	WW-BL	15	1.1		1706 -			1-	1706 -	- 1707 -	1711	2S2	22					
			SS-BL	10	NM						d40			4PT	2800	3				
			SS-BL	5	0.8															
			SS-BL	4	0.6															

Date	SFD's						Solar Flares						Solar Radio Emissions						Ionospheric Effects					
	UT		Path		f Mc/s	Δf, cps (+)	Δf, cps (-)	ΔA km	-ΔP km	UT		UT		Type	Freq Mc/s	Int or Peak Flux		UT		Beg - Max - End	Type	Imp		
1962	Beg - Max	- End								Beg	- Max	- End	Beg	- Max			Beg	- Max	- End					
10-18	2123	-2125D-2130	WWH-AN WWV-BL	15 10	2.1 0.5 NR	15 5 4	0.5 0.3 0.4			2111E-2135U-2155	1-	2005 - 2125 -	2125	-	9Pre 2S2	2800 2800	2 14							
10-20	1955	-1956E-1959	WWV-BL SS-BL	15 10	0.6 0.4	15 5	0.6 0.4	0.1		1951 -1959	-2011	1-												
10-20	2117	-2119 -2127	WWV-BL SS-BL	15 10	0.3 0.2	15 5	0.3 0.4	0.2		NFR														
10-25	1941	-1943 -1945	WWV-BL SS-BL	15 10	0.2 0.2	15 5	0.2 0.1	0.1		1942 -1944 -1946	1-	1938.45-	-	1939	III			26-41	1-					
10-27	1840	-1841 -1843	WWV-BL SS-BL	15 10	0.4 0.6	15 5	0.4 0.6	0.6		1836 -1843 -1901	1-	1838.15- 1841 -1841.5- 1841.3 - 1845.15-	1839.15 1841.5-1843 1842.15 -1846		III	16-41 2S2	1+	16-41 2800	11					
11-07	1411	-1411D -1413 -1415	WW-AC MN-AC	10 10	1.0 1.0	WWV-BL SS-BL	15 10	0.6 0.4			NFR							III	16-41 2S2	1+	16-41 16-41	11		
11-14	1840	-1841D-1845D	WWV-BL SS-BL	15 10	0.6 0.4	WWV-BL SS-BL	15 10	0.6 0.4			NFR							III	16-41 2S2	1+	16-41 22-41	1-		
11-16	1629	-1631E-1633	WWV-BL SS-BL	15 10	0.6 1.3	WWV-BL SS-BL	15 10	0.6 0.4			NFR													
11-16	2214	-2215 -2217	WWV-BL SS-BL	15 10	0.5 0.7	WWV-BL SS-BL	15 10	0.5 0.4			NFR													

Date	SFD's						Solar Flares						Radio Emissions						Ionospheric Effects			
	UT		Path	f Mc/s	Δf , cps		ΔA db	$-\Delta P$ km	UT		Imp	UT		Type	Freq Mc/s	Int or Peak Flux		UT		Type	Imp	
	Beg	Max - End			(+)	(-)			Beg	Max - End		Beg	Max - End			Beg - Max - End	Beg - Max - End					
1962 11-24	2219 -2221 -2226	WWH-AN WW-BL	WWH-AN WW-BL	15 15 10 5	1.5 0.2 NM 0.3	15 0.2 NM 0.5	2218 -2222 -2230D	1-	2222 -	- 2223	III	1941	2									
11-30	1641 -1643 -1645D	WW-BL	WW-BL	15 10 5 4	NR 0.3 0.2 0.3	15 10 5 4	1644 -1648 -1652	1-														
11-30	1928 -1930 -1933	WW-BL	WW-BL	15 10 5 4	NM 0.8 NM 0.3	15 10 5 4	1927 -1932 -1937	1	1830 - 1918 - 2028			353	2800	3								
12-17	1629 -1630 -1640	WW-BL	WW-BL	15 10 20 10	0.8 1.4 12.0 3.5	15 10 10 5	1630 -1633 -1640	1-	1625.5-1630.5-1632	d31		252	2800	40								
		MN-NA	MN-NA	10 10 10 5	0.6 0.6 0.6 0.3	10 10 10 4						401	2800	2								
		MN-AC	MN-AC	10 10 10 5	0.6 0.6 0.6 0.3	10 10 10 4																
12-17	1732 -1733 -1735	WW-BL	WW-BL	15 10 5 4	0.1 0.2 NM 0.2	15 10 5 4																
12-18	1654 -1656 -1657	WW-BL	WW-BL	15 10 5 4	NM 0.3 NM 0.2	15 10 5 4	1654 -1656 -1711	1-														
12-20	0827-0828D-0832	MN-NA	MN-NA	20 10 10 10	0.5 0.8 0.6 0.5	20 10 10 10	0815 -		-0830		1											
12-22	0918-0919-0923	MN-NA	MN-NA	20 10 10	0.2 0.5 0.2	20 10 10	0918D-				1-											



